UNIVERSITÀ DEGLI STUDI DI PADOVA

Head Office: Università degli Studi di Padova

Department of Biology

_____

Ph.D. COURSE IN: BIOSCIENCES
CURRICULUM: CELL BIOLOGY AND PHYSIOLOGY
SERIES XXXI

Investigating the role of the Roc/GTPase domain of the Parkinson's disease kinase LRRK2 in regulating protein function and activity

Thesis written with the financial contribution of Fondazione CARIPARO

Coordinator: Prof. Ildikò Szabò
Supervisor: Prof. Elisa Greggio
Co-Supervisor: Dr. Patrick A. Lewis

Ph.D. student: Susanna Cogo

"The scientist is not a person who gives the right answers,
he is one who asks the right questions."

Claude Lévi-Strauss

Index

Abstract

Parkinson's disease (PD) is the second most common neurodegenerative disease of the modern era. Although PD aetiology is still uncertain, approximately 10% of patients suffer from a monogenic form of PD.

Mutations in *Leucine-rich repeat kinase 2* (*LRRK2*) are the most common cause of autosomal dominant, late onset familial PD and increase PD risk. LRRK2 possesses dual Roc/GTPase and kinase domains, bridged by a COR scaffold. Given the robust association with PD and the presence of a "druggable" kinase activity, substantial efforts have been made to explore LRRK2 functions in health and disease. The current understanding of LRRK2 biology comes from the characterisation of knockout models or the manipulation of its kinase activity, especially since the most common pathological mutation is the G2019S in the kinase domain and kinase activity is associated with increased cellular toxicity.

Conversely, Roc has received less attention, probably because of the challenges related to the measurement of *in vitro* GTPase activity. Nevertheless, the cross-talk between the two enzymatic modules and the signalling properties of Roc make the GTPase domain a key element in determining the biochemical and cellular properties of LRRK2. Therefore, a thorough characterisation of the intramolecular mechanisms of LRRK2 regulation as well as the signalling cascades orchestrated by the kinase is of high priority to provide alternative therapeutic targets in those cases where kinase inhibition proves badly-tolerated or ineffective.

In this scenario, this project has focused on a comprehensive characterisation of the role of LRRK2-Roc in regulating protein biochemistry and the binding with the previously identified interactor p21-activated kinase 6 (PAK6). As a functional readout, two pathways convincingly linked to LRRK2, i.e. autophagy and neurite remodelling, have been investigated.

Specifically, we characterised a murine cellular model where endogenous Lrrk2 has been genetically engineered to disrupt guanine nucleotides binding in terms of Lrrk2 expression levels, basal autophagy and the ability to respond to specific autophagic stimuli. We observed that lack of nucleotide binding in Roc

affects protein steady-state levels and possibly the response to autophagy-inducing treatments. The second part of the study was dedicated to the characterisation of the interaction between LRRK2 and PAK6. PAK6 regulates actin-cytoskeletal dynamics and it was demonstrated by our group to interact with Roc and to promote neurite outgrowth *in vivo* through its kinase activity in a LRRK2- and GTP-dependent manner. More recently, we demonstrated that the two proteins bidirectionally modulate each other and overexpression of PAK6 is able to rescue the defects in neurite outgrowth associated with the G2019S pathological mutation. We then went a step further and, in collaboration with Dr. Patrick Lewis at University of Reading, we evaluated the impact of PAK6 pharmacological inhibition on autophagy, given the established role of LRRK2 and the importance of actin cytoskeleton in assisting the process, as well as the involvement of PAK6 homolog PAK1 in promoting autophagy through the AKT/mTOR/ULK1 axis. Our results show clear alterations in the autophagic markers analysed after treatment with an inhibitor of PAK6 kinase activity. Second, we characterised the effects of a *de novo* substitution in PAK6 in terms of kinase activity, localisation and neurite development as well as interaction with LRRK2, and the consequences of a PD mutation in Roc in terms of binding with PAK6. While the PAK6 variant does not affect the properties of the protein, the presence of a mutation in LRRK2-Roc impairs the interaction with PAK6, with possible consequences on downstream pathways.

Overall, our data suggest that any alterations in Roc have severe implications for the steady-state levels of the protein, its activities and binding with partners, with a predicted impact on its subcellular localisation and downstream signalling.

Riassunto in lingua italiana

La malattia di Parkinson (MP) è la seconda malattia neurodegenerativa più comune dell'era moderna. Nonostante un'eziologia incerta, il 10% dei pazienti soffre di una forma monogenica di MP.

Mutazioni nel gene *Leucine-rich repeat kinase 2* (*LRRK2*) sono la causa più comune di MP autosomica dominante ad insorgenza tardiva e aumentano il rischio di sviluppare la MP. LRRK2 possiede una duplice attività enzimatica: GTPasica nel dominio Roc e chinasica, collegate da un dominio COR. Date la robusta associazione con la MP e la presenza di un'attività chinasica modulabile dal punto di vista farmacologico, sono stati compiuti notevoli sforzi per esplorare il ruolo fisiopatologico di LRRK2. L'attuale comprensione della biologia di LRRK2 proviene dallo studio di modelli *knockout* o dalla manipolazione dell'attività chinasica, dato che la mutazione patologica più comune è la G2019S nel dominio chinasico e l'attività chinasica è associata ad aumentata tossicità cellulare.

Al contrario, Roc ha ricevuto minore attenzione, probabilmente a seguito delle difficoltà nel misurare l'attività GTPasica *in vitro*. Tuttavia, l'interazione tra i due moduli enzimatici e le proprietà di *signalling* di Roc rendono il dominio GTPasico un elemento chiave nel determinare le proprietà biochimiche e cellulari di LRRK2. Una caratterizzazione completa dei meccanismi intramolecolari di regolazione e delle cascate di segnale orchestrate dal dominio chinasico è dunque un requisito essenziale per individuare strategie terapeutiche alternative qualora l'inibizione dell'attività chinasica fosse mal tollerata o inefficace.

Questo progetto si è focalizzato su una caratterizzazione globale del ruolo di Roc nel regolare le proprietà biochimiche di LRRK2 ed il legame con un interattore precedentemente identificato, p21-activated kinase 6 (PAK6). A livello funzionale, sono stati investigati due processi associati a LRRK2 in modo convincente: autofagia e rimodellamento dei neuriti.

Più precisamente, abbiamo caratterizzato un modello cellulare murino, in cui Lrrk2 endogena è stata ingegnerizzata geneticamente per impedire il legame dei nucleotidi guaninici, in termini di stabilità della proteina, autofagia basale e capacità di rispondere a stimoli autofagici. Abbiamo osservato che l'assenza di legame coi nucleotidi nel Roc influenza i livelli di Lrrk2 e la risposta all'induzione

del flusso autofagico. La seconda parte dello studio riguarda la caratterizzazione dell'interazione LRRK2-PAK6. PAK6 regola le dinamiche del citoscheletro di actina. Il nostro gruppo ha dimostrato che PAK6 interagisce con Roc e promuove la crescita dei neuriti *in vivo* grazie alla sua attività chinasica in dipendenza da LRRK2 e dal GTP. Di recente, abbiamo dimostrato che le due proteine esercitano una vicendevole modulazione e la sovra-espressione di PAK6 può recuperare i difetti nella crescita dei neuriti associati alla mutazione G2019S in LRRK2. Abbiamo quindi fatto un passo ulteriore e, in collaborazione con il Dr. Patrick Lewis all'Università di Reading, abbiamo valutato l'impatto dell'inibizione farmacologica di PAK6 sull'autofagia, visto il ruolo assodato di LRRK2 e l'importanza del citoscheletro di actina nel processo, così come il coinvolgimento dell'omologo di PAK6, PAK1, nel promuovere l'autofagia tramite l'asse AKT/mTOR/ULK1. I nostri risultati mostrano chiare alterazioni nei *markers* autofagici analizzati a seguito del trattamento con un inibitore dell'attività chinasica di PAK6. Abbiamo poi caratterizzato gli effetti di una sostituzione *de novo* in PAK6 in termini di attività chinasica, localizzazione, sviluppo dei neuriti ed interazione con LRRK2, e le conseguenze di una mutazione patologica nel Roc in termini di legame con PAK6. Mentre la variante di PAK6 non influenza le proprietà della proteina, la mutazione nel Roc riduce l'interazione con PAK6.

Globalmente, i nostri dati suggeriscono che qualunque alterazione di Roc abbia severe conseguenze per i livelli basali di LRRK2, l'attività della proteina ed il legame con gli interattori, con un probabile impatto sulla localizzazione subcellulare e le cascate di segnale a valle.

Chapter 1
Introduction

1. Parkinson's disease

201 years after the publication of "An Essay on the Shaking Palsy", where James Parkinson very accurately described the disease now bearing his name (Parkinson, 1817; Parkinson, 2002), a significant progress has been made in the understanding of the genetic and biochemical defects underlying the second most common neurodegenerative disease worldwide (Deng et al., 2018). While Parkinson's disease (PD) had been associated with the loss of cells in the *substantia nigra pars compacta* (*SNpc*) 100 years after its description, dopamine (DA) was identified as a neurotransmitter only in 1957 (Tretiakoff, 1919; Carlsson et al., 1957; Carlsson et al., 1958; Jankovic, 2008). A few years later, when DA levels were demonstrated to be reduced in the *striatum* of PD patients, levodopa, a precursor of DA, started to be administered which greatly improved the motor symptoms associated with PD (Ehringer and Hornykiewicz, 1960; Birkmayer and Hornykiewicz, 1961; Andén et al., 1970; Hornykiewicz et al., 2002; Jankovic, 2008). Today, the neuropathology of the disease is very well defined. PD is characterised by the selective loss of DA neurons in the *SNpc* and, at later stages, in other specific brain regions, such as the cortex and the brainstem (Jellinger et al., 1991; Braak et al., 1998). The second, distinctive hallmark of the disease is the accumulation of cytoplasmic proteinaceous inclusions known as Lewy bodies (LBs) (Figure 1) and Lewy neurites in certain brain nuclei of individuals affected by *Paralysis agitans*, in recognition of Fredrich Lewy's description of intraneuronal structures within both the somata and the neurites (Lewy, 1912). However, not all PD cases appear with LBs, and LBs can occur in diseases other than PD, such as dementia with LBs and other forms of parkinsonism (Gwinn-Hardy, 2002; Hardy and Lees, 2005). A brief overview of the non-conventional forms of PD will be given in section 1.1.

The discovery by Spillantini and colleagues of alpha-synuclein (α-syn) as the major component of LBs, back in 1997, represented a great revolution in the PD timeline (Spillantini et al., 1997). Soon after, at the beginning of the 21th century, the idea of PD as a prion-like pathology started to spread, particularly after the studies by Braak and colleagues reporting a reproducible pattern of

progression for parkinsonian pathology (Braak et al., 2003; Visanji et al., 2013). According to Braak's model, the disease begins at the level of the vagus nerve and the olfactory structures, to then ascend until it finally reaches the cortex, in a progression that is determined by the differential susceptibility of the diverse neuronal populations. Although multiple studies have later contradicted this staging scheme (Jellinger et al., 2008; Parkkinen et al., 2008; Beach et al., 2009), which undoubtedly presents certain limitations, the body of evidence sustaining a transcellular transmission of α-syn is quite robust (Kordower et al., 2008; Li et al., 2008; Desplats et al., 2009; Hansen et al., 2011; reviewed in Visanji et al., 2013).

PD is very common in the elderly, with a prevalence of 1% among the individuals over 60 years and 4% in the population over 85 years (Eriksen et al., 2005; Deng et al., 2013), although the onset of the disease can also occur at very young age, up to the third decade of life (Obeso et al., 2017). The precise aetiology of PD remains elusive and is very likely multifactorial, i.e. derived from a combination of genetic and environmental protective or predisposing factors (Eriksen et al., 2005; Obeso et al., 2017). For many years, certain lifestyles, e.g. farming, plus the exposure to specific environmental factors such as pesticides and/or toxins – e.g. MPTP, paraquat and maneb/mancozeb –, metals and solvents, have been associated with an increased risk of developing PD, even though a precise cause-effect relationship is still lacking (Pezzoli and Cereda, 2013; Goldman, 2014; Obeso et al., 2017). More recently, given the early symptoms appearing at the level of the gut and the olfactory apparatus, a putative role for an infectious agent in initiating the disease was proposed. On the other hand, protective behaviours that lower PD risk have been identified, including cigarette smoking and caffeine intake (Obeso et al., 2017).

In addition to the abovementioned environmental factors, there is a relevant genetic component contributing to PD onset. In this regard, 2017 was important not only for being the bicentenary of James Parkinson's publication, but also because it marked the 20th anniversary of the discovery of the first gene causing familial PD, i.e. *SNCA*, encoding α-syn (Polymeropoulos et al., 1997). This discovery opened a new era in PD research, with genetics taking centre stage, from the identification of novel genes mutated in familial forms of PD, to the generation of genetic models of the disease in parallel to the pre-existing toxin-

based ones (rotenone, 6-OHDA, MPTP, paraquat) (Bové et al., 2005). Indeed, genetic animal models, although with their own limitations, gave an important pulse to the research in the field (Obeso et al., 2017).
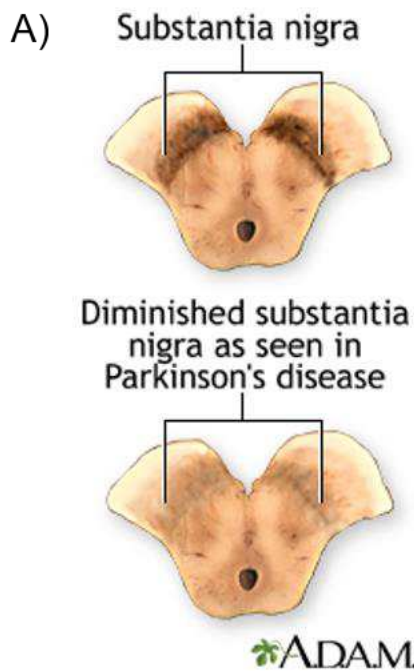
Figure 1. Pathological hallmarks of PD. (A) Comparison between the *SNpc* of a control and that of a PD patient, where a clear depigmentation – due to the loss of dopaminergic neurons – is observed (adapted from the U.S. National Library of Medicine, National Institutes of Health (NIH), https://medlineplus.gov/ency/article/000755.htm). (B) Representative immunohistochemical labelling of LB inclusions within neurons of the *SNpc*, that constitute a pathological hallmark of the disease (Dauer and Przedborski, *Neuron*, 2003).
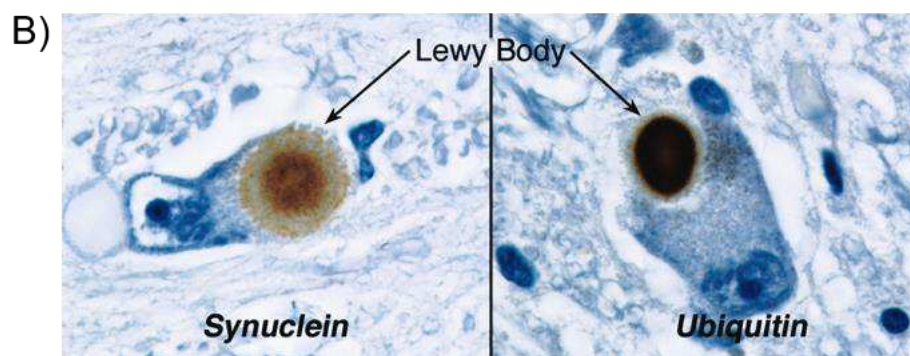
Notably, it appears now evident that genetic background contributes in determining the predisposition to PD at multiple levels, not restricted to the inheritance of gene mutations that cause monogenic forms of the disease. The overall susceptibility can indeed be defined by the combined occurrence in the genome of 1) very rare coding mutations within genes associated with Mendelian PD, 2) rare coding mutations acting as risk factors, and 3) risk factors identified by genome-wide association studies (GWAS), i.e. non-coding single nucleotide

polymorphisms (SNPs) in disease-associated loci that are very common and confer only a moderate risk of developing PD ("missing heritability" problem) (Keller et al., 2012; Gasser, 2015; Singleton and Hardy, 2016). The complex genetic architecture, in combination with the influence exerted by the environment and lifestyles, explains the large heterogeneity observed among PD patients in terms of both age of onset and clinical manifestations (Obeso et al., 2017).

1.1 Clinical manifestations & diagnosis

Clinicians usually group the prominent motor features of PD under the acronym TRAP: Tremor at rest, Rigidity, Akinesia (or Bradykinesia) and Postural instability. In addition to these, symptoms like flexed posture and freezing are more generally an indication of parkinsonism, defined as a clinical syndrome characterised by lesions in the basal ganglia, predominantly in the *SNpc*, of which PD represents the 80% of the cases (reviewed in Jankovic, 2008; International Parkinson and Movement Disorder Society). Non-motor symptoms – which can be present at different extents and in different combinations – include sleep disturbances, olfactory dysfunction, cognitive impairment, psychiatric symptoms and autonomic dysfunction, very often anticipating the occurrence of motor symptoms (Lang, 2011; Obeso et al., 2017; Deng at al., 2018).

Diagnosis is based on clinical evaluation and, in classical PD cases, confirmed *post-mortem* by pathological finding of neuronal loss in the *SNpC* and LBs on autopsy (Jankovic, 2008). The clinical criteria for diagnosing PD are represented by a combination of key motor features, associated and exclusive/specific symptoms, and the response to levodopa, as indicated by the UK Parkinson's Disease Society Brain Bank and the National Institute of Neurological Disorders and Stroke (Gelb et al., 1999; Tarakad and Jankovic, 2017). Regarding the severity of the phenotype, different rating scales are often employed, even though their reliability has not been fully evaluated due to the high heterogeneity of the disease (Jankovic, 2008). The differentiation among PD and other parkinsonian syndromes, grouped under the term "atypical parkinsonism", is fundamental in planning the treatment and predicting the prognosis. Indeed,

patients affected by atypical parkinsonism are usually characterised by a worse prognosis and do not benefit from levodopa treatment. Examples of atypical parkinsonism are progressive supranuclear palsy (PSP), multiple system atrophy (MSA), and dementia with LBs (Trenkwalder and Arnulf, 2011). In the case of PSP, LB inclusions are not increased as compared to controls, further supporting the notion that PD and the parkinsonian spectrum of disorders can arise without α-syn accumulation (Jellinger, 2003).

1.2 PD therapeutics

One of the major limitations in PD field is the current absence of a treatment able to halt or slow the progression of the disease (Jankovic et al., 2018). Levodopa remains the treatment with the highest efficacy in alleviating the motor symptoms (Birkmayer and Hornykiewicz, 1961; Andén et al., 1970; Lotia and Jankovic, 2016; Tarakad and Jankovic, 2017), but at a cost, i.e. the appearance of complications such as motor fluctuations and dyskinesia after prolonged use. To bypass this obstacle, emerging levodopa formulations aim at prolonging its effect and/or improving its delivery. In parallel, alternative strategies could be approached both as monotherapies or as adjuvant therapies. Among them, DA agonists or deep brain stimulation are currently employed with good success (Tarakad and Jankovic, 2017). In some cases, tremor can be ameliorated with botulinum toxin, which has been proven efficacious in the treatment of multiple neurologic and non-neurologic disorders (Jankovic, 2018). In the last years, the exploration of alternative routes based on gene therapy *via* adeno-associated viral (AAV) vectors for the silencing of *SNCA*, or carrying the DNA encoding human aromatic-L-amino-acid decarboxylase (AADC) – i.e. the last enzyme in DA production –, immunotherapy – mainly *via* the production of antibodies against α-syn – or cell transplantation has also been undertaken. Despite the fact that these approaches are at the moment more encouraging in terms of safety rather than in terms of clinical efficacy, the efforts and investments in this area confer it a great potential from a therapeutic point of view (Zharikov et al., 2015; Lee and Lee, 2016; Deverman et al., 2018; Lee et al., 2018).

1.3 Genetics of PD

Although a clear definition of PD aetiology is still missing, and the vast majority of PD cases is likely caused by a combination between the exposure to environmental risk factors and a predisposing genetic background (Kalinderi et al., 2016), about 15% of patients have family history and 5-10% suffer from a monogenic, Mendelian form of the disease (Deng et al., 2018). To date, 13 disease-causing genes have been associated with parkinsonism. A summary of the known *PARK* genes, together with their protein product, the mode of inheritance and the associated clinical manifestation is listed in Table 1.

The very first genetic modification linked to PD was the G209A point mutation (A53T in the protein product) in the *SNCA* gene, located within the *PARK1* locus on chromosome 4 (Polymeropoulos et al., 1997). Several other point mutations, together with duplications and triplications of the entire locus, were later added to the list of PD-causing alterations (Singleton et al., 2003; Chartier-Harlin et al., 2004; Ibáñez et al., 2004; Singleton and Gwinn-Hardy, 2004; Deng and Yuan, 2014), with a clear genomic dosage-related phenotype, i.e. a more severe phenotype and a higher penetrance in the case of multiplications as compared to the effect of single mutations (Chartier-Harlin et al., 2004; Singleton and Gwinn-Hardy, 2004; Deng et al., 2018). Twenty years after Spillantini's labelling of α-syn in LBs, there is still some uncertainty about the physiological function of α-syn, whereas its pathological accumulation in the form of toxic fibrils is better understood and of high interest for therapeutic design (Poewe et al., 2017). More recently, mutations in *CHCHD2/PARK22* and *VPS13C/PARK23* – whose protein products are likely involved in mitochondrial metabolism – have been associated with different parkinsonian manifestations, i.e. autosomal dominant, late onset PD and autosomal recessive, early onset parkinsonism, respectively (Table 1) (Funayama et al., 2015; Lesage et al., 2016; Singleton and Hardy, 2016; Ferreira and Massano, 2017). Interestingly, Lesage and co-authors reported an effect of VPS13C loss of function in the mitochondria quality control system orchestrated by the previously identified PD-related proteins Parkin and PINK1 (PTEN-induced putative kinase 1). Mutations in *PRKN/PARK2* were found

very early in 1998 to be the cause of severe, autosomal recessive juvenile parkinsonism. Parkin is an E3 ubiquitin ligase, participating to the degradation of proteins *via* the ubiquitin-proteasome system (UPS). Mitochondria quality control is guaranteed through selective autophagy of depolarised mitochondria (mitophagy), occurring when PINK1, a serine-threonine kinase encoded by *PINK1/PARK6*, recruits, phosphorylates and activates parkin on damaged mitochondria. In the same pathway we can position the adaptor protein FBXO7 (*FBXO7/PARK15*). Another *PARK* locus causing early-onset PD is *PARK7*, where *DJ-1* is located. DJ-1 has been shown to buffer oxidative stress. Finally, *PARK14/PLA2G6* enters the list of mitochondria-related genes. PLA2G6 is a calcium (Ca^{2+}) independent phospholipase particularly important for the homeostasis of mitochondrial membrane (Kitada et al., 1998; Bonifati, 2003; Shojaee et al., 2008; Paisán-Ruiz et al., 2009; Seirafi et al., 2015; Kalinderi et al., 2016; Deng et al., 2018).

One of the most intriguing aspects of the majority of neurodegenerative diseases, and one that applies to PD, is that, although displaying a large heterogeneity in terms of clinical manifestation, the molecular defects underlying the pathology can be grouped under a relatively small number of cellular pathways. In addition to the abovementioned control of mitochondrial homeostasis, a substantial number of *PARK* genes is involved in "cellular transport and trafficking". Starting with the dominantly inherited forms, *PARK17/VPS35* encodes a component of the retromer that is key for the transport of proteins from endosomes to the trans-Golgi network (TGN). Interestingly, VPS35 has been shown in association with multiple PD-related genes/proteins, including parkin. Similarly, moving to the recessive mode of inheritance, ATP13A2 (*ATP13A2/PARK9*) is an ATPase involved in cargo sorting at the endo-lysosomal level, found to be mislocalised in PD. Of extremely high interest is also the set of proteins involved in clathrin-mediated endocytosis, specifically of synaptic vesicles (SVs), represented by the exclusively neuronal protein auxilin (*DNAJC6/PARK19*) and the phosphatase synaptojanin-1 (*SYNJ1/PARK20*) (Ramirez et al., 2006; Vilariño-Güell et al., 2011; Zimprich et al., 2011; Edvardson et al., 2012; Krebs et al., 2013; Quadri et al., 2013; Kalinderi et al., 2016; Cao et al., 2017; Deng et al., 2018).

PARK SYMBOL	GENE NAME	PROTEIN PRODUCT	MODE OF INHERITANCE	CLINICAL MANIFESTATION
PARK1	*SNCA*	α-syn	AD	Early onset PD
PARK2	*PRKN*	Parkin	AR	Early onset PD
PARK4	*SNCA*	α-syn	AD	Early onset PD
PARK6	*PINK1*	PINK1	AR	Early onset PD
PARK7	*DJ-1*	DJ-1	AR	Early onset PD
PARK8	*LRRK2*	LRRK2	AD	Late onset PD
PARK9	*ATP13A2*	ATP13A2	AR	Parkinsonism
PARK14	*PLA2G6*	PLA2G6	AR	Parkinsonism
PARK15	*FBXO7*	FBXO7	AR	Parkinsonism
PARK17	*VPS35*	VPS35	AD	Late onset PD
PARK19	*DNAJC6*	Auxilin	AR	Parkinsonism
PARK20	*SYNJ1*	Synaptojanin-1	AR	Parkinsonism
PARK22	*CHCHD2*	CHCHD2	AD	Late onset PD
PARK23	*VPS13C*	VPS13C	AR	Parkinsonism

Table 1. List of PD-related genes. The name of the gene and the respective protein product associated with each *PARK* locus are indicated. The mode of inheritance and the clinical manifestation consequent to variations in each of the causative genes are also reported (AD= autosomal dominant; AR= autosomal recessive).

Finally, *leucine-rich repeat kinase 2* (*LRRK2/PARK8*) might be considered a unifying element in the frame of PD, as mutant *LRRK2* represents the most common cause of familial PD cases, and it interacts at different levels with other *PARK* genes or with their protein products, e.g. α-syn, VPS35, ATP13A2, auxilin, synaptojanin-1 (Paisán-Ruiz et al., 2004; Zimprich et al., 2004; Henry et al., 2015; Islam et al., 2016; Inoshita et al., 2017; Mir et al., 2018; Nguyen and Krainc, 2018; Novello et al., 2018). A separate paragraph will be dedicated to a comprehensive discussion about LRRK2 and its relevance to PD.

Mutations in PD-causing genes are usually characterised by a high penetrance but a low frequency (Gasser, 2015). Therefore, in most cases, the

susceptibility to PD likely depends on a combination of risk factors rather than on the presence of single genetic variations. Figure 2 schematises the complex genetic architecture of PD. Coding mutations in *GBA* and *LRRK2*, with intermediate frequency in the population, were associated with an increased risk of developing PD (Sidransky et al., 2009; Gasser, 2015). Homozygous mutations in *GBA*, encoding the beta-glucocerebrosidase enzyme, cause a lysosomal storage disorder known as Gaucher's disease, while increasing the risk of developing PD at the same extent of heterozygous variants (Deng et al., 2018). Similarly, heterozygous mutations in *SPMD1* (encoding the sphingomyelin phosphodiesterase 1), where homozygous variations lead to Niemann-Pick disease, have been associated to PD-risk (Foo et al., 2013; Gan-Or et al., 2013; Schuchman and Desnick, 2017).
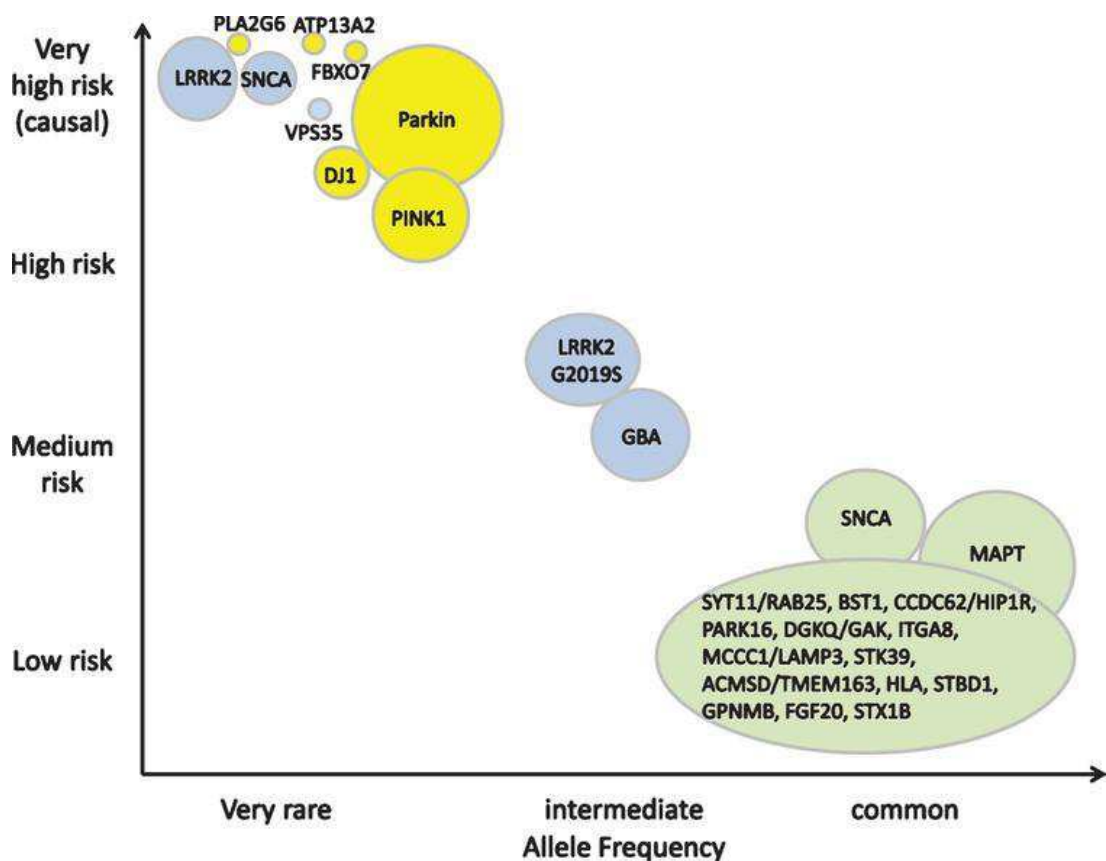
Figure 2. Genetic architecture of PD. The overall predisposition to PD is either dictated by the presence of very rare mutations in genes associated with Mendelian forms of the disease or defined by the presence of SNPs conferring moderate to low risk that contribute to the definition of susceptibility (Gasser, *Journal of Parkinson's Disease*, 2015).

In addition to these risk-increasing coding variants, the advent of genome-wide association studies (GWAS) has helped in the identification of around forty loci carrying common SNPs, mainly located in noncoding regions, that mildly increase PD risk (Figure 3) (Nalls et al., 2014; Gasser et al., 2015; Kalinderi et al., 2016; Singleton and Hardy, 2016; Chang et al., 2017; Deng et al., 2018).

Figure 3. Graphical representation of PD genes and loci. A) The human genome is depicted as a circle, with numbers indicating the chromosomes. The genes containing causative mutations are in blue; red indicates genes where coding SNPs associated with moderate risk have been identified; the loci identified by GWAS, containing low risk alleles, are indicated in black and named by proximal gene symbols (Singleton and Hardy, *Neuron*, 2016). B) Using an analogous scheme, the loci identified through the latest GWAS meta-analysis are depicted around a circular genome. Black and gray indicate previously identified loci, whereas the red labels refer to novel associations with PD. Gray lines spanning multiple genes indicate the presence of multiple candidate genes within the same locus (Chang et al., *Nature Genetics*, 2017).

Even considering the complete picture that has emerged to date regarding the genetics of PD, the estimates suggest that only one tenth of the heritable component has been unveiled (Keller et al., 2012; Singleton and Hardy, 2016). Thus, there is still a great burden of information residing in our DNA, which could

help in the detailed definition of those networks that are deregulated in disease and in the consequent design of more specific therapeutic approaches.

2.   *Leucine-rich repeat kinase 2 (PARK8)*

Among all the genetic contributors to the incidence of PD, *LRRK2* certainly occupies a relevant place in that it represents the single most common cause of disease (Paisán-Ruiz et al., 2013). *LRRK2* encodes a large, complex protein with dual GTPase and kinase activities, surrounded by multiple protein-protein and protein-lipid interaction domains, e.g. a WD40 domain in the C-terminal region (Figure 4) (Hatano et al., 2007; Piccoli et al., 2014; Vancraenenbroeck et al., 2014; Lystad and Simonsen, 2016). The presence of a Roc (Ras of complex proteins) GTPase and COR (C-terminal of Roc) bidomain allocates LRRK2 in the family of ROCO proteins (Tomkins et al., 2018). Given this complex architecture, LRRK2 very likely plays both signalling and scaffolding roles during signal transduction. LRRK2 is expressed in multiple tissues and organs during development and adulthood, with moderate to high expression in the brain, heart, lungs, kidneys and circulating immune cells (Biskup et al., 2007). Not surprisingly, considered the elevated levels and the proposed function in the immune response (Greggio et al., 2012; Härtlova et al., 2018), variations within the *LRRK2* locus have been associated with multibacillary leprosy and inflammatory bowel disease (IBD) (reviewed in Cogo et al., 2017). In addition, PD-patients carrying the G2019S mutation in LRRK2 were demonstrated to develop certain types of cancer with a higher frequency with respect to non-carriers (Agalliu et al., 2015). Within the brain, both neurons and glial cells express LRRK2, particularly in the *striatum*, which receives the dopaminergic projecting fibres from the *SNpc* (West et al., 2014).

We will now provide an overview of LRRK2 genetics, biochemistry and biology, and comment on the therapeutic potential of targeting LRRK2 in PD. Some aspects that are particularly relevant to the scope of this thesis will be discussed in greater detail in the following chapters.
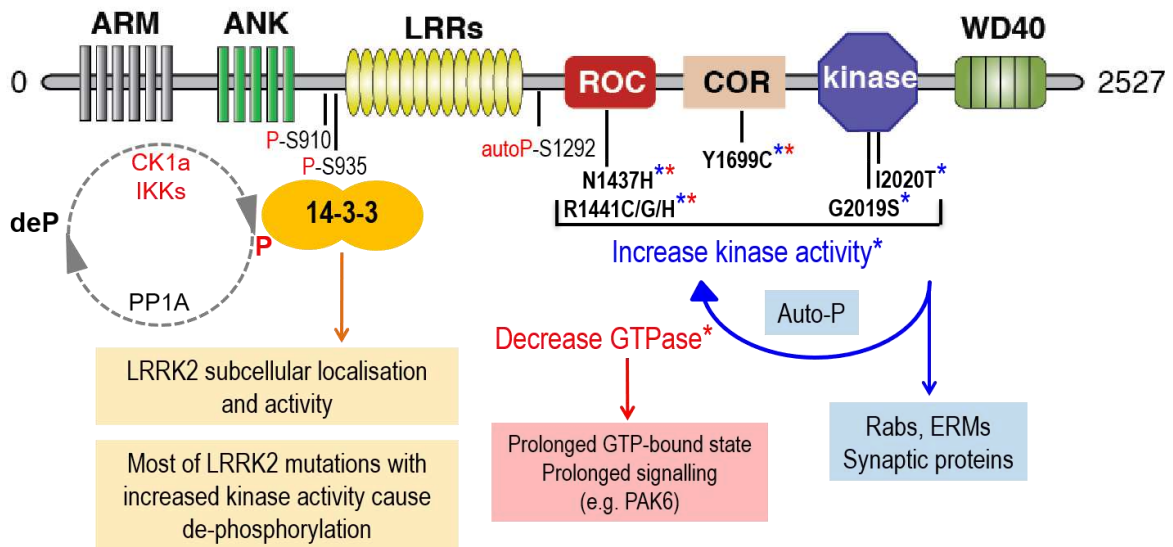
Figure 4. LRRK2 domain architecture and biochemistry. Schematic representation of LRRK2 with domain organisation and disease segregating mutations. The catalytic core is surrounded by interaction domains. The coloured asterisks refer to the alterations in the enzymatic activities and the consequent functional outcomes associated with the pathological mutations. The main autophosphorylation and phosphorylation sites, as well as the kinases and phosphatases mediating this event, are also indicated. Phosphorylation at Ser910/Ser935 induces the binding of 14-3-3 proteins. (Adapted from Cogo and Greggio, *The Neuroscience of Parkinson's Disease*, accepted for publication).

2.1 *LRRK2* genetics

The attention towards the *PARK8* locus arose for the first time in 2002 from the discovery by Funayama and collaborators of a large Japanese kindred affected by an autosomal dominant form of PD. The "Sagamihara family", named after the Japanese region of origin, was carrying changes in a novel PD locus, indeed termed *PARK8*, mapping on chromosome 12 (Funayama et al., 2002). Two years passed before the publication of two back-to-back studies identifying *LRRK2* as the candidate gene within that locus (Paisán-Ruiz et al., 2004; Zimprich et al., 2004), encoding the homonymous protein. LRRK2 is also named dardarin after the Basque term "*dardara*", meaning tremor, since one of the first families recognised to carry *PARK8* mutations was from Basque origins.

The heterogeneity that has previously been described within the totality of PD cases holds true also among individuals that carry mutations in the same gene. Indeed, this family displayed a wide clinical-pathological spectrum, ranging from typical PD to dementia and amyotrophy, pure nigral degeneration and a diffuse pathology composed by LBs, tau – whose accumulation is a hallmark of Alzheimer's disease – and ubiquitin-positive inclusions (Zimprich et al., 2004; Ballatore et al., 2007). Since this initial discovery, multiple aminoacid substitutions were proposed as disease-causing mutations. However, a clear segregation has been demonstrated for only seven of them, distributed within the catalytic tridomain of LRRK2, namely N1437H, R1441C, R1441G, R1441H, Y1699C, G2019S and I2020T (Figure 4) (Paisán-Ruiz et al., 2004; Zimprich et al., 2004; Goldwurm et al., 2005; Zabetian et al., 2005; Greggio and Cookson, 2009; Ross et al., 2009; Aasly et al., 2010). The most common mutation is the G2019S, found in 5% of familial cases and 2% of apparently idiopathic PD in Caucasian populations. However, these frequencies can raise up to 40% of familial cases and 13%-40% of sporadic cases in those ethnic groups where the degree of consanguinity is high, such as Ashkenazi Jewish and North African Berber Arab populations (Hernandez et al., 2016). Importantly, an individual carrying a mutation does not necessarily develop PD, as the penetrance is age-dependent, incomplete and variable according to the mutation. For example, in the case of the G2019S substitution, the penetrance varies between 25% and 42.5% at age 80, meaning that the probability of manifesting the disease for these subjects is relatively low compared to carriers of the R1441G mutation, whose penetrance reaches 95% in later life (Hernandez et al., 2016). Focusing on the risk factors, i.e. the coding variants within *LRRK2* that increase the predisposition to idiopathic PD, the R1628P and G2385R substitutions represent the most common susceptibility variants, increasing the risk of PD of about twofold (Farrer et al., 2007). Additional variants, associated with a lower increase in lifetime risk of PD (odd-ratio ~1.2), are represented by noncoding variants in the promoter region of *LRRK2*, that have been uncovered by GWAS (Simón-Sánchez et al., 2009). The latter mutations are likely to act by influencing the levels of expression, demonstrating the pleomorphic nature of *PARK8* as a risk locus (Singleton and Hardy, 2011; Singleton and Hardy,

2016), i.e. a genomic region harbouring variants that increase disease risk by different mechanisms (Roosen and Cookson, 2016).

2.2   LRRK2 biochemistry

The dual enzymatic activity of LRRK2 is a peculiarity possessed by only three proteins in the human proteome (Tomkins et al., 2018). As mentioned above, LRRK2 belongs to the family of ROCO proteins, characterised by the presence of a Roc-COR bidomain, where Roc exerts the enzymatic role by acting as a GTPase, while COR functions as a platform for dimerization (reviewed in Civiero et al., 2017a). The other enzymatic activity in the protein is a serine-threonine kinase, autophosphorylating at multiple sites and phosphorylating several cellular substrates. The most relevant, *bona fide* autophosphorylation site is Ser1292. Located at the junction between the LRR and Roc domains, Ser1292 is employed as a faithful indicator of LRRK2 kinase activity (Sheng et al., 2012). Since mutations in *LRRK2* segregate with PD, and the common G2019S substitution within the kinase domain increases kinase activity of ~2-3 fold (Greggio and Cookson, 2009), this activity has been extensively investigated and pursued as a promising therapeutic target. After more than ten years of research, an impressive number of interactors and substrates have been nominated for LRRK2. The list of LRRK2 interactors accounts approximately 450 proteins back in 2015 (Figure 5) (Manzoni et al., 2015), and it is growing daily. A possible and appealing explanation for these numbers is the so called "date-hub hypothesis" (Manzoni, 2017), according to which LRRK2 role might be extremely flexible depending on the macromolecular complexes it forms in different cell-types, developmental stages and under specific stimuli. This hypothesis is likely in that it takes into account the high degree of complexity of the protein, together with its differential expression across tissues.

The increase of *in vitro* kinase activity associated with the G2019S mutation probably depends on structural reasons. Indeed, the presence of a serine in the activation loop of the kinase domain was suggested to lock the kinase in a more active state (Jaleel et al., 2007; Greggio and Cookson, 2009). Instead, for several

years, no effect in terms of *in vitro* kinase activity towards a number of putative substrates was measured for the other pathogenic mutations in the kinase (I2020T), Roc (R1441C/G) and COR (Y1699C) domains (Greggio and Cookson, 2009). Surprisingly, the development of the first antibody against Ser1292 autophosphorylation revealed that, in addition to the G2019S, the majority of pathogenic mutants show an augmented activity as compared to the wild type (WT) when autophosphorylation is assessed in the cellular context (Sheng et al., 2012).
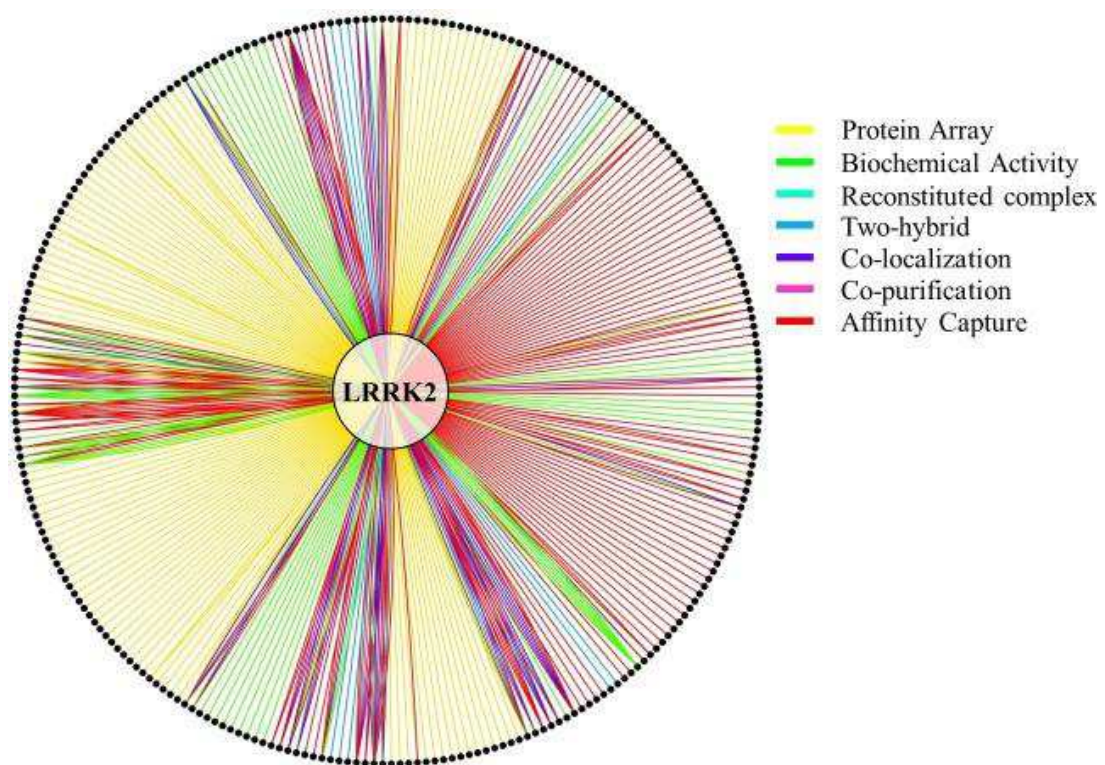
Figure 5. The complexity of LRRK2 interactome. Graphical representation of LRRK2 linked to its candidate interactors (depicted as black dots). Colours symbolise the different methods adopted to detect the interaction (Manzoni et al., *PeerJ*, 2015)**.**

Another turning point in LRRK2 research occurred in 2016, with the validation by Steger and collaborators of a subset of Rab GTPases as *bona fide* substrates of LRRK2 kinase activity (Steger et al., 2016). This work confirmed the 2-3 fold increased kinase activity of the G2019S, but also showed, in analogy to LRRK2 autophosphorylation on Ser1292, that the level of Rab8 and Rab10

phosphorylation in cells but not *in vitro* is greatly enhanced by the majority of LRRK2 pathogenic mutations. In addition to that, they showed that the impact of mutations located outside the kinase domain is even greater with respect to the G2019S (Steger et al., 2016). This pointed how *in vitro* assessment of enzymatic activity can provide limited information and needs to be interpreted with caution.

The presence of domains mediating protein-to-protein interactions in addition to the catalytic core suggests that LRRK2 may also play a scaffolding role during signal transduction. Although PD-segregating mutations sit in the catalytic core of the protein and affect either the kinase (G2019S and I2020T) or the GTPase (R1441C/G/H and Y1699C) activities (Figure 4), the presence of multiple scaffolding modules emphasises the importance of studying full-length LRRK2 within its physiological environment. Indeed, it is likely that different mutations result in different but converging gain-of-function mechanisms, with many of them requiring a more complex cellular machinery (co-factors, interactors, compartmentalisation) that cannot be mimicked *in vitro* with recombinant proteins. The gain-of-function mechanism proposed for PD-mutations is supported by the possibility to rescue the neurotoxic phenotype associated with mutant LRRK2 (G2019S, Y1699C and R1441C) by genetically inactivating the kinase activity through substitution of key catalytic residues (Greggio et al., 2006; Smith et al., 2006; Greggio and Cookson, 2009).

The other fundamental platform in the signalling towards downstream targets is represented by the Roc/GTPase domain. Although for many years LRRK2-Roc has received limited attention, in part due to technical challenges of measuring GTPase activity *in vitro*, early observations pointed how mutations in the Roc-COR domain lowered GTP hydrolysis (reviewed in Taymans, 2012). The consequence for this is a prolonged permanence in the GTP-bound state, and, in turn, a sustained signalling. Very recently, an elegant work from Wim Versées's group – conducted on a bacterial homolog of LRRK2, i.e. the Roco protein from *Chlorobium tepidum* – shed important light into the G-protein cycle of ROCO proteins, with possible implications for LRRK2 and PD-associated mutations. They showed that ROCO proteins cycle between a monomeric and a dimeric form depending on the nucleotide load. More specifically, ROCO proteins are dimers when in the nucleotide-free or GDP-bound forms, while switching into monomers

upon GTP-binding. The result is a monomer to dimer cycle during GTP hydrolysis (Deyaert et al., 2017a). Notably, due to the prohibitive molecular weight of LRRK2, the poor yields achieved from the purification of the full-length protein and the elevated conservation maintained within the ROCO protein family, multiple structural and functional studies have focused on bacterial or amoeboid homologs of LRRK2 (Gotthardt et al., 2008; van Egmond et al., 2008; Gilsbach et al., 2012; Kortholt et al., 2012; Rudi et al., 2015; Deyaert et al., 2017b). Meanwhile, the dimeric nature of LRRK2 has been extensively described in the literature before. It was indeed shown very early in 2008 (Greggio et al., 2008), and later on confirmed by electron microscopy (EM) (Civiero et al., 2012). Interestingly, in 2011, Daniëls and colleagues proposed that pathological mutations in the Roc-COR bidomain, namely R1441C/G and Y1699C, weaken dimerization and consequently lower LRRK2 GTPase activity (Daniëls et al., 2011). Another important milestone in the field of LRRK2 research dates back in 2016, when Guaitoli and collaborators generated the first model of dimeric LRRK2 based on cross-linking experiments and EM maps (Guaitoli et al., 2016). According to this model, LRRK2 dimerization occurs *via* the interaction of two Roc-COR domains and it is the dimeric state that renders LRRK2 an active serine-threonine kinase. Importantly, the tightly packed, homodimeric nature of LRRK2 has been further confirmed through Cryo-EM analysis (Sejwal et al., 2017). A further level of complexity is added by the observation that dimeric, active LRRK2 predominantly localises at membranes (Berger et al., 2010; reviewed in Civiero et al., 2017a).

The role of Roc as a signalling output is additionally supported by the notion that a large number of interactors map within this domain. Among them, the actin-cytoskeleton regulator p21-activated kinase 6 (PAK6), was shown to interact with GTP-loaded Roc (Beilina et al., 2014; Civiero et al., 2015; Civiero et al., 2017b), indicating that the binding of some cellular effectors is guanine nucleotide-dependent, similar to the canonical mechanism for small GTPases.

Finally, LRRK2 is a phospho-protein, able to autophosphorylate at multiple sites (Greggio et al., 2009; Kamikawaji et al., 2009; Gloeckner et al., 2010; Sheng et al., 2012) but at the same time finely tuned by heterologous phosphorylation. Importantly, casein kinase 1α (CK1α) and the IkB family of kinases phosphorylate a cluster of serines located at the N-terminus of LRRK2, including Ser910 and

Ser935 (Figure 4) (Chia et al., 2014). These sites are relevant for a handful of reasons: first, Ser910 and Ser935 are often exploited as an indirect indication of LRRK2 kinase inhibition. Indeed, although not being autophosphorylation sites, these residues become dephosphorylated as a consequence of LRRK2 kinase inhibition (Dzamko et al., 2010; Deng et al., 2011; Zhao et al., 2012), probably mediated by an indirect, feedback effect on a kinase or a phosphatase regulated by LRRK2-dependent phosphorylation. Monitoring the phospho-state of Ser910 and Ser935 as a readout of LRRK2 activation state has proven a particularly useful tool, especially given the technical challenges in the detection of phospho-Ser1292, related to the low tone of autophosphorylation at Ser1292 in combination with the poor sensitivity of the antibodies against this site. Second, phosphorylation at Ser910 and Ser935 triggers the binding of 14-3-3 proteins, which is important to regulate the subcellular localisation of LRRK2, its kinase activity and substrates/interactors availability (Nichols et al., 2010). Phosphorylation is counter-regulated by phosphatases, the most validated one being PP1 (Figure 4) (Lobbestael et al., 2013).

2.3 LRRK2 pathobiology

In terms of function, LRRK2 has been linked to multiple cellular processes, including autophagy, endo-lysosomal pathways, cytoskeletal dynamics, synaptic vesicle trafficking and inflammation (Figure 6), although the detailed molecular mechanisms have not been fully uncovered yet.

Given the role of LRRK2 in multiple human diseases, invertebrate and rodent models have been generated over the past decade to gain a better understanding of LRRK2-mediated pathways and processes. Murine models remain the gold standard for the *in vivo* modelling of most human diseases, due to the striking sequence similarity between human and mouse genomes – about 85% of identity in coding regions – (Batzoglou et al., 2000). However, the pattern of expression throughout the brain, as well as the biochemical properties of murine and human LRRK2 were shown to display substantial differences, possibly ascribable to the less conserved regions of the protein (West et al., 2014;

Langston et al., 2018). These differences need to be taken into account especially when testing compounds for therapeutic purposes. Initially, Lrrk2 knockout (KO) mice were developed in order to investigate the physiological roles of LRRK2 in neurons and non-neuronal cells. Indeed, although pathogenic mutations in LRRK2 lead to a gain of function in the protein product (Blauwendraat et al., 2018), these models gave pivotal hints about the biology of murine Lrrk2. In particular, they informed that the loss of Lrrk2 impacts on autophagy in peripheral organs (Herzig et al., 2011; Tong et al., 2012), a phenotype that turned useful to evaluate the safety issues related to Lrrk2 kinase inhibition.
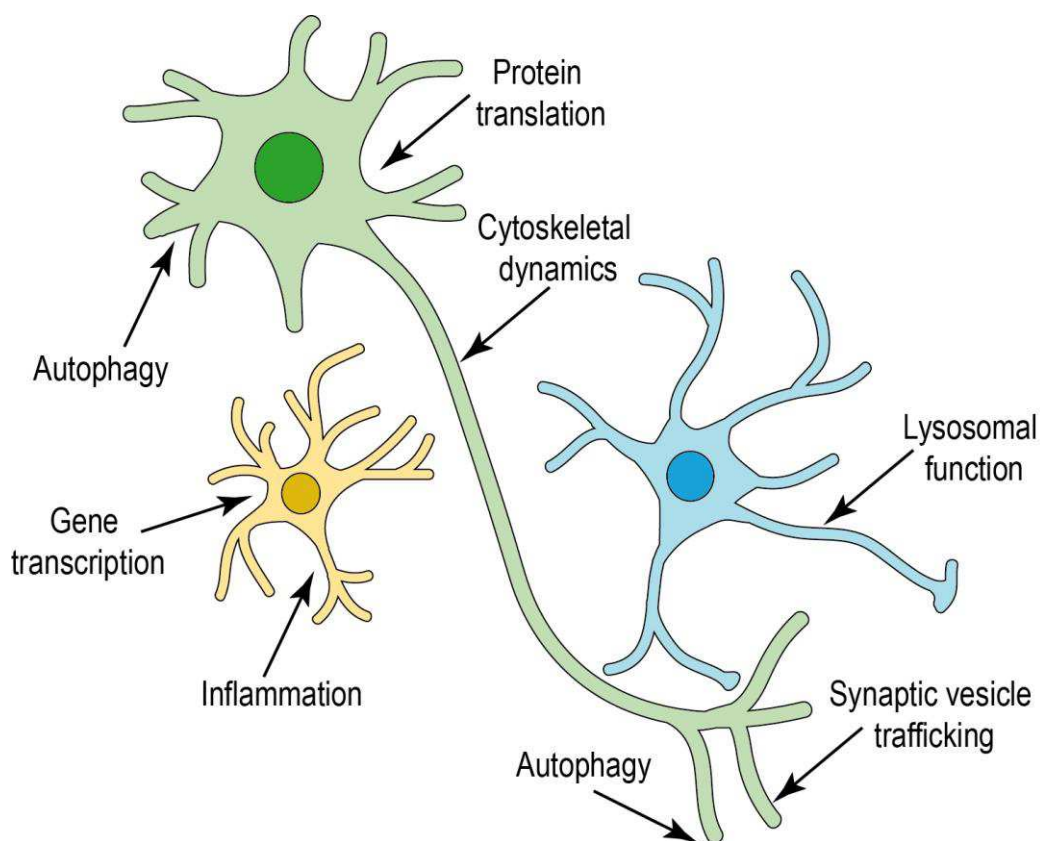
Figure 6. Proposed functions of LRRK2 in different brain cells. LRRK2 was associated with multiple processes in brain cells, in support of the statement that PD is not exclusively a neuronal pathology (Cogo and Greggio, *The Neuroscience of Parkinson's Disease*, accepted for publication).

Disappointingly, the transgenic mice expressing mutant Lrrk2 or over-expressing mutant forms of the human protein do not display obvious PD-related

phenotypes, such as loss of dopaminergic neurons, accumulation of α-syn in LBs or motor deficits, but only mild defects in DA neurotransmission, which might be interpreted as preclinical symptoms of PD (reviewed in Volta and Melrose, 2017; Xiong et al., 2017). One of the main issues associated with the modelling of age-related pathologies is that animal models do not develop neurodegenerative phenotypes due to a relatively short lifespan as compared to humans. Nevertheless, animal models represent powerful tools in the reconstruction of the pathways that are physiologically relevant and potentially deregulated during pathology. In addition to the mouse, *Drosophila melanogaster* and *Caenorhabditis elegans* have been exploited to model LRRK2 biology. Both organisms possess only one LRRK-like protein, namely dLRRK and Lrk-1, respectively. Also in this case, KO models turned useful in understanding the molecular pathways where LRRK2 homologs – and potentially LRRK2 itself – are involved but, more interestingly, the overexpression of endogenous or human LRRK2 in the fly or in the worm was very often associated with a clear PD phenotype. On the other hand, zebrafish LRRK2 models (zLRRK2) are to date underdeveloped and poorly characterised (reviewed in Xiong et al., 2017).

We will now emphasise those LRRK2-mediated pathways that might be particularly relevant for PD, and give a brief overview about the role exerted by LRRK2 at the synapse through a strict interplay with cytoskeletal components, and in regulating the inflammatory response, protein translation and the autophagy-lysosomal pathway. Additional sections within the following chapters will be dedicated to an extensive discussion of LRRK2 contribution in the regulation of autophagy and cytoskeletal dynamics, and the possible link between the two pathways.

2.3.1 LRRK2 at the synapse

Neurons require a highly specialised machinery to maintain an efficient vesicle traffic, given that the distance between the cell body and the dendrites or axons can be extremely long if compared to the typical distances covered within the compartments of non-neuronal cells. This machinery is represented by the vesicles, together with the cytoskeletal elements providing the physical tracks to

move across the cellular compartments. In this frame, the actin cytoskeleton plays an essential role in shaping pre- and postsynaptic elements, controlling the traffic of neurotransmitter-containing SVs at the presynapse and receptor-containing endosomes at the postsynapse, to mediate synaptic plasticity (i.e. long-term potentiation and depression) (Cingolani and Goda, 2008). While the role of LRRK2 in shaping neuronal processes will be discussed later, we will now focus on underlining the contribution of the actin cytoskeleton in supporting the exo-endocytic machinery.

The importance of LRRK2 in orchestrating cellular traffic was reinforced after the validation of Rab GTPases as substrates of LRRK2 kinase activity (Steger et al., 2016; Lis et al., 2018; Liu et al., 2018; Madero-Pérez et al., 2018; Purlyte et al., 2018). Multiple lines of evidence suggest a role for LRRK2 at the synapse. In this context, LRRK2 could either exert its scaffolding role, acting as a bridge between vesicles and the cytoskeleton that permits the assembly of local signalling, and/or influence the activity of the synaptic machinery *via* phosphorylation of substrates in the different compartments. Recently, LRRK2 was shown to interact both physically and functionally with vesicles and actin at the presynapse (Parisiadou and Cai, 2010; Cirnaru et al., 2014). The binding between LRRK2 and SVs is mediated by the interaction with actin and a number of presynaptic proteins including Endophilin A (Matta et al., 2012), synapsin I (Cirnaru et al., 2014), Rab5a (Yun et al., 2015), N-ethylmaleimide sensitive fusion (NSF) protein (Belluzzi et al., 2016), auxilin (Nguyen and Krainc, 2018) and the microtubule (MT)-binding protein Futsch (Lee et al., 2010). These studies demonstrated how the rate of SV cycling and fusion (Matta et al., 2012; Cirnaru et al., 2014; Yun et al., 2015; Belluzzi et al., 2016; Nguyen and Krainc, 2018), the release of neurotransmitter (Cirnaru et al., 2014), and the development of synapses (Lee et al., 2010) are influenced by the kinase activity of LRRK2 or its homologs. Therefore, LRRK2 phosphorylates presynaptic components, consequently modulating the exo-endocytic machinery, and the presence of mutant LRRK2 very likely affects the process. In support of this notion, defects in the trafficking of DA receptor were observed in striatal neurons in presence of G2019S-Lrrk2 (Rassu et al., 2017), which could depend on deregulated actin dynamics. Interestingly, a work from Cai's group in which they performed a

comprehensive characterisation of the dendritic morphology in developing spiny projecting neurons (SPNs), revealed substantial alterations that are also suggestive of impaired actin mobilisation. They indeed found a significant decrease in dendritic spines and increase in dendritic filopodia in Lrrk2-KO brains as compared to the WT littermates, with morphological alterations in the spines and hyperphosphorylated cofilin – a protein that is part of the cascade ultimately leading to actin polymerisation (Ostrowska and Moraczewska, 2017) – within the first postnatal days (Parisiadou et al., 2014). Accordingly, a complementary study in G2019S-Lrrk2 SPNs demonstrated that these neurons possess larger spines, accompanied by an augmented postsynaptic activity, during development (Matikainen-Ankney et al., 2016). Phenotypically, the G2019S knockin (KI) mouse exhibits hyperactivity at young ages. This is paralleled by an increased release of glutamate and DA in the *striatum*, that however declines with age (Longo et al., 2014; Volta et al., 2017). It is important to underline how pre-symptomatic LRRK2 mutation carriers similarly exhibit augmented DA turnover in comparison to manifest idiopathic PD patients (Sossi et al., 2010), suggesting the G2019S KI mouse might represent a valuable pre-symptomatic model to investigate early pathogenic mechanisms of PD.

2.3.2 LRRK2 in the regulation of inflammation and protein translation

The role of LRRK2 in the immune system was first shown in 2010, when Gardet and co-authors demonstrated that LRRK2 expression is particularly elevated in human immune cells and can additionally be induced by IFN-γ stimulation in intestinal tissues upon Crohn's Disease inflammation (Gardet et al., 2010). The high expression of LRRK2 both in circulating and tissue immune cells, together with its upregulation after the recognition of microbial patterns, were later confirmed by multiple studies (Hakimi et al., 2011; Cook et al., 2017). In parallel to this, genetic evidence further reinforced the link between LRRK2 and inflammation, with different GWAS indicating that common variants in the *LRRK2* locus increase the risk of developing IBD (Franke et al., 2010) and leprosy (Zhang et al., 2009).

In the brain, the resident macrophages acting as the first line of defence of

the innate immune system are represented by microglia. After the association of LRRK2 with PD, several studies focused on the understanding of the role mediated by LRRK2 in this particular cell population. The early studies were mainly conducted in primary microglia from mouse brain and suggested that Lrrk2 deficiency attenuates inflammatory response (Moehle et al., 2012) through a mechanism involving cAMP/protein kinase A (PKA) signalling (Russo et al., 2015; Greggio et al., 2017). More recent studies performed on resident microglia failed to detect Lrrk2 (Kozina et al., 2018). These findings might imply that the nigral neuronal loss observed in mice systematically injected with lipopolysaccharide (LPS) – and exacerbated by the presence of mutant LRRK2 – may be triggered by peripheral circulating inflammatory molecules or infiltrated T cells and/or monocytes rather than by dysfunctional microglia (Kozina et al., 2018).

Of interest, a few studies interrogated the existence of a link between LRRK2 and α-syn aggregation. Multiple experiments showed that LRRK2 KO can modulate aggregation, whereas the G2019S mutation can fuel it, leading to a phenotype that is reverted by kinase inhibition (Volpicelli-Daley et al., 2016; Schapansky et al., 2018; reviewed in Lewis, 2018). In this regard, a couple of studies suggested the contribution of a strong microglial component in the process (Schapansky et al., 2015; Maekawa et al., 2016).

In myeloid cells, LRRK2 was found to regulate phagocytosis, through a process involving the modulation of actin cytoskeleton (Parisiadou and Cai, 2010), *via* interaction with and phosphorylation of the regulatory protein WAVE2 (Kim et al., 2018). Recent data from Max Gutierrez's lab demonstrate a role for LRRK2 in inhibiting *Mycobacterium tuberculosis* phagosome maturation in macrophages *via* the class III PI3K/Rubicon complex, further supporting the notion that LRRK2 is a key checkpoint in the cellular control of microorganism infection (Härtlova et al., 2018).

A few works investigated the impact of LRRK2 on transcriptional regulation and it is interesting to point the close correlation with its role in mediating the inflammatory response. Once again, Lrrk2 knockdown (KD) proved fundamental in modelling the physiological roles of the protein. Indeed, several studies reported a reduction in NF-kB transcriptional activity and a consequent decrease in the release of signalling cytokines after Lrrk2 KD (Gardet et al., 2010; Kim et al., 2012;

Russo et al., 2015; Wandu et al., 2015), as well as a decrease in the nuclear translocation of the transcription factor NFAT (Liu et al., 2011). Later on, the reduced responsivity of cells lacking Lrrk2 has been correlated with an increase in the expression of CX3CR1, a receptor known to promote migration of microglial cells while suppressing their inflammatory activity (Ma et al., 2016).

At the very beginning of the investigation of LRRK2 role in protein synthesis, the fruit fly *Drosophila melanogaster* represented a valuable model. Loss of function models lacking the fly homolog dLRRK display a reduction in phosphorylation and an increase in activation of 4E-BP1, a key negative regulator of protein translation. The opposite observation was made in presence of pathological mutations, that were therefore suggested to induce an abnormal activation of specific synthesis pathways (Imai et al., 2008; Tain et al., 2009).

Along the same lines, the ribosomal protein s15 was recently recognised as a substrate of LRRK2/dLRRK kinase activity in human neurons and Drosophila. The functional consequence of phosphorylation by LRRK2/dLRRK is an increase in protein synthesis, that was augmented in presence of PD-mutations (Martin et al., 2014a). Interestingly, the treatment with the cap-dependent translation inhibitor 4EGI-1 is able to rescue this phenotype (Martin et al., 2014b).

Back in 2012, G2019S-Lrrk2 was proposed to promote transcription after a genome-wide characterisation of mRNA expression in KO and G2019S-Lrrk2 mouse models (Nikonova et al., 2012), even though the data regarding this putative function are conflicting (Devine et al., 2011). Finally, pathogenic LRRK2 was also shown to modulate translation *via* interference with microRNA-mediated translational repression (Gehrke et al., 2010).

Taking all of these data into consideration, we can identify two major sets of functions: one, suggestive of a more generalised action of LRRK2 on the transcriptional/translational machinery, and a second, more restricted, directed towards NF-kB and its downstream targets. The fact that the diseases associated with mutations/variants in LRRK2 – PD, multibacillary leprosy and IBD (Cogo et al., 2017) – are characterised by a very strong immune component, does not therefore seem accidental.

2.3.3 The role of LRRK2 in the autophagy-lysosomal pathway

LRRK2 was firstly reported to play a role in macroautophagy (hereafter referred to as autophagy) back in 2008, when Plowey and co-authors reported this pathway to be involved in the neurite shortening associated to G2019S-LRRK2 pathological mutation in differentiated SH-SY5Y cells (Plowey et al., 2008).

After the first report supporting a role for LRRK2 in the autophagic process, multiple studies followed, aiming at unravelling the molecular details of this regulation. The findings by Plowey et al. were indeed later confirmed both in primary midbrain cultures from mice overexpressing human G2019S-LRRK2 and in iPSCs derived from idiopathic and LRRK2-PD patients. Both models displayed reduced neurite complexity accompanied by autophagic abnormalities in the aged brain (Ramonet et al., 2011; Sánchez-Danés et al., 2012). In parallel, knocking down LRRK2 in human stable cell lines was shown to increase the autophagic flux (Alegre-Abarrategui et al., 2009). The great number of studies that followed returned controversial information about the direction in which LRRK2 is regulating autophagy. For example, kidneys derived from KO mice showed an age-dependent, bi-phasic alteration of degradative pathways, including autophagy (Tong et al., 2010; Tong et al., 2012). By looking at the ratio LC3-I/LC3-II and at the levels of p62 – two validated markers for autophagosome formation and degradation, respectively (Tanida et al., 2008; Bjørkøy et al., 2009) –, as well as at α-syn accumulation, the authors highlighted an initial increase in autophagic activity, correlating with a higher clearance of α-syn at young ages, and a following decrease in autophagy with α-syn and lysosomal protein accumulation at 20-months (Tong et al., 2012). To further complicate the picture, Herzig and collaborators characterised in parallel a different KO model displaying lysosomal accumulation in kidneys and lungs without alterations in the autophagosomal marker LC3 at early stages (Herzig et al., 2011). More recently, Jie Shen's lab generated a double KO mouse model lacking both Lrrk1 and Lrrk2. Interestingly, the animal developed an age-dependent degeneration of dopaminergic neurons, with accumulation of autophagic vacuoles (Giaime et al., 2017), suggestive of an at least partial compensation between the two homologs. When looking at the hyperactive forms of Lrrk2, introduction of the G2019S mutation in the

endogenous murine gene did not lead to obvious histopathological changes (Herzig et al., 2011). Mechanistically, LRRK2 overexpression was initially proposed to promote the autophagic flux by activating a Ca^{2+}-dependent protein kinase kinase-β (CaMKK-β)/ adenosine monophosphate (AMP)-activated protein kinase (AMPK) pathway, involving NAADP receptors (such as two pore channel 2, TPC2), with a concomitant alkalinisation of lysosomal pH (Gómez-Suaga et al., 2012). A subsequent work demonstrated how the inhibition of TPC2 could rescue the alterations of lysosomal morphology in G2019S-LRRK2 patient fibroblasts (Hockey et al., 2015). In agreement with these findings, a similar phenotype was observed in primary astrocytes from transgenic mice overexpressing G2019S-Lrrk2. These cells display enlarged lysosomes with impaired activity and upregulation of ATP13A2, which could be rescued by inhibiting Lrrk2 kinase activity (Henry et al., 2015).

Given the importance of LRRK2 kinase activity in mediating toxicity (Greggio et al., 2006; Smith et al., 2006), multiple studies, conducted in different cell lines, investigated the effects of kinase inhibition on the autophagic pathway, often returning apparently opposite outcomes. The literature indeed reports that i) on one hand, the lack of kinase activity induces autophagy through an mTOR (mammalian target of rapamycin)-independent, Beclin-1-dependent pathway while ii) on the other side, the increase in autophagosomal markers observed after LRRK2 inhibition is suggested to be partly related to an impaired fusion with the lysosome (Manzoni et al., 2013a; Saez-Atienzar et al., 2014; Manzoni et al., 2016). Surprisingly, the removal – usually *via* KD – of LRRK2 kinase activity or its increase – achieved in most cases through expression of the G2019S form – led in some studies to the same phenotype. This statement is exemplified by a work in immune cells where LRRK2 silencing led to defective induction of autophagy and impaired degradation of substrates (Schapansky et al., 2014), paralleled by a study reporting similar findings after G2019S-LRRK2 overexpression in concomitance with proteasomal inhibition (Bang et al., 2016). Similarly, analysis of patient-derived fibroblasts bearing LRRK2 mutations highlighted i) an increased basal autophagy in presence of the G2019S substitution (Bravo-San Pedro et al., 2013), and, conversely, ii) deficits in the ability to respond to starvation and/or mTOR inactivation (Manzoni et al., 2013b). At the beginning of the year, a very

interesting work by Jeremy Nichol's lab revealed that p62 is an interactor and a substrate of LRRK2 kinase activity, and that p62 phosphorylation leads to increased neurotoxicity (Kalogeropulou et al., 2018). This work confirmed an interaction that had already been observed back in 2016 (Park et al., 2016). In addition, LRRK2 was demonstrated to exert an inhibitory function on the more selective chaperone-mediated autophagy (CMA), with an increase in the levels of LAMP2A as a response (Orenstein et al., 2013).

In parallel to these studies conducted in cellular systems and mouse models, a substantial branch of the literature describes a connection between autophagy and LRRK2 in non-mammalian animal models such as *Caenorhabditis elegans* and, once more, *Drosophila melanogaster*. Interestingly, both organisms support a role for LRRK2 in autophagy. Expressing mutant human LRRK2 in the worm exerts an inhibitory action on autophagy, that potentiates the physiological, age-dependent impairment of the autophagic flux (Ferree et al., 2012; Saha et al., 2015). The fruit fly permitted to uncover a specific branch of autophagy happening at the synapse, highly dependent on the LRRK2/dLRRK substrate EndophilinA, that mediates the curvature of the autophagosomal membrane (Soukup et al., 2016; Soukup and Verstreken, 2017). Of interest, dLRRK loss of function (upon the introduction of missense mutations in the protein) fully recapitulates the phenotype observed in mouse models, i.e. a global impairment of the endo-lysosomal system, with accumulation of autophagosomes and enlarged lysosomes unable to degrade their content, as well as early endosomes filled with mono-ubiquitylated cargo proteins. Notably, the lysosomal abnormalities correlated to the lack of dLRRK can be compensated by the overexpression of a constitutively active form of the small GTPase Rab9, which promotes retromer-dependent recycling from late endosomes to the Golgi (Dodson et al., 2014). This evidence supports the relevance of Rabs as substrates of LRRK2 kinase activity, and the potential impact of a general deregulation in vesicle trafficking on cell homeostasis. A simplified schematic of the putative roles of LRRK2 in the autophagy-lysosomal pathway is depicted in Figure 7.
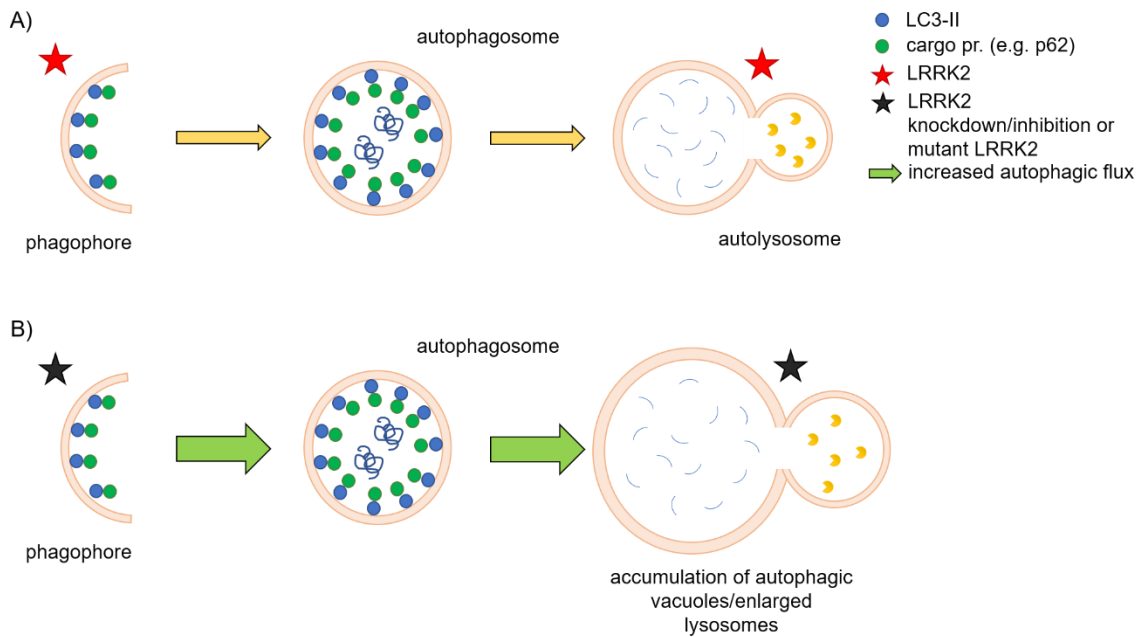
Figure 7. Putative roles of LRRK2 in the autophagy-lysosomal pathway. (A) LRRK2 likely regulates autophagy at multiple levels. (B) Removal of LRRK2, its kinase activity or expression of mutant forms of the protein result in an increase in the autophagic flux together with an accumulation of enlarged lysosomes (Cogo and Greggio, *The Neuroscience of Parkinson's Disease*, accepted for publication).

2.4 LRRK2 as a therapeutic target

The "druggable" nature of LRRK2 as a kinase attracted much attention as a candidate therapeutic target for PD in the last fifteen years. In addition, autophosphorylation at Ser1292 and phosphorylation of specific Rabs are currently being evaluated as biomarkers to test the efficacy of inhibition (Wang et al., 2017a; Lis et al., 2018). Based on the well-established association between LRRK2 kinase activity and cellular toxicity (Greggio et al., 2006; Smith et al., 2006), and the increased phosphorylation of substrates displayed by pathogenic LRRK2 (Steger et al., 2016), multiple drug discovery programs targeting LRRK2 are currently active. This intense work led to the generation of more than 100 inhibitors, some of which are highly potent and selective, as reviewed in Taymans

and Greggio, 2016. The greatest progress in this regard comes from the DNL201 molecule developed by Denali Therapeutics, that very recently entered and successfully passed a phase I clinical trial in a randomised study performed in healthy volunteers (http://investors.denalitherapeutics.com/news-releases/news-release-details/denali-therapeutics-announces-positive-clinical-results-lrrk2#ir-pages). This result is extremely promising in the perspective of additional trials with patient versus control cohorts. However, studies performed in non-human primates highlighted potential safety issues associated with the abundance of LRRK2 in peripheral organs, lungs *in primis* (Fuji et al., 2015). Fortunately, the on-target side effects associated with LRRK2 kinase inhibition outside the central nervous system (CNS) are reversible.

Given the dual enzymatic activity of LRRK2, an alternative route, equally attractive but less explored due to the difficulties in generating highly selective compounds, is the design of inhibitors targeting the GTPase activity of LRRK2 (Li et al., 2015). To this respect, acting on the modulation of specific interactions that are deregulated in disease conditions might represent a more finely tuned strategy to reduce the probability of undesired side effects.

The past fifteen years of research have undoubtedly led to enormous progress in the understanding of LRRK2 physiopathology. On the other hand, several aspects are still debated in the community, likely reflecting the complexity of the protein, its still unclear splicing pattern and its genomic and/or proteomic interactions, that are very likely tissue specific. These factors, in combination with environmental stresses and a certain lifestyle, are probably key to drive the process that ultimately leads to the onset of PD. As a general consideration, understanding the shared pathways between LRRK2 and idiopathic PD cases will give important insight on the translatability of genetic models, with remarkable implications in terms of prevention and/or patient management.

.

Chapter 2

Aim of the project

3. The central role of Roc in LRRK2 physiopathology

The contribution of the Roc domain to PD pathogenesis is supported by the fact that several mutations map within this domain (i.e. N1437H and R1441C/G/H). In addition to mutations that clearly segregate with PD, further substitutions were proposed during the years to be disease-associated. One example is the R1441S variation, that confirms the nature of Arg1441 as a mutational hotspot (Mata et al., 2016). In addition to them, the Roc domain also contains mutations that have been identified only in individuals but not in families, namely the I1371V substitution, as well as protective variants, such as the R1398H (Giordana et al., 2007; Nixon-Abell et al., 2016).

The presence of a phosphate-binding, P-loop motif between aminoacids 1341 and 1348 enables LRRK2 to bind guanine nucleotides – GTP and GDP – with similar affinity in the μM range, and LRRK2 possesses a GTPase activity that can be measured *in vitro*. As previously mentioned, pathological mutations tend to decrease the rate of GTP hydrolysis, and this is in some cases accompanied by an increase in GTP binding (reviewed in Nguyen and Moore, 2017). Importantly, while mutations in the Roc do not affect kinase activity *in vitro*, with the only exception of N1437H (Aasly et al., 2010), they behave quite differently in cells, where they increase phosphorylation of substrates to a greater extent as compared to mutations in the kinase domain (Steger et al., 2016). This evidence might support the idea that the GTPase activity of the Roc domain regulates LRRK2 kinase activity. As a proof of concept, the removal of key residues in the P-loop region of Roc – *via* introduction of the hypothesis-testing K1347A or T1348N mutations – was demonstrated to have a deleterious effect on both GTP binding and kinase activity (Biosa et al., 2013), indicating that possibly GTP-binding capacity is the actual requirement for LRRK2 kinase activity (Taymans et al., 2011). In the past, LRRK2 has been classified as an unconventional GTPase. Nevertheless, there is some evidence supporting its interaction with classical regulatory proteins for small GTPases, namely ARFGAP1 and ARHGEF7 (Haebig et al., 2010; Xiong et al., 2012). An alternative model that was proposed is that of LRRK2 acting as a G-protein activated by nucleotide-dependent dimerization

(GAD), on the basis of the structure of bacterial ROCO proteins (Gotthardt et al., 2008), even though also this hypothesis has some limitations. For example, isolated, monomeric Roc maintains GTPase activity (Liao et al., 2014). Further investigation is therefore required to gain better understanding about the regulation of LRRK2 GTPase cycle.

If it is true, on one side, that the Roc/GTPase domain can impact on the modulation of kinase activity, plenty of literature sustains a cross-regulation between the two catalytic cores of the protein. The kinase domain, indeed, autophosphorylates Roc at multiple sites, including T1343, T1348, S1403, T1404, T1410, T1491, and T1503 (West et al., 2007; Greggio et al., 2008; Gloeckner et al., 2010). The exact effect of each autophosphorylation event on LRRK2 GTPase activity is not clear yet. A recent study performed with isolated Roc suggests that autophosphorylation enhances GTP hydrolysis and promotes dimerization (Liu et al., 2016). In addition, GTPase activity could be modulated by heterologous phosphorylation. PKA, for example, phosphorylates S1444, creating a docking site for 14-3-3 proteins whose binding leads to a decrease in kinase activity. Importantly, phosphorylation on this residue is impaired by the presence of PD-mutations on R1441 (Muda et al., 2014).

From a functional point of view, GTP binding and GTPase activity were associated to induced neuronal toxicity (West et al., 2007). Another key feature of Roc is that it likely acts as a "molecular hub" in the initiation of signalling cascades, based on the large number of interactors binding to this domain (Gandhi et al., 2008; Cho et al., 2014; Law et al., 2014; Parisiadou et al., 2014; Civiero et al., 2015; Schreij et al., 2015; Athanasopoulos et al., 2016 are some examples), that is also important in the process of dimerization (reviewed in Civiero et al., 2017a).

Based on all these properties, the GTPase domain of LRRK2 appears an exceptionally good candidate for therapeutic targeting, with the implication that a clearer picture of the complex intramolecular regulation of enzymatic activities and scaffolding regions, and the way in which Roc contributes to LRRK2-linked phenotypes is required. This could potentially offer an alternative approach to kinase inhibition, in those cases where the treatment is not well tolerated or not beneficial. Despite the fact that the pharmacological targeting of GTPases is

certainly challenging because of the low selectivity of compounds, there are some reports of molecules with positive effects on LRRK2 toxicity (Li et al., 2015). However, the modulation of specific interactions that are deregulated in disease conditions seems a more finely tuned strategy to reduce the probability of undesired side effects. In a review paper published in 2015, Cromm and co-authors discuss a multiplicity of alternative routes for the targeting of small GTPases (Figure 8) (Cromm et al., 2015). Keeping in mind that LRRK2 is not small and demonstrates divergence from the canonical behavior of the small GTPases, the advances in terms of drug discovery that come from the field of small GTPases might be, at least partially, translated to LRRK2.
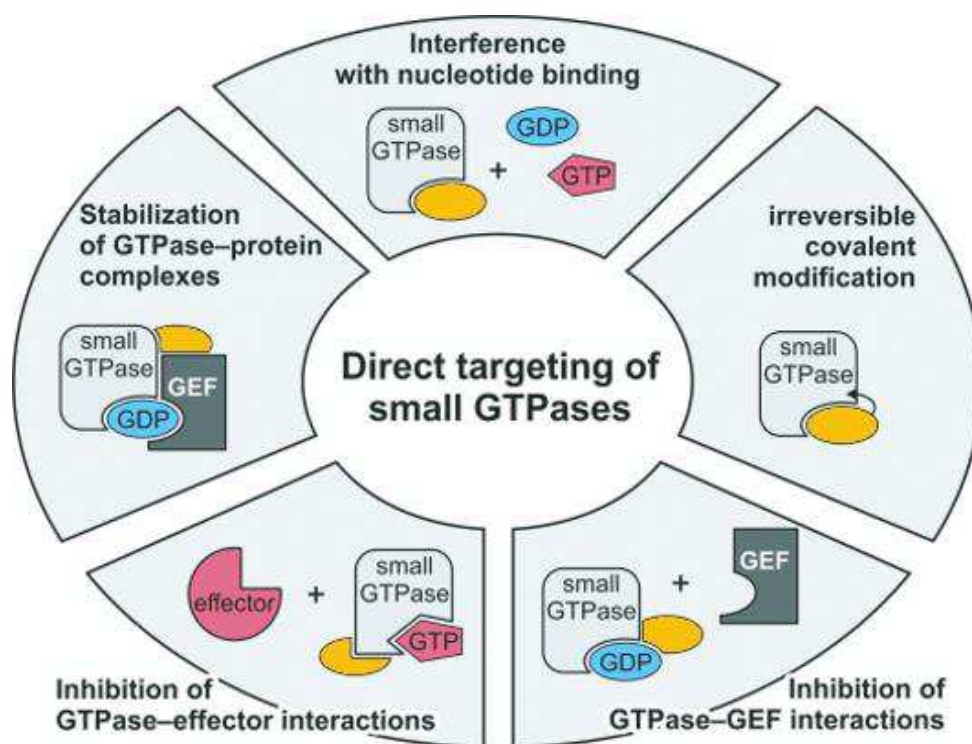
Figure 8. Strategies for targeting small GTPases. In addition to the interference with nucleotide binding, multiple therapeutic routes could be undertaken to target GTPases, such as post-translational covalent modification and/or intervention on the interaction with binding partners, e.g. effectors or regulators (Cromm et al., *Angewandte Chemie International Edition*, 2015).

4. Aim of the project

In this frame, this PhD project has focused on the understanding of how LRRK2-Roc domain influences the properties of the entire protein, from different perspectives and through several approaches.

First, this thesis will discuss the consequences of genetically depleting LRRK2 nucleotide binding capacity at the endogenous level. We indeed performed a characterisation of isogenic, genetically engineered RAW264.7 WT, Lrrk2-KO and T1348N-Lrrk2 cell lines. These lines – murine blood macrophages – have been generated by the Michael J. Fox Foundation (MJFF) in collaboration with ATCC. Given the abundance of Lrrk2 expression in this cellular system, we had the opportunity to analyse for the first time the effects of the lack of endogenous GTPase activity. This system constitutes a useful tool to gain insight regarding the signalling outputs of this complex protein. In particular, we will comment on how the lack in GTP-binding affects Lrrk2 steady-state levels and describe some functional data obtained by evaluating autophagy in these cell lines.

The second part of the thesis will be dedicated to the role of Roc as a signalling output. In this regard, we aimed at further characterising the previously established interaction between LRRK2-Roc and the actin-cytoskeleton regulator PAK6, which might potentially be relevant in the pathogenesis of PD (Civiero et al., 2015; Civiero et al., 2017b). We will provide some data describing the impact of LRRK2 pathological mutations and PAK6 variants in the formation of the complex. Also, we will give an overview of preliminary data obtained from the investigation of a potential role for the LRRK2-PAK6 complex in the autophagic pathway.

Given the limited attention that LRRK2-Roc has received in the past fifteen years as compared to the kinase domain (Nguyen and Moore, 2017), there is still some dearth of knowledge about the intra- and intermolecular signalling mechanisms of LRRK2. Moreover, the challenges associated with the study of a large and relatively slow GTPase significantly delayed any progress in this regard. This is the reason why we believe such a complex and fundamental question needs to be addressed from multiple points of view.

Chapter 3
Materials and Methods

5.   Materials and Methods

5.1   Constructs and chemicals

3xFlag-PAK6 WT was previously cloned (Civiero et al., 2015), and the S236L variant was generated using the Quick-Change II site-directed mutagenesis kit (Stratagene). GFP-LRRK2 WT and mutants cloned in pDEST53 (Life Technologies) were previously described (Greggio et al., 2006). 2xmyc-GFP cloned into a pCMV-2xmyc vector adapted from a pCMV-tag-3B (Stratagene, La Jolla, CA, USA) as previously described (Greggio et al., 2007) and 3xFlag-GFP were used as negative controls in the pull-down assays. For neurite tracing, pEGFP (Novagen) was employed. For the pharmacological treatments, the following compounds were employed (working concentrations are in brackets): cycloheximide (CHX, 1ng/µl, Santa Cruz Biotechnologies, sc-3508), Torin-1 (200nM, Cayman Chemicals, CAY10997), PAKs PF-3758309 (10µM, MedChem, HY-13007), LRRK2 IN-1 (5µM, Division of Signal Transduction Therapy, School of Life Sciences, University of Dundee, UK).

5.2   Animals

C57BL/6 Lrrk2 WT and (mouse) G2019S-Lrrk2 BAC mice were obtained from Jackson Laboratory [B6.Cg-Tg(Lrrk2*G2019S)2Yue/J]. Housing and handling of mice were done in compliance with national guidelines. All animal procedures were approved by the Ethical Committee of the University of Padova and the Italian Ministry of Health (license 1041/2016-PR).

5.3   Mammalian cell cultures, treatment and transfection

5.3.1   Stable cell lines

RAW264.7 and H4 cells purchased from ATCC, as well as HEK293T cells (Life Technologies), were cultured in Dulbecco's modified Eagle's *medium* (DMEM, Life Technologies) supplemented with 10% foetal bovine serum (FBS,

Life Technologies). Cell lines were maintained at 37°C in a 5% CO_2 controlled atmosphere. 0.25% trypsin (Life Technologies), supplemented with 0.53mM EDTA, was employed to generate subcultures. Twenty-four hours after plating, when at 80% confluency, cells were subjected to the various treatments. RAW264.7 cells were treated with 1ng/µl CHX for the duration indicated in paragraph 7.2. Starvation was performed through an over-night incubation in a serum-free *medium*, followed by a 2-hour pulse in Hank's Balanced Salt Solution (HBSS, Life Technologies). Torin-1 treatment was either performed for 150 minutes or aligned with the duration of the other treatments when adopted as a control. H4 cells underwent treatment with PF-3758309 for the doses and times indicated in the figures. The final working concentration was 10µM for 4 hours. IN-1 treatment was performed for 4 hours. DMSO vehicle was included as a negative control.

5.3.2 Transfection

HEK293T were transiently transfected with plasmid DNA using polyethylenimine (PEI, Polysciences). Briefly, a DNA:PEI ratio of 1:2 was employed. To assay PAK6 cellular autophosphorylation and the activation in presence of LRRK2 overexpression, a total amount of 4µg DNA was dissolved in 250µl of OPTI-MEM (Life Technologies) and the respective amount of PEI was added to 250µl of OPTI-MEM. After 5 minutes the two solutions were mixed together and incubated for 20 minutes to allow the formation of DNA/PEI complexes. The mix was then added to the cells that had previously been plated in 6-well plates (Sarstedt) and experimental procedures were carried out after 48-72 hours. For the purification procedure and the subsequent kinase or pull-down assays, cells were plated onto 150mm dishes and transfected with 40µg of DNA dissolved in 1ml of OPTI-MEM and 80µl of PEI added to 1ml. In the case of the GFP control constructs, which display a higher efficiency in terms of both transfection and expression, only 10µg DNA were transfected, to obtain comparable purification yields.

5.3.3 Primary neuronal cultures

Primary cortical neurons were obtained from E16-18 (embryonic days 16-18) or postnatal between day 0 and 1 (P0-P1) mice with the Papain Dissociation System (Worthington Biochemical Corporation). High-density (750-1000 cells/mm^2) and medium-density (150-200 cells/mm^2) neuronal cultures were plated onto 6-well plates or on 12mm glass coverslips in 24-well plates, respectively, and grown in Neurobasal *medium* (Life Technologies) supplemented with 5% FBS, 2% B27 supplement (Invitrogen), 0.5mM Glutamine (Life Technologies), penicillin (100Units/ml) and streptomycin (100µg/ml) (Life Technologies), and 2.5µg/ml fungizone (Life Technologies), in a 5% CO_2 atmosphere at 37°C. After 7 days, 50% of the Neurobasal *medium* was removed and replaced with fresh one. For neurite tracing, transfections with 3xFlag-PAK6 WT or S236L and EGFP were performed at day *in vitro* (DIV) 3 using Lipofectamine 2000 (Life Technologies). Neurons were fixed at DIV7. The EGFP-PAK6 co-transfection was visualised by immunofluorescence under a fluorescence microscope (Leica 5000B) and the EGFP staining was submitted to neurite complexity analysis using the NeuronJ plugin in ImageJ (Meijering et al., 2004). For Western Blot analysis, neuronal samples were harvested in RIPA (Radio Immuno Precipitation Assay) Buffer (Cell Signaling Technology) and processed as described below.

5.4 Western Blot

For Western Blot (WB) analysis, after a double wash in Dulbecco's Phosphate Buffered Saline (DPBS), stable cells were harvested in RIPA Buffer (Sigma Aldrich) supplemented with protease inhibitors (Halt™ protease inhibitor cocktail, Thermo Scientific) and phosphatase inhibitors (Halt™ phosphatase inhibitor cocktail, Thermo Scientific). Neurons and total brain lysates were harvested in RIPA Buffer (Cell Signaling Technology) supplemented with protease inhibitors (Halt™ protease inhibitor cocktail, Thermo Scientific) and phosphatase inhibitors (Halt™ phosphatase inhibitor cocktail, Thermo Scientific). 10 to 30µg of

total protein samples were resolved on NuPAGE, Novex precasted Bis-Tris 4–12% gels (Invitrogen), in MOPS running buffer, NuPAGE, Novex precasted Bis-Tris 12% gels (Invitrogen) in MES running buffer (Invitrogen) or 7.5% Tris-glycine polyacrylamide gels in SDS/Tris-glycine running buffer, according to the size-resolution required. The resolved proteins were transferred to polyvinylidenedifluoride (PVDF) membranes (Bio-Rad), through a Trans-Blot® Turbo™ Transfer System (Bio-Rad). PVDF membranes were subsequently blocked in Tris-buffered saline plus 0.1% Tween (TBS-T) plus 5% non-fat milk for 1 hour at 4°C and then incubated over-night at 4°C with primary antibodies in TBS-T plus 5% non-fat milk. Membranes were then washed in TBS-T (3x10 minutes) at room temperature (RT) and subsequently incubated for 1 hour at RT with horseradish peroxidase (HRP)-conjugated α-mouse or α-rabbit IgG. Blots were then washed in TBS-T (4x10 min) at RT and rinsed in TBS-T, and immunoreactive proteins were visualised using ECL (GE Healthcare). Densitometric analysis was carried out using the Image J software. The antibodies used for WB are as follows: rabbit α-LRRK2 (MJFF2 c41-2, ab133474, abcam, 1:300 to 1:1000), mouse α-β-actin (A1978, Sigma-Aldrich, 1:20000), mouse α-ubiquitin (P4D1, sc-8017, Santa Cruz Biotechnology, 1:500), rabbit α-ULK1 (D8H5, 8054, Cell Signaling Technology, 1:500), rabbit α-phospho-ULK1 (Ser757, 6888, Cell Signaling Technology, 1:500), rabbit α-SQSTM1/p62 (5114, Cell Signaling Technology, 1:500), mouse α-p62 (610833, BD Transduction Laboratories, 1:1000), rabbit α-LC3B (NB100-2220, Novus Biologicals, 1:5000), rabbit α-PAK6 (HPA031124, Prestige® Sigma-Aldrich, 1:1000), rabbit α-phospho-PAK4/5/6 (SAB4504052, Sigma-Aldrich, 1:1000), mouse α-GAPDH (TA150046, OriGene, 1:10000), α-Flag® M2-HRP (A8592, Sigma-Aldrich, 1:20000).

5.5 Cellular Thermal Shift Assay

The Cellular Thermal Shift Assay (CETSA) was performed based on the protocol described by Jafari et al., 2014 and Axelsson et al., 2016. Briefly, 7 million cells per genotype (WT versus T1348N-Lrrk2) were detached with trypsin, subjected to a double wash in DPBS and resuspended in DPBS supplemented

with protease inhibitors before being harvested through a sequence of 4 freeze/thaw steps in liquid nitrogen. Subsequently, the lysate was carefully resuspended and 50µl aliquots were prepared in PCR strips. The samples were subjected to a gradient of temperatures – 37 to 62°C – for 5 minutes on a T100™ Thermal Cycler (BioRad). A 4°C sample was prepared following the same protocol to act as the reference for normalisation. Similarly, a 95°C sample was the control for complete aggregation. The separation between the soluble and the insoluble components was performed *via* a centrifugation step at 4°C and 16300g for 30 minutes. Supernatants were collected without disturbing the pellet and prepared for gel electrophoresis and WB by addition of Sample Buffer (by dilution of a 4X stock solution: 200mM Tris-HCl pH 6.8, 8% SDS, 400mM DTT, 40% glycerol and 0.4% Bromophenol Blue). Data were fitted using the Boltzmann sigmoid (Niesen et al., 2007) equation within GraphPad Prism.

5.6 Semi-quantitative PCR

Prior to moving to quantitative PCR (qPCR), an optimisation step was performed through standard, semi-quantitative PCR in a T100™ Thermal Cycler (BioRad). Total RNA was extracted from WT, KO and T1348N-Lrrk2 cells using the RNeasy Mini Kit (QIAGEN) according to the manufacturer's recommendations. cDNA was obtained by retro-transcription with the ImProm-II™ Reverse Transcription System (Promega). The WT samples were then used for the optimisation step. A gradient, semi-quantitative PCR was performed with the Wonder Taq polymerase (EuroClone). For *Lrrk2* amplification, primers (indicated as LQ) were designed at the N-terminus of the LRR domain, where the epitope recognised by the MJFF2 antibody is located. Three housekeeping genes – *Actb* (coding for β-actin), *Tfrc* (transferrin receptor) and *Pcx* (pyruvate carboxylase) – as well as a control primer pair for *Lrrk2* (indicated as LS) were included. The sequences of forward (Fw) and reverse (Rv) primers are listed below.

Lrrk2 – LQ:
Fw: AAGTCCAACTCAATTAGTGTAGGGGAAGT

Rv: AGATAGGTCTAACGACGTGATGTGTTCT

Lrrk2 – LS:
Fw: GCAGGTCGTGAGGAATTCTACAGC
Rv: CCAACCACAGGCTGATCTCGG

Actb:
Fw: TACCACCATGTACCCAGGCATT
Rv: ACTCATCGTACTCCTGCTTGCTGA

Tfrc:
Fw: TATAAGCTTTGGGTGGGAGGCA
Rv: AGCAAGGCTAAACCGGGTGTATGA

Pcx:
Fw: ACTGGCAGGTAGTTGCTCACATATTCA
Rv: ACATGACCTAGTGTGGAGGGCAA

The PCR reaction was conducted as follows: one initial denaturation step at 95°C for 4 minutes, followed by 29 cycles of denaturation at 95°C for 1 minute, annealing at either 56.3°C, 57.7°C or 60°C for 1 minute and extension at 72°C for 1 minute. A final extension step was applied at 72°C for 10 minutes. Amplified cDNA was resolved *via* electrophoresis on 2.5% agarose gels and visualised by the Molecular Imager® Gel Doc XR+ (BioRad).

5.7 Immunocytochemistry and confocal microscopy

For immunocytochemistry (ICC), cells were cultured onto 12mm glass coverslips in 12- or 24-well plates that had previously been coated with poly-L-lysine (Sigma-Aldrich). RAW264.7 cells were fixed after the described treatment using 4% paraformaldehyde (PFA) and subsequently subjected to staining. Transfected HEK293T cells were fixed in PFA after 2 days. Neurons were fixed at

DIV7, as previously described. The antibodies used for ICC are the following: rabbit α-LC3B (NB100-2220, Novus Biologicals, 1:200), rabbit α-SQSTM1/p62 (ab91526, abcam, 1:200), rabbit α-PAK6 (HPA031124, Prestige® Sigma-Aldrich, 1:300), mouse α-GFP (11814460001, Roche, 1:200) and fluorescent secondary antibodies (α-rabbit Alexa-568 and α-mouse Alexa-488, Life Technologies, both 1:200). Phalloidin 647 (ab176759, abcam) was employed for the staining of filamentous actin (F-actin), as per manufacturer's instructions. Proteins were afterwards visualised by confocal microscopy (Zeiss LSM700).

5.8 Protein purification from mammalian cells

For the purification protocol, cells were plated onto 150mm dishes, transfected with 40µg plasmid DNA and solubilised after 48-72 hours in 1ml of Lysis Buffer supplemented with 1% Triton® X-100 or 0.5% Tween® 20 (Sigma-Aldrich) and protease inhibitor cocktail. All the non-commercial buffer utilised, together with their composition and the application for which they have been used are listed in Table 2. After clearing of the lysate by centrifugation at 20000g for 30 minutes at 4°C, the supernatants were incubated for 2 hours with 40µl of anti-Flag® M2 Affinity Gel (Sigma-Aldrich) at 4°C.

For kinase assays, resins were subsequently washed twice with each of the Washing Buffers (WBu) supplemented with Tween® 20 (Table 2). Centrifugation steps (7500g x 1 minute) were performed between washes to pellet the resin. Proteins were eluted in 200µl WBu5 by competition with an excess of 3xFlag peptide at a final concentration of 150ng/µl. The samples were centrifuged to collect supernatants and resins separately.

For pull-down-assays, one wash per each of the Triton® X-100-supplemented WBus was performed (Table 2). A final wash in the buffer used for the pull-down reaction (Pull-down Buffer, Table 2) was applied.

BUFFER NAME	COMPOSITION	APPLICATION
Tween® 20 Lysis Buffer	20mM Tris-HCl pH 7.5, 150mM NaCl, 1mM EDTA, 2.5mM sodium pyrophosphate, 1mM β-glycerophosphate, 1mM sodium orthovanadate, 0.5% Tween® 20, protease inhibitor cocktail	Kinase assays
Tween® 20 WBu1	20mM Tris-HCl, pH 7.5, 500mM NaCl, 0.5% Tween® 20	Kinase assays
Tween® 20 WBu2	20mM Tris-HCl, pH 7.5, 300mM NaCl, 0.5% Tween® 20	Kinase assays
Tween® 20 WBu3	20mM Tris-HCl, pH 7.5, 150mM NaCl, 0.5% Tween® 20	Kinase assays
Tween® 20 WBu4	20mM Tris-HCl, pH 7.5, 150mM NaCl, 0.1% Tween® 20	Kinase assays
Tween® 20 WBu5	20mM Tris-HCl, pH 7.5, 150mM NaCl, 0.02% Tween® 20	Kinase assays
Kinase Assay Buffer	25mM Tris-HCl, pH 7.5, 5mM β-glycerophosphate, 0.1mM sodium orthovanadate, 2mM DTT, 10mM $MgCl_2$, 0.02% Tween® 20	Kinase assays
Triton® X-100 Lysis Buffer	20mM Tris-HCl pH 7.5, 150mM NaCl, 1mM EDTA, 2.5mM sodium pyrophosphate, 1mM β-glycerophosphate, 1mM sodium orthovanadate, 1% Triton® X-100, protease inhibitor cocktail	Pull-down assays
Triton® X-100 WBu1	20mM Tris-HCl, pH 7.5, 500mM NaCl, 1% Triton® X-100	Pull-down assays
Triton® X-100 WBu2	20mM Tris-HCl, pH 7.5, 300mM NaCl, 1% Triton® X-100	Pull-down assays
Triton® X-100 WBu3	20mM Tris-HCl, pH 7.5, 150mM NaCl, 1% Triton® X-100	Pull-down assays
Triton® X-100 WBu4	20mM Tris-HCl, pH 7.5, 150mM NaCl, 0.1% Triton® X-100	Pull-down assays
Triton® X-100 WBu5	20mM Tris-HCl, pH 7.5, 150mM NaCl, 0.02% Triton® X-100	Pull-down assays

Pull-down Buffer	50mM Tris-HCl, pH 7.5, 1mM EDTA, 0.27M sucrose, 5mM sodium pyrophosphate, 1mM sodium orthovanadate, 1% Triton® X-100	Pull-down assays
Pull-down WBu	50mM Tris-HCl, pH 7.5, 1mM EDTA, 0.27M sucrose, 5mM sodium pyrophosphate, 1mM sodium orthovanadate, 1% Triton® X-100, 0.5M NaCl	Pull-down assays
HBSP⁺	20mM HEPES, pH 7.4, 150mM NaCl, 0.005% Tween® 20	Surface plasmon resonance

5.9 Pull-down assays

After the purification step (performed as previously described), bait proteins on the resins were incubated with lysates overexpressing the prey proteins, as discussed in the Results sections. The pull-down reaction was conducted over-night in the Pull-down Buffer. The following morning, resins were washed three times with the Pull-down Buffer supplemented with 0.5M NaCl (Pull-down WBu, Table 2) and processed for WB analysis.

5.10 *In vitro* kinase assays

Purified 3xFlag-PAK6 WT or S236L were eluted in Kinase Assay Buffer (Table 2) and incubated for 1 hour at 30°C in the presence of ^{33}P-ATP (1µCi) and 10µM cold ATP. The incorporated ^{33}P-ATP was detected by autoradiography by a Phospho-Imager system (Cyclone, Perkin-Elmer). Total protein loading was checked by staining the same membranes with the Coomassie Brilliant Blue staining for PVDF.

5.11 Surface plasmon resonance

To conduct the surface plasmon resonance (SPR) experiments, 3xFlag-PAK6 was obtained by large scale purification followed by elution with Flag-peptide in Tween® 20-supplemented buffers as previously described. Similarly, double-tagged Strep/Flag-LRRK2 was purified by affinity with the *Strep*-Tactin® Superflow® system (IBA) and the *Strep*-tag purification Buffer Set as in Gloeckner et al., 2009. The Roc-COR WT, R1441C and Y1699C fragments purified from *E. coli* were kindly provided by Dr. Arjan Kortholt. 20µM proteins were resuspended in HBSP$^+$ running buffer (Table 2) supplemented with 10mM EDTA and 0.5mM DTT to unload any residual nucleotide bound to the proteins. After a 20-minute incubation on ice, the buffer was exchanged through Zeba Spin Desalting Columns, 40K MWCO (Thermo Scientific) and substituted by HBSP$^+$ supplemented with 0.5mM $MgCl_2$ and 250µM GppCp (Jena Bioscience). CM5 Biacore Sensor chips (GE Healthcare) were prepared by standard chemical immobilisation. Equivalent response levels (RU) were reached in the different chips in order to obtain comparable values among the measurements. For each run, 5 measurements were conducted in Single Cycle Kinetics mode on a Biacore™ X100 system (GE Healthcare). The dissociation step was performed with 2M $MgCl_2$.

5.12 Data analysis software

Relative band intensities were measured with the freeware ImageJ software. Total protein levels were normalised over the loading control – β-actin – whereas the phospho/total ratios were calculated as the relative abundance of phospho- over total protein, previously normalised to their respective loading controls. Graphs and statistical analysis were realised using GraphPad PRISM 5.

Chapter 4

Nucleotide-binding capacity is important for Lrrk2 stability

6. Introduction

6.1 The role of Roc in the autophagic function of Lrrk2

The term "autophagy" was initially introduced by Christian de Duve in 1963 to indicate the degradation of cytoplasmic material in the lysosome, but the molecular characterisation of the process only began in the early '90s, with the report of autophagic bodies accumulation in the yeast vacuole after nutrient deprivation and depletion of proteinases by Ohsumi and colleagues (de Duve, 1963; Takeshige et al., 1992). Nowadays, autophagy is a well-recognised process through which intracellular components and organelles, either self or foreign, are delivered to the lysosome for degradation and recycling (Yu et al., 2017), and the mechanisms underlying this process start to be uncovered in greater detail. Nevertheless, the more the understanding of autophagy advances, the more its complexity and dynamic nature are recognised, including the existence of several so called "non-canonical" ways, parallel to the "canonical" pathways, that cells undertake to degrade the materials they need to eliminate and/or recycle. To give a brief overview, autophagy initiates with the activation of the ULK (Unc-51 Like Autophagy Activating Kinase) kinase complex – composed of ULK1, ULK2, ATG13, RB1CC1/FIP200 – and its translocation at specific sites on the endoplasmic reticulum (ER) (Figure 9) (Hurley and Young, 2017; Yu et al., 2017). This can be accomplished essentially through two ways: the first one, through release of mTOR inhibition, *via* dephosphorylation of ULK1 Ser757 in mouse/Ser758 in human; the other one, by the activating phosphorylation on ULK1 Ser555 in mouse/Ser556 in human, mediated by AMPK (Khan and Kumar, 2012; Papinski and Kraft, 2016). ULK1 activation constitutes an early event able to transduce pro-autophagic signals through phosphorylation of many substrates. Among them, one of the most important is Beclin-1, which is part of the class III phosphatidylinositol 3-kinase complex I. This phosphorylation is pivotal for activating the complex and promoting autophagy, thanks to the production of phosphatidylinositol 3-phosphate (PI(3)P) (Hurley and Young, 2017). This initial series of finely tuned events leads to the formation of the autophagosome, a double-membrane bound organelle containing the material(s) to be degraded,

which ultimately fuses with the lysosome (Yu et al., 2017). The lipidation of LC3 by conjugation with phosphatidylethanolamine (PE) for recruitment and insertion into the autophagosomal membrane is adopted as a marker for the progression of autophagy (Tanida et al., 2008), whereas the reduction in the levels of the cargo protein p62 – a ubiquitin-binding scaffold recognising and binding proteins for the sequestration into the autophagosome (Kalogeropulou et al., 2018) – is generally accepted as an indicator of the fusion with the lysosome and consequent degradation of the waste materials (Bjørkøy et al., 2009).

The influence of LRRK2 on the autophagic pathway, as well as the contribution of the kinase activity to the process, have been robustly characterised in the last decade (reviewed in Manzoni, 2017), although a detailed picture of the molecular events orchestrated by LRRK2 is still lacking. On the contrary, there is no current understanding about the impact of Roc/GTPase activity on the process. We decided to perform a comprehensive characterisation of a cellular model where endougenous Lrrk2 is unable to bind guanine nucleotides, therefore deprived of GTPase activity, exploiting the autophagic pathway as a readout i) to investigate the cellular impact of GTP binding loss and ii) to potentially dissect the influence of the two catalytic activities on Lrrk2-mediated pathways.
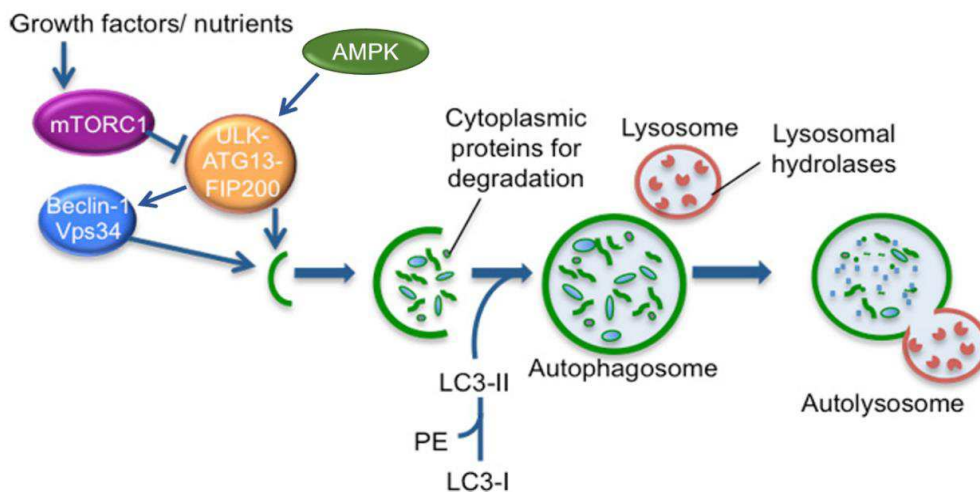
Figure 9. Schematic of the autophagic flux. Release of mTOR inhibition on ULK1, ULK1 activation by AMPK and/or activation of the Beclin-1 complex initiate autophagosome formation. Autophagy progresses till the final fusion of autophagosomes with lysosomes and the digestion of the cytoplasmic material that needs to be degraded (adapted from the Babraham Institute website).

7. Results

7.1 The T1348N mutation in Roc impacts on Lrrk2 steady-state levels

In order to gain a better understanding about the impact of LRRK2 GTPase activity in regulating the biochemical properties of the protein and LRRK2 cellular functions, we decided to exploit the multiple advantages of the isogenic RAW264.7 murine macrophage cell lines, recently generated by the MJFF in collaboration with ATCC. These cells have been engineered with the Zinc Finger Nuclease Technology for gene editing (Geel et al., 2018). In addition to the parental (WT) line, a Lrrk2-KO and a Lrrk2-KI leading to a mutation in a key aminoacid (T1348N) that disables nucleotide binding are available. We initially evaluated the expression levels of Lrrk2 in the three different cell lines, since it was already known from the literature that ectopic expression of GTP-binding deficient mutants of LRRK2 is significantly reduced with respect to the WT (Taymans et al., 2011; Biosa et al., 2013). When looking at the basal expression profile of T1348N-Lrrk2, we indeed observed an average 8-fold reduction in comparison with the levels of WT-Lrrk2 (Figure 10), suggesting that the mutation is affecting the steady-state levels of the protein. One possibility to consider is that the reduced intensity of the staining could depend on the fact that the T1348N mutation interferes with the binding of the antibody to its epitope. However, the mapping site of the epitope recognised by the antibody (close to LRR region, as shown in Davies et al., 2013), combined with the fact that GTP-binding deficient, tagged construct detected with antibodies directed against the tag display a similar behaviour (Biosa et al., 2013), make this hypothesis unlikely.
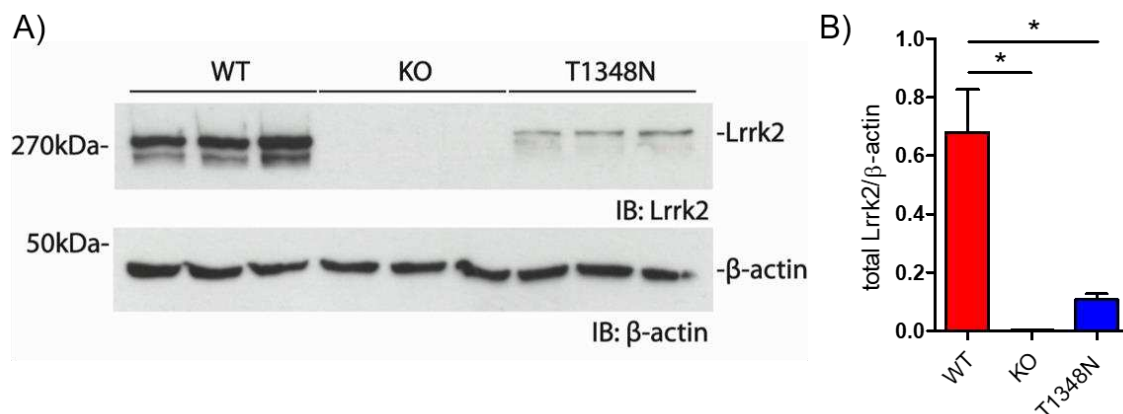
Figure 10. The T1348N mutation impairs Lrrk2 steady-state levels in RAW264.7 cells. (A) Representative WB and (B) quantification of total Lrrk2 over β-actin (n=2 independent experiments; n=3 technical replicates per experiment; mean ± SEM; one-way ANOVA with Turkey's multiple comparison test; *P≤0.05).

Given the absence of mechanistic data explaining the reasons at the basis of such a strong reduction, we then sought to understand how the T1348N mutation impacts on Lrrk2 steady-state levels.

7.2   CHX treatment did not reveal significant alterations in WT versus T1348N-Lrrk2 half-life

We initially hypothesised that the strategic position of the mutation, located in a key residue within the P-loop in the active site of the Roc domain (Nguyen and Moore, 2017), could account for the differential stability with respect to WT-Lrrk2, by affecting the rate of degradation of the protein. To compare the half-lives of WT versus T1348N-Lrrk2, we decided to pharmacologically block protein synthesis using CHX. After drawing a calibration curve with increasing concentrations of the compound – from 1 to 50ng/μl – we decided to employ 1ng/μl CHX for the following treatments, since it was the lowest dose that we proved effective without being lethal to our system. We thus followed the degradation of one specific pool of proteins over time, collected the samples at different time points, and analysed the degradation profile of Lrrk2 *via* WB. Based on data from the literature reporting an approximate half-life of 9 hours for

ectopically expressed LRRK2 (Wang et al., 2008), we initially performed a 24-hour time-course, evaluating Lrrk2 expression after 3, 6, 12 and 24 hours. As a negative control, we selected β-actin, whose half-life is reported to be at least 48 hours (Antecol et al., 1986). The results obtained from this experiment are reported in Figure 11. Surprisingly, we did not observe any decay in Lrrk2 levels for any of the genotypes in our experimental conditions. As a positive control for CHX treatment, we probed our membranes for ubiquitin, which is commonly adopted to monitor the overall response of the cell to treatments involving degradation pathways. As expected, the pool of ubiquitinated proteins significantly decreased over time, although not reaching the zero, compatibly with the presence of longer-lived proteins (Figure 12).
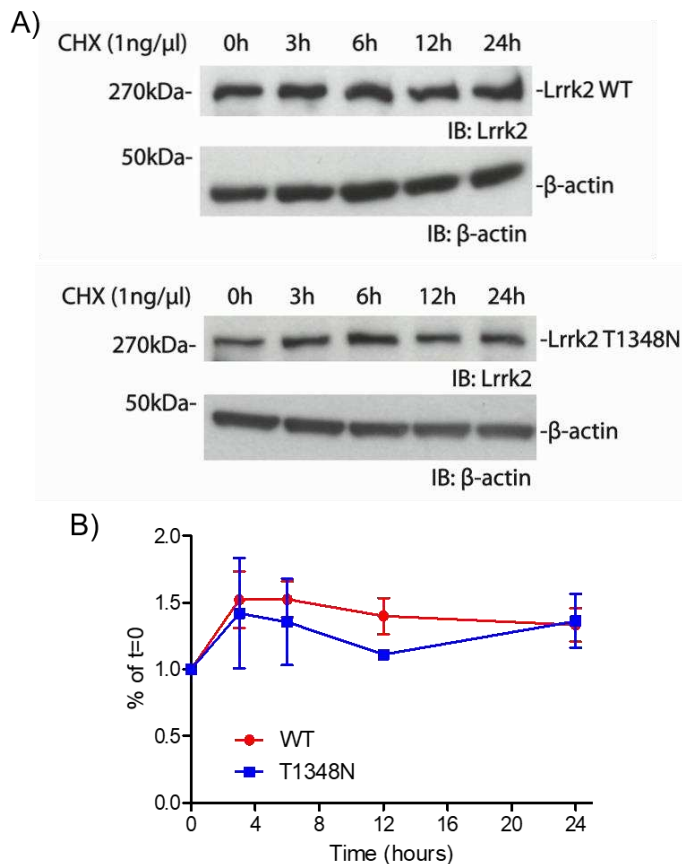
Figure 11. WT and T1348N-Lrrk2 are stable after a 24-hour treatment with 1ng/µl CHX. (A) Representative WB depicting the time-course for WT (top panel) and T1348N-Lrrk2 (bottom panel). β-actin was employed as a loading control, given its long half-life. (B) Protein content was normalised over time=0 (n=3 independent experiments; n=3 technical replicates per experiment).

Longer exposure
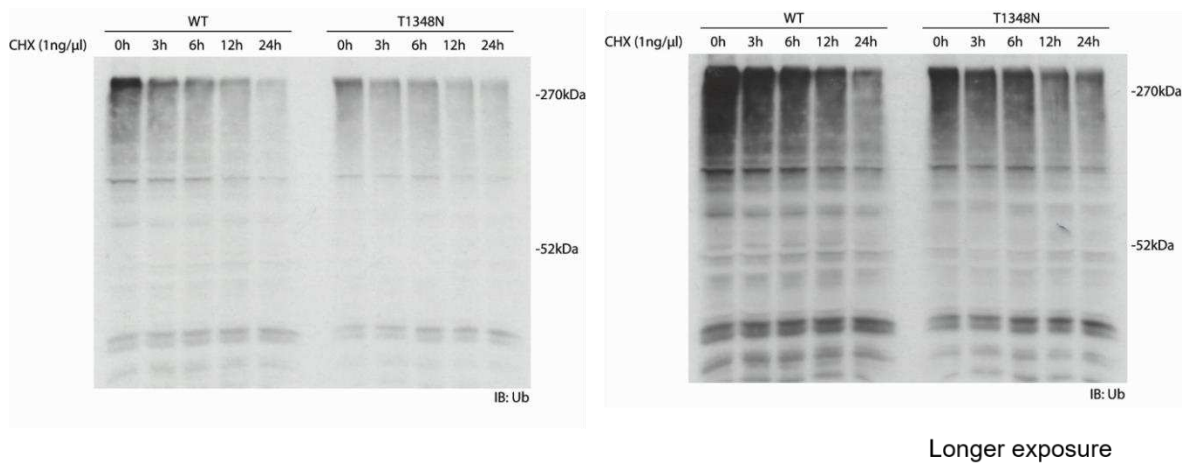
Figure 12. The pool of ubiquitinated proteins confirms the efficacy of CHX treatment. The probing of membranes with an α-ubiquitin antibody was exploited as a positive control for CHX treatment. As shown from the representative WB, the total pool of cellular proteins decreased over time, despite the fact that certain populations remained stable, coherently with a longer half-life. Interestingly, high-molecular weight species display, on average, shorter half-lives compared to low-molecular weight proteins.

Therefore, after excluding the presence of technical issues impacting on the outcome of the experiment, we wanted to investigate the possibility that endogenous Lrrk2 possesses a longer half-life in our experimental model. For this reason, we set up a second round of treatment, prolonging the exposure of cells to CHX up to 48 hours (time points: 0, 6, 12, 18, 24 and 48 hours). Also in this case, we did not observe any significant decay in WT nor in T1348N-Lrrk2 levels, as depicted in Figure 13. However, we could appreciate a partial destabilisation of the T1348N mutant at the latest time point.
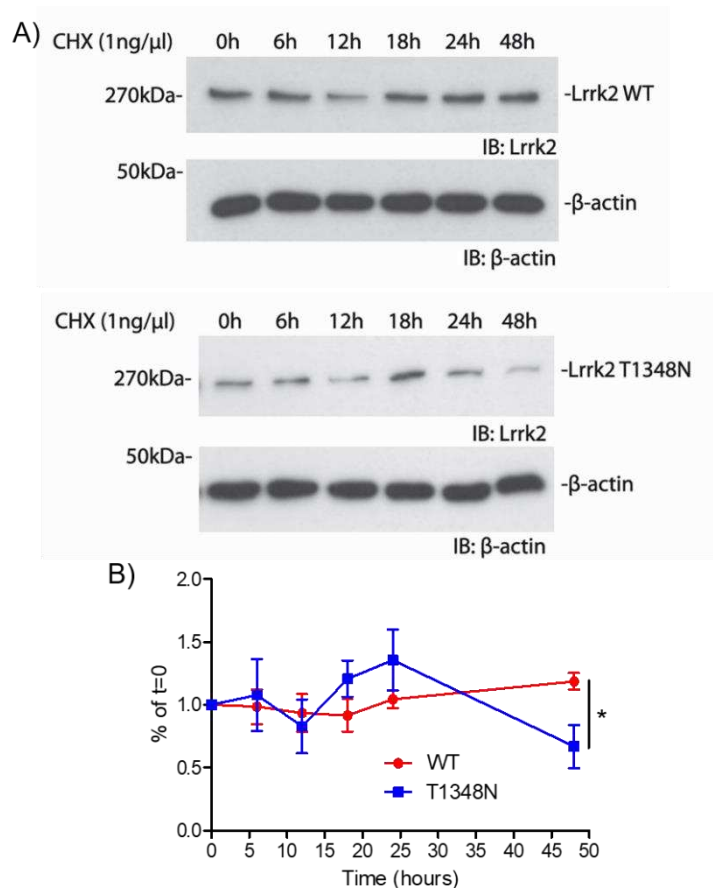
Figure 13. T1348N-Lrrk2 is partially destabilised after 48 hours of treatment with 1ng/µl CHX. (A) Representative WB depicting the time-course for WT (top panel) and T1348N-Lrrk2 (bottom panel). β-actin was employed as a loading control, given its long half-life. (B) Protein content was normalized over time=0 (n=3 independent experiments; n=2-3 technical replicates per experiment; unpaired t-test; *P≤0.0479).

7.3 WT and T1348N-Lrrk2 display different denaturation profiles

One possible explanation for the dramatic loss of T1348N-Lrrk2 in our RAW264.7 mutant cell line is that the aminoacidic substitution and/or the permanent apo- (i.e. depleted of nucleotide binding) state of Lrrk2 could interfere with the appropriate folding of the protein.

The approach we selected to employ to test our "misfolding hypothesis" is the recently developed CETSA technique (Axelsson et al., 2016; Jafari et al., 2014) to monitor the thermal stability of WT and T1348N-Lrrk2. Briefly, we compared the denaturation profiles of whole lysates from WT and T1348N-Lrrk2 RAW264.7 cell lines, subjected to a gradient of temperatures as described in the Materials and Methods section, to maintain any of the interacting molecules that have an influence on the stability of Lrrk2. Even though additional replicates are

mandatory to calculate precise and statistically robust values in terms of temperature of aggregation (T_{agg50} = the temperature at which 50% of the protein is lost in the insoluble fraction) for WT and T1348N-Lrrk2, our preliminary data indicate a different trend between the curves obtained by looking at the proteins within their cellular environment (Figure 14). In particular, while the WT protein displays the expected sigmoidal behaviour, with an approximate T_{agg50} of about 43°C, the T1348N mutant shows a more variable and drastic "on-off" trend, supporting the idea of an at least partial unfolding of the protein.
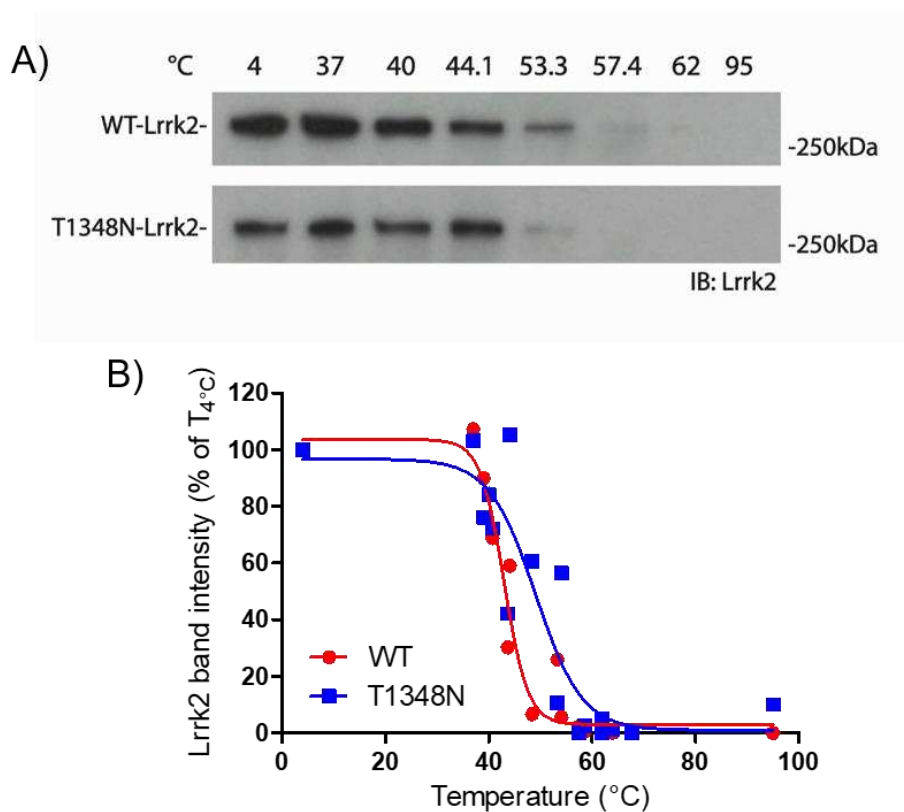
Figure 14. WT and T1348N-Lrrk2 possess different thermal stability profiles. (A) Preliminary data (n=2 independent experiments) indicate a different behaviour between the two proteins, with possible implications for the melting temperature. Longer exposures revealed the presence of high molecular weight aggregates in the T1348N mutant but not in the WT samples (data not shown). (B) The graph shows the denaturation curve for WT and T1348N-Lrrk2 (n=2 independent experiments). While WT-Lrrk2 displays a typical sigmoid trend, with an apparent temperature of aggregation (T_{agg50}) around 43°C, the fitting for the T1348N is ambiguous, meaning that an estimate of T_{agg50} based on these data would be inaccurate. Data were fitted using the Boltzmann sigmoid (Niesen et al., *Nature Protocols*, 2007) equation within GraphPad Prism.

Another possible explanation for the reduced levels of T1348N-Lrrk2 could reside in an instability at the mRNA level. Although we believe this hypothesis is less likely, we have no elements to exclude that the mutation is impacting on the transcript rather than on the protein, or even that it is affecting both levels.

Therefore, in parallel to the previously described approaches, we designed and validated through standard, semi-quantitative PCR a set of primer pairs that we will use to compare the expression profile of *Lrrk2* in all three the cell lines (WT, Lrrk2-KO, T1348N-Lrrk2) through qPCR. In particular, we have designed a primer pair for *Lrrk2* on the N-terminal region of the LRR domain, where the epitope recognised by the MJFF2 antibody is located (Davies et al., 2013). In addition, based on the literature and on the commercially available platforms for high-throughput gene expression analyses on murine datasets, we selected three genes with variable expression to act as housekeeping controls: *Actb* (coding for β-actin), *Tfrc* (transferrin receptor) and *Pcx* (pyruvate carboxylase). As a positive control for our reaction, we included a primer pair that we had in house and that was designed for the amplification of *Lrrk2* in standard, semi-quantitative PCR, which leads to a larger product. The result obtained from the validation is depicted in Figure 15. In particular, we subjected the samples (400ng cDNA obtained from WT RAW264.7 cells) to a gradient of temperatures, in order to select the best condition for the annealing of the primer pairs. The bottom panel shows comparable efficiencies of amplification between 56.3 and 57.7°C for all the primer pairs tested. Also, the products were of the expected size, i.e. around 200 base pairs (bp). When increasing the temperature up to 60°C, we could still obtain good amplification yields, although observing the formation of primer dimers. Therefore, we are now planning to move to the qPCR reaction performing the annealing step at 58°C, since at that temperature we obtained the cleanest bands without the formation of primer dimers.
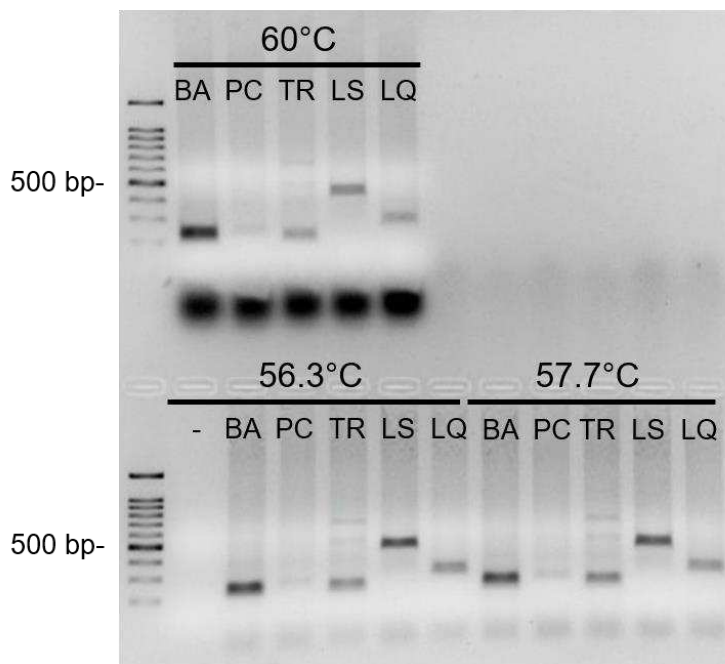
Figure 15. Optimisation of the conditions for qPCR through semi-quantitative PCR. 400ng cDNA per sample were subjected to a gradient PCR reaction (the temperatures are indicated in the picture) as described in the Material and Methods section (- = negative control; BA = *Actb*/β-actin; PC = *Pcx*/pyruvate carboxylase; TR = *Tfrc*/transferrin receptor; LS = *Lrrk2*/Lrrk2 for semi-quantitative PCR; LQ = *Lrrk2*/Lrrk2 for qPCR).

7.4 The T1348N mutation in Lrrk2 impacts on p62 levels

Given the established role of LRRK2 in autophagy (Tong et al., 2012; Manzoni et al., 2013a; Manzoni et al., 2013b; Manzoni et al., 2016; Giaime et al., 2017; reviewed in Roosen and Cookson, 2016; Manzoni, 2017), we decided to adopt this process as a functional readout to investigate whether and how the lack of nucleotide-binding, hence GTPase activity, influences the signalling properties of Lrrk2.

We initially wished to assess whether the mutation was affecting basal autophagy. We therefore evaluated *via* WB a panel of key autophagic markers that are useful indicators of the progression of the autophagic flux at different steps: 1) the activating, pro-autophagic de-phosphorylation of ULK1 on Ser757, which is an index of mTOR inactivation, 2) the lipidation of LC3, crucial event in the early stages of autophagosome formation and 3) the levels of p62, which normally decrease at later stages because of the degradation of autophagic materials (Klionsky et al., 2016). Our preliminary data indicate no major differences in the levels of basal autophagy, but point towards a significant accumulation of p62 in absence of Lrrk2 GTPase activity, as highlighted in Figure

16. This could be suggestive of a blockade in the autophagic flux.

We next wondered whether the absence of GTPase activity could become relevant in the mediation of the response to stress conditions. We therefore induced autophagy either by nutrient deprivation – achieved by an over-night starvation in serum-free media, followed by a 2-hour pulse with HBSS – or by inhibition of mTOR kinase activity through the use of the highly selective Torin-1 compound. Up to date, our preliminary data highlighted some interesting observations, that deserve further validation. In terms of LC3 lipidation, we could observe a response to both treatments in WT cells, despite the high level of basal activation that was already evident in the previous set of experiments (Figure 16; Figure 17A, left panel). However, this basal level appeared higher in KO cells, where autophagy-inducing treatments were unable to significantly increase the level of LC3-II (Figure 17A, middle panel). On the other hand, the T1348N mutant cells exhibited a peculiar behaviour, as they could respond to starvation but not to the treatment with Torin-1 (Figure 17A, right panel). In all cases, we noticed that the induction of autophagy was leading to a conversion of LC3-I into LC3-II rather than a mere accumulation of LC3-II, therefore we decided to quantify lipidated LC3 as a ratio between the two forms (Figure 17B).

With respect to ULK1, phospho-ULK1 and p62 we did not appreciate substantial differences in the response among the genotypes. As expected, both starvation and mTOR inhibition *via* Torin-1 led to an almost complete dephosphorylation of ULK1. Interestingly, the behaviour of p62 was coherent but opposite between the two stimuli: it tended to accumulate with starvation while decreasing after Torin-1 treatment, as summarised in the representative Figure 18.
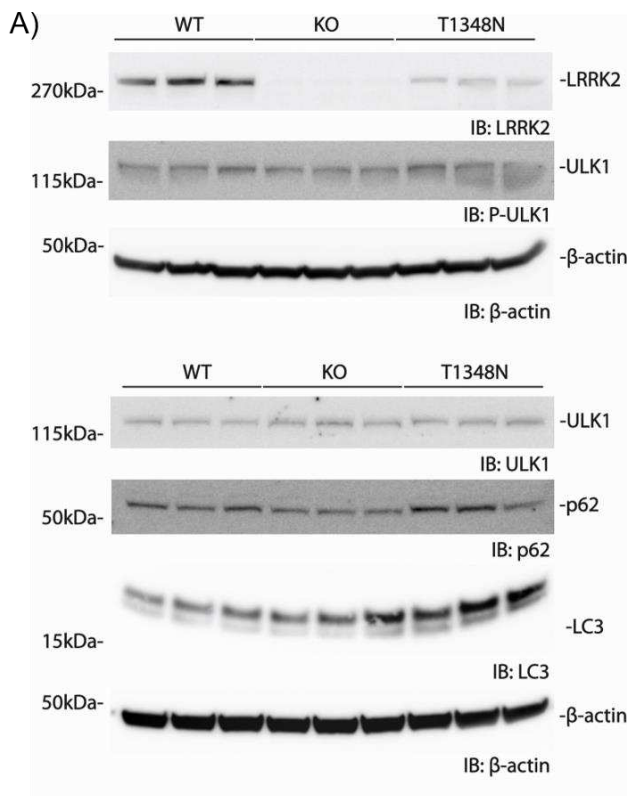
Figure 16. Loss of GTP-binding impacts on p62 levels in basal conditions. (A) Representative image of the impact of T1348N-Lrrk2 mutation on the autophagic markers analysed. As shown from the quantification in (B), the only significant alteration registered relates to the levels of p62, (n=2 independent experiments for p62; n=5 independent experiments for all the other markers; n=3 technical replicates per experiment; mean ± SEM; one-way ANOVA with Turkey's multiple comparison test; *P≤0.05; **P≤0.01. Within each biological replicate, values were normalised over the WT sample. To take into account the variability of the WT measurements during statistical analysis, SEM was manually calculated and included in the graphs).

Figure 17. LC3 lipidation appears differentially impaired in KO and T1348N-Lrrk2 RAW264.7 cell lines in response to stress stimuli. (A) Representative WBs illustrating the differential ability of RAW264.7 cells to respond to nutrient deprivation and/or mTOR inhibition. (B) Quantification of the ratio between LC3-II and LC3-I (n=2 independent experiments for WT and KO cell lines; n=1 for T1348N-Lrrk2 RAW264.7 cells; n=3 technical replicates per experiment; mean ± SEM; one-way ANOVA with Turkey's multiple comparison test; *P≤0.05; **P≤0.01).

Figure 18. Starvation and Torin-1 trigger autophagy with different specificity and in a different time scale. (A) Representative WBs depicting the diverse behaviour in terms of p62 after nutrient deprivation and treatment with Torin-1, even though both stimuli activate the mTOR pathway, as shown by ULK1 de-phosphorylation in (B). (C) Quantification panel (n=2 independent experiments for WT and KO cell lines; data for T1348N-Lrrk2 RAW264.7 cells were not included due to low quality WBs; n=3 technical replicates per experiment; mean ± SEM; one-way ANOVA with Turkey's multiple comparison test; *P≤0.05; **P≤0.01).

7.5   RAW264.7 are highly reactive cells

As a complementation to the data we have just described, we sought to perform some immunofluorescence analysis on our RAW264.7 cell lines, in absence or presence of a stress stimulus. We initially chose starvation in order to check whether i) the alteration in the levels of p62 observed in WB in basal conditions was accompanied by a subcellular re-localisation of the protein; ii) we could reproduce the differential response to starvation in terms of LC3 lipidation in absence and presence of Lrrk2 using a different technique. Figure 19 shows a panel of representative pictures obtained for LC3 (A) and p62 staining (B), respectively. As exemplified from the first panel of pictures, the staining for LC3 was very diffuse and difficult to interpret in all the conditions tested. In addition, nutrient deprivation, although inducing a change in cell morphology, did not lead to the expected increase in LC3 puncta, which is normally observed when autophagy is induced (Pugsley, 2017). With respect to p62, even though there seems to be a partial reorganisation of the protein in the T1348N mutant, the unexpectedly

elevated intensity of the staining even at basal, i.e. non-stimulated conditions, hampers the comparison among genotypes, as well as between untreated versus treated conditions. Therefore, a conclusion we could draw based on this experiment, which is further supported by the high levels of basal LC3 lipidation shown in Figures 16 and 17, is that a constant, hyperactive condition might conceal certain differences in the handling of autophagy among the genotypes, being an obstacle to the study of this process in this cell line.
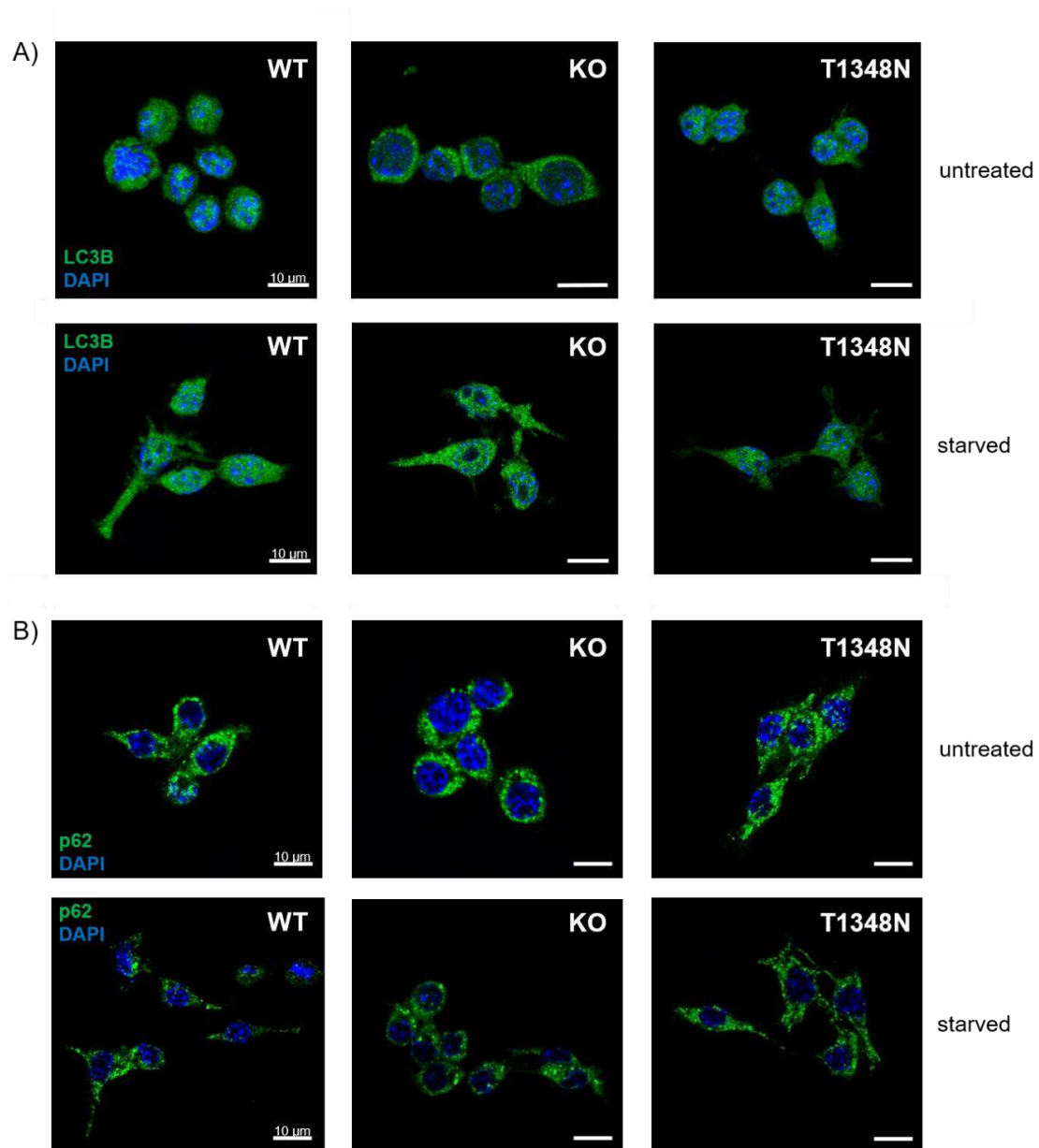
Figure 19. Immunofluorescence staining of (A) LC3 and (B) p62 in WT, Lrrk2-KO and T1348N-Lrrk2 cell lines. Representative images depicting LC3 and p62 cellular distribution, in green. DAPI is in blue. Scale bars: 10μm.

8. Discussion

As expected, the use of RAW264.7 cell lines has proven useful in order to gain a better understanding of the importance of nucleotide binding, hence GTPase activity, in Lrrk2 cellular function. The results reported in this chapter led us to hypothesise that the ablation of guanosine nucleotide binding for Lrrk2 may affect the stability of the protein, confirming previous reports from the literature regarding ectopically expressed LRRK2 (Taymans et al., 2011; Biosa et al., 2013). This could be due to multiple reasons.

We firstly hypothesised that the differential expression could coincide with a more rapid rate of degradation in the case of T1348N-Lrrk2, which we tested through CHX treatment. Surprisingly, in our experimental conditions, we could appreciate a significant reduction in T1348N-Lrrk2 as compared to the WT counterpart only after 48 hours of treatment. In addition to that, we did not observe the expected decay in Lrrk2 levels over time that is the consequence of protein degradation. Despite the fact that literature reports a half-life of 9 hours for exogenously expressed LRRK2 (Wang et al., 2008), some works indicate a much longer half-life (~38 hours for WT-LRRK2) (Orenstein et al., 2013). Indeed, it has to be noted that the treatment with CHX is a technically challenging experiment, in that it is cell-type and construct-specific. Therefore, one very simple explanation is the half-life of endogenous Lrrk2 in RAW264.7 cell might be longer than 24-hours. However, there are additional possibilities that we need to take into account in the interpretation of the results. First, considering that we are employing low doses of the compound due to the sensitivity of the system – higher concentrations and/or longer times are extremely toxic to the cells – it could be that protein synthesis is only partially blocked. An alternative option we are currently testing could be that, due to structural reasons and/or the inability of binding nucleotides, only a fraction of the T1348N mutant is properly folded, while the remaining is rapidly degraded, and we could not follow this population due to the technical challenges of the experiment with CHX. To check for this, we plan to use specific combinations of drugs to individually block the cellular degradation pathways, i.e. the UPS, macroautophagy and CMA (Orenstein et al., 2013; Ciechanover & Kwon, 2015). We expect to see an accumulation of T1348N-Lrrk2 up to WT levels when

blocking its preferential way of degradation. In addition, blocking global protein synthesis likely affects overall cellular homeostasis and may therefore complicate data interpretation. In this regard, we initially considered to perform ^{35}S pulse chase assays, however it turned not to be a feasible option due the difficulty in immunoprecipitating endogenous Lrrk2.

The results obtained from the CETSA seem to, at least partially, support this "misfolding hypothesis". If we cannot definitely conclude that T1348N-Lrrk2 is unproperly folded, since we have conducted the assay with the whole lysate, i.e. in presence of endogenous ligands and/or binding partners, the "on-off" behaviour of the mutant protein may suggest that T1348N-Lrrk2 is maintained in solution by the presence of chaperones assisting the folding. According to this hypothesis, once the T_{agg50} of the chaperone is reached, mutant Lrrk2 rapidly switches towards the insoluble fraction. These data are still preliminary, and further investigation is required to confirm our hypothesis. For example, we need to repeat the CETSA in different conditions – e.g. with the purified proteins, in presence of nucleotide-unloading agents, chaperone inhibitors etc. – to rule out the exact mechanistic details of the process. However, this result supports the hypothesis that the lack of GTP-binding is affecting the stability of T1348N-Lrrk2 either by exerting a direct impact on the protein structure or by interfering with the intramolecular signalling towards the kinase domain, the interaction with binding partners and, possibly, the quaternary structure of Lrrk2 itself.

In parallel to the investigation at the protein level, we are also planning qPCR experiments to check for mRNA expression. We do not expect to observe significant differences in the transcripts, since such a small modification in the genome might not impact on mRNA levels. However, regulation of mRNA stability is a very complex process operated at multiple steps (Wu and Brewer, 2012), and we need to exclude the possibility that the mutation is located in a key position for the binding of regulatory elements.

As a functional readout, we looked at autophagy, given the established role of LRRK2 in this process (Roosen and Cookson, 2016; Manzoni, 2017). We initially evaluated basal autophagy, by assessing markers of different steps *via* WB, with the aim of obtaining a complete picture of the pathway. As described in paragraph 7.4, we only detected significant alterations in the levels of p62, which

was found to accumulate in T1348N-Lrrk2 as compared to WT and KO controls. Since p62 decrease is generally considered as an indication of the autophagosome degradation in the lysosome (Bjørkøy et al., 2009), this might suggest a blockade of the autophagic flux. However, autophagy is a highly dynamic process and multiple experiments are needed before drawing definite conclusions. In general, this finding is particularly interesting given that p62 has been recently described as a substrate of LRRK2 kinase activity (Kalogeropulou et al., 2018). Further investigation is required to uncover the mechanistic details of how GTPase activity is impacting on the pathway.

When we induced autophagy through alternative approaches – starvation and Torin-1 – we observed that KO cells display basally high levels of LC3, coherently with literature reports regarding the characterisation of cellular and animal models lacking LRRK2 or its homologs (Tong et al., 2012). Conversely, the results obtained from the T1348N cell line were more surprising. Indeed, these cells could efficiently lipidate LC3 in response to nutrient deprivation, but failed to do so after the treatment with Torin-1. This result seems to collide with the mTOR-independent regulation of autophagy by LRRK2 and the abnormal response to starvation observed in fibroblasts bearing PD-mutations in LRRK2 (Manzoni et al., 2013b; Manzoni et al., 2016), and might imply that Roc integrity is participating to the dynamics of the process through a more articulated mechanism. However, it is important to underline that, in most cases, we observed a decrease in LC3-I rather than an increase in LC3-II after autophagy-inducing treatment. This is not surprising, since the literature reports that LC3-I tends to decrease during short starvation periods and to disappear during longer periods of nutrient deprivation (Mizushima and Yoshimori, 2007). Given the high level of basal activation that we observed in these cell lines through different methodologies, it is possible that the autophagosome turnover is particularly high, and for this reason we were not able to detect a significant increase of lipidated LC3. We are currently performing some EM analysis on untreated samples, as well as on samples where we induced and/or blocked the autophagic flux, in order to check for any ultrastructural alterations in the autophagosomal appearance. On the other side, the differential response observed in terms of p62 between the two treatments was very reproducible among the genotypes. In particular, p62 tended to accumulate with

starvation, while being rapidly degraded after Torin-1 treatment. One simple possibility is that the starvation protocol has not fully induced macroautophagy. To double check for this, it is possible to follow the degradation of alternative cargo proteins, e.g. NBR1 (neighbour of BRCA1 gene), or to monitor the cascades initiated by mTOR inactivation and/or AMPK activation, exploiting specific phospho-antibodies against the members of the pathway. However, this result is not surprising, if we consider that the specificity and the time scale of the two stimuli are very different, and points out how the choice of a treatment in place of a different one, and the consequent interpretation of the results, must be extremely careful. Indeed, while Torin-1 is specifically inhibiting mTOR kinase activity, nutrient deprivation induces autophagy by activating a broader range of pathways – e.g. serum starvation initiates the mTOR cascade, whereas glucose starvation promotes AMPK-mediated signalling (Chen et al., 2014; Hardie and Lin, 2017). Finally, the immunofluorescence analysis revealed a basal condition of stress/hyperactivation in our cell lines, that strengthens the evidence of elevated LC3 lipidation as shown by WB. This is coherent with their macrophagic nature, since macrophages always maintain an active autophagic/phagocytic machinery to readily face any inflammatory threat within the body (Vural and Kehrl, 2014; Bah and Vergne, 2017), but has to be taken into account as it could hamper a detailed study of the autophagic process in this cell line.

Overall, our data suggest that a functional GTPase domain is essential for the stability of Lrrk2, but in terms of basal autophagic machinery is only affecting the levels of p62. Conversely, its integrity might be fundamental in the ability to respond to specific stimuli and in the activation of certain pathways.

Chapter 5

**Exploring the GTP-binding domain of LRRK2
as a platform for signalling outputs**

9. Introduction

9.1 LRRK2 at the crossroad between autophagy and cytoskeletal dynamics

In the previous chapters, we have comprehensively discussed the relevance of LRRK2 in autophagy-related cascades. We mentioned how LRRK2 is likely acting as a negative regulator of autophagy, influencing different steps of the pathway. Indeed, either its knockout or the inhibition of its kinase activity promote autophagosome formation, while enlarged lysosomes accumulate, in a phenotype that is shared among LRRK2 pathological mutations (Tong et al., 2012; Manzoni et al., 2013a; Dodson et al., 2014; Henry et al., 2015). Despite a quite clear phenotypical characterisation, however, the molecular signalling underlying this effect is only partially understood. In this regard, one still unresolved question is related to the contribution of other domains, in addition to the kinase, in the determination of signal specificity. For example, besides the dual, cross-talking enzymatic activity, LRRK2 possesses a WD40 domain that might acquire particular relevance in this pathway being a common motif among many autophagic proteins due to its ability to bind phosphoinositide (Lystad and Simonsen, 2016). An additional degree of complication adds up if we consider the well-established relation of LRRK2 with the cytoskeleton.

The association between LRRK2 and cytoskeletal elements has been reported multiple times (Parisiadou and Cai, 2010). Initially, Gandhi and co-authors demonstrated the interaction between Roc and tubulins (Gandhi et al., 2008), proposing a link of LRRK2 with microtubules (MTs). MTs are essential in guaranteeing the trafficking between the cell body and the periphery and in mediating synaptic plasticity (Parisiadou and Cai, 2010; Kapitein and Hoogenraad, 2015). Later on, this connection was reinforced by the evidence of a co-localisation between LRRK2 and βIII-tubulin in mouse brain (Lin et al., 2009) and the phosphorylation of mouse-purified β-tubulin by recombinant human LRRK2 (Gillardon, 2009). This phosphorylation, occurring at T107, was shown to be significantly increased by the G2019S mutation, and was suggested to enhance MT stability in the presence of MT-associated proteins (Gillardon, 2009). LRRK2

has also been associated with tubulin acetylation. Back in 2014, LRRK2-KO models were shown to display increased β-tubulin acetylation, suggesting that LRRK2 binding to MTs might interfere with the process (Law et al., 2014). Interestingly, R1441C and Y1699C-LRRK2 selectively bind deacetylated MTs *in vitro* and this was proposed to explain, at least partially, the impairment in axonal transport observed in primary neurons and in Drosophila, given that prevention of MT deacetylation was sufficient to rescue this phenotype (Godena et al., 2014). LRRK2 also interacts with tau and promotes its phosphorylation *via* cyclin-dependent kinase 5 (Cdk5) (Shanley et al., 2015). Of note, mutant G2019S-LRRK2 – but not WT – markedly enhances neuron-to-neuron transmission of tau in mice (Nguyen et al., 2018), supporting the pathological evidence that a subgroup of LRRK2 patients exhibit tau pathology (Rajput et al., 2006)..

In addition to MTs, LRRK2 also binds actin *in vitro* and promotes its polymerisation (Meixner et al., 2011). As previously mentioned, in neurons actin is fundamental for neurite outgrowth and synapse formation and maintenance (Parisiadou and Cai, 2010). LRRK2 phosphorylates moesin, one of the ERM proteins that, together with ezrin and radixin, connects the actin cytoskeleton to the plasma membrane (Jaleel et al., 2007). ERMs are localised at the actin-rich sites in filopodia, where they orchestrate neurite outgrowth by organising filopodia architecture (Mangeat et al., 1999). Importantly, when neurons isolated from G2019S-LRRK2/Lrrk2 mouse models are cultured *in vitro*, they display a reduced neuritic complexity as compared with the non-transgenic counterpart (MacLeod et al., 2006; Sepulveda et al., 2013; Civiero et al., 2017b) and both phosphorylated ERMs and F-actin-enriched filopodia are increased in G2019S-LRRK2 neurons, which might be a partial justification for such defects (Parisiadou et al., 2009).

In the context of defining the outgrowth and complexity of the neuritic network, a particularly relevant role is covered by PAK6. PAK6 is a guanine nucleotide-dependent interactor of LRRK2-Roc, that was initially identified through a high-throughput proto-array screening conducted by our lab in collaboration with Dr. Mark Cookson at NIH (Beilina et al., 2014), and subsequently validated with multiple techniques (Civiero et al., 2015; Civiero et al., 2017b). PAKs are serine-threonine kinases with key roles in signal transduction. The family is subdivided into type I PAKs (PAK1-3), that are activated by Rho GTPase binding, and type II

PAKs (PAK4-6) that are re-localised – but not activated – by GTPases to specific signalling sites and locally activated by binding with SH3 domains and consequent release of pseudo-substrate inhibition (Civiero and Greggio, 2018). One of the best-established roles of PAKs is related to actin cytoskeleton remodelling *via* the LIM kinase (LIMK)-cofilin pathway. Activated PAKs phosphorylate LIMK1, in turn phosphorylating cofilin. The functional meaning of this phosphorylation is the inhibition of cofilin actin-severing activity. Therefore, PAKs initiate a phosphorylation cascade ultimately leading to the stabilisation of F-actin (Minden, 2012; Civiero et al., 2015). Interestingly, PAK6 displays high and almost exclusive expression in the brain, particularly in the dopaminergic fibres of the *SNpc* (Mahfouz et al., 2016). Pak6 knockout mice are viable and fertile, whereas double Pak5/Pak6 KO models exhibit cognitive and locomotor activity defects, as well as neurite shortening (Nekrasova et al., 2008). Previous work from the lab demonstrated that active PAK6 stimulates neurite complexity *in vivo* in the striatum in a LRRK2-dependent manner, indicating a cooperation between the two kinases in actin-dependent neurite-remodelling (Civiero et al., 2015). More recently, we showed that the two proteins bidirectionally modulate each other, since PAK6 can influence LRRK2 phospho-state in a pathway involving the phosphorylation of the common interactor 14-3-3γ (Civiero et al., 2017b). Indeed, phosphorylation of 14-3-3γ by PAK6 induces loss of affinity for LRRK2 phospho-Ser935, which is left unprotected and can be readily dephosphorylated (Figure 20) (Civiero et al., 2017b). Of note, phosphorylation of Ser910/935 and, consequently, 14-3-3 binding, are reduced in the majority of LRRK2 pathogenic mutants, a biochemical state that can be phenocopied by LRRK2 pharmacological inhibition (Nichols et al., 2010). Intriguingly, dephosphorylated LRRK2 redistributes into MTs and vesicle-related structures (Nichols et al., 2010; Kett et al., 2012). Moreover, PAK6 overexpression is able to rescue the defects in neurite outgrowth associated with the G2019S-LRRK2 pathological mutation through this pathway (Figure 21) (Civiero et al., 2017b). This set of data highlights the importance of 14-3-3s in influencing LRRK2 cellular redistribution and substrates/partners availability, suggesting a possible explanation of the reason why Roc-COR pathogenic mutants phosphorylate substrates, e.g. Rab proteins, to a higher extent as compared to the G2019S mutant (Steger et al., 2016), which is structurally

affecting the kinase domain, and indeed has consequences also on *in vitro* kinase activity. In addition, it supports the idea that LRRK2 is very likely involved in the regulation of multiple pathways, according to its compartmentalisation and the macro-complexes in which it is integrated, as well as to the cell-type in which it is expressed. In this regard, expression of G2019S-LRRK2 in microglia was shown to retard the response to brain injury *via* exerting a negative regulation on focal adhesion kinase (FAK), with a consequent impairment in microglial motility (Choi et al., 2015). This idea of LRRK2 behaving as a multifaceted protein hints at a broader regulation of the cellular traffic and, more specifically, the autophagic pathway, involving a strict interplay between vesicles and the cytoskeletal machinery.
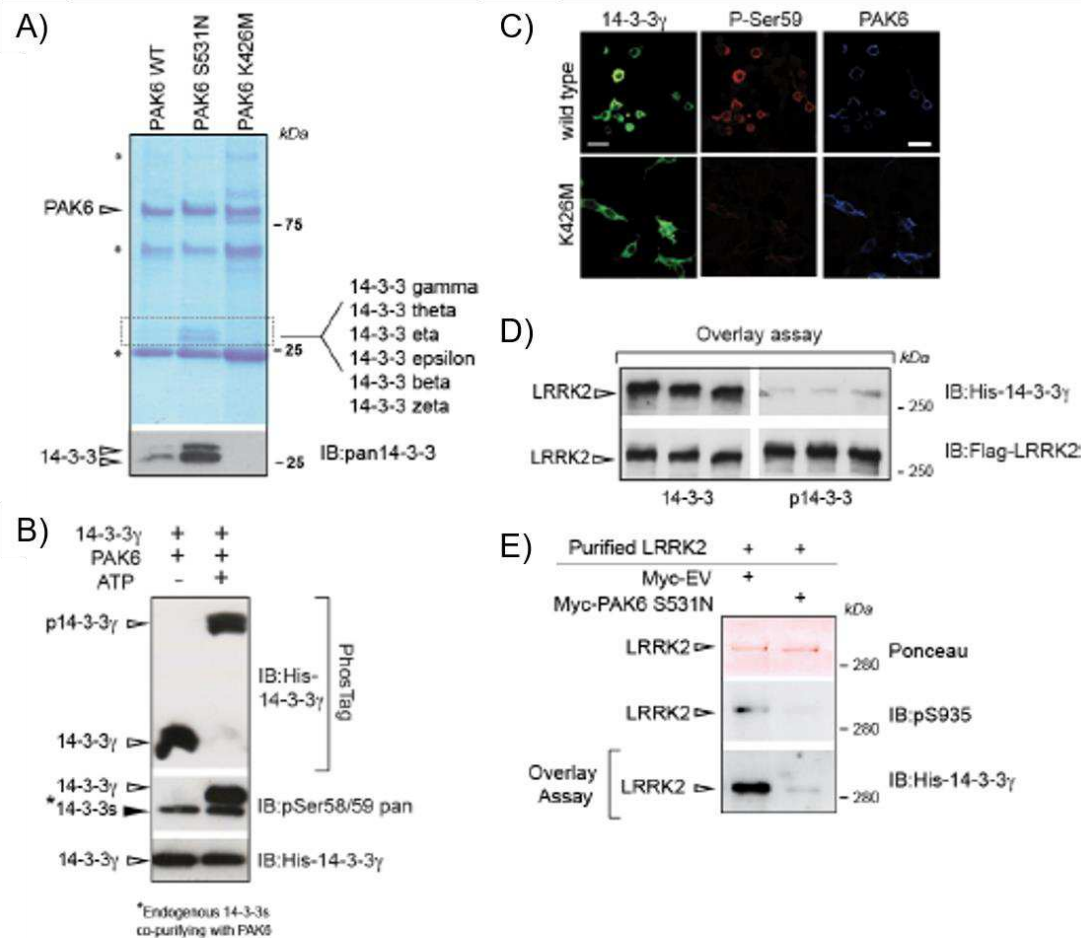
Figure 20. Interplay between LRRK2, PAK6 and 14-3-3γ. (A) Active PAK6 (i.e. WT and the hyper-active S531N mutant) but not a kinase-dead form (K436M) can pull-down endogenous 14-3-3s. (B) PAK6 phosphorylates 14-3-3γ *in vitro* at S59. (C) ICC in HEK293T cells confirms that WT,

but not kinase-dead PAK6 phosphorylates 14-3-3γ in cells. (D) Overlay assays prove that 14-3-3γ phosphorylated by PAK6 loses affinity for LRRK2. (E) The cellular consequence of PAK6 kinase activity on LRRK2 is the dephosphorylation of P-Ser935 and the impaired binding of 14-3-3γ, as demonstrated by immunoprecipitation and overlay assays (adapted from Civiero et al., *Frontiers of Molecular Neuroscience*, 2017b).
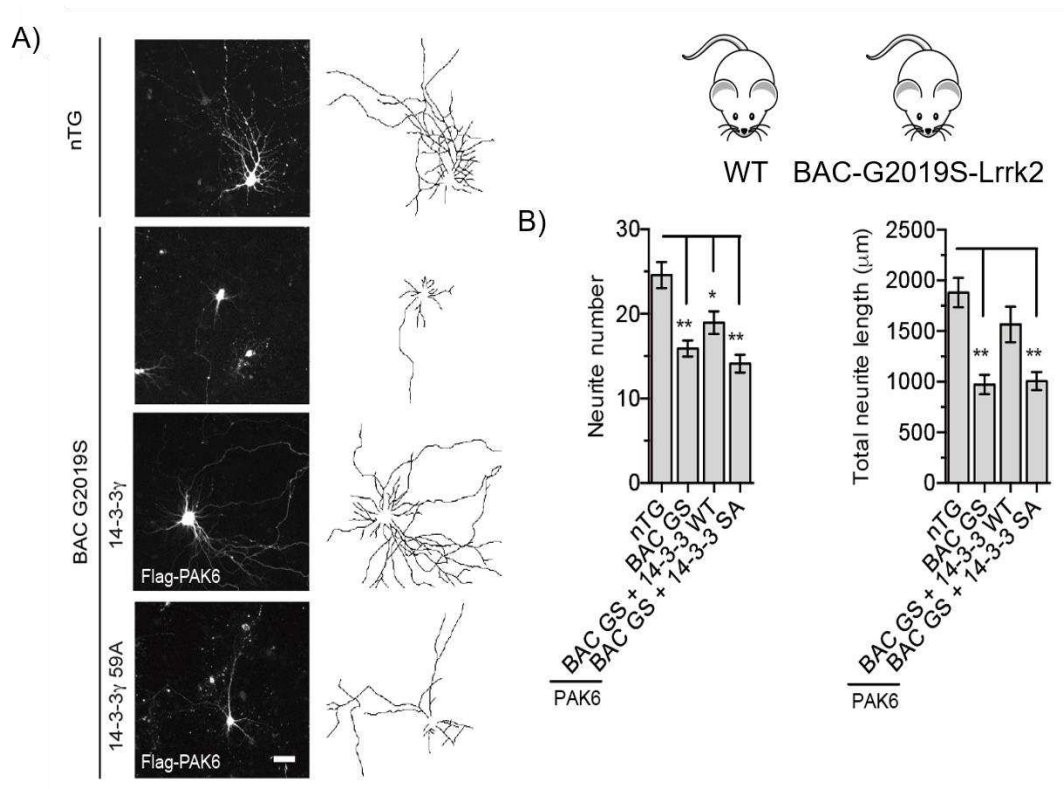
Figure 21. G2019S-Lrrk2 neurite shortening is restored by PAK6-mediated 14-3-3γ phosphorylation. (A) Representative images of primary neurons from nTg and BAC G2019S-Lrrk2 mice transfected with an empty vector or 3xFlag-PAK6 S531N together with YFP-14-3-3γ WT and the non "phosphorylatable" S59A form. mCherry was employed to trace neurites. (B) Neurite number and length were quantified with the NeuronJ plugin from ImageJ (n=3 independent cultures; n=30-40 neurons traced; mean ± SEM; two-way ANOVA with Turkey's multiple comparison test; *P≤0.05 and **P≤0.01) (adapted from Civiero et al., *Frontiers of Molecular Neuroscience*, 2017b).

That microfilaments and MTs play essential roles in coordinating the delivery of membranes first and shaped vesicles later during autophagy is nowadays well acknowledged, even though the mechanistic details of the process have not been fully uncovered yet. Despite the first indications from yeast that actin cytoskeleton only participates to selective forms of autophagy (Reggiori et al., 2005; reviewed in Monastyrska et al., 2009), studies conducted in mammalian cells suggest that it is also required for the autophagic response to starvation (Aguilera et al., 2012). Interestingly, the KO of *Atg7* – a key autophagy gene whose protein product is involved in the pathway of LC3 lipidation (Xiong, 2015) – in mouse causes severe defects in actin organisation (Zhuo et al., 2013). In addition, recent work in mammalian models attributes to the actin cytoskeleton the important tasks of i) providing and supporting the membranes for the formation of the autophagosome, ii) loading the growing phagophore with the materials that need to be digested and iii) guiding, in cooperation with MTs, the shaped autophagosomes to the lysosomes throughout the cell (reviewed in Kruppa et al., 2016; Kast and Dominguez, 2017). In this scenario, LRRK2 might contribute to the regulation of autophagy not only through a direct action on the autophagic machinery (e.g. by phosphorylation of key autophagic components, like the membrane curvature inducing protein EndophilinA – Soukup and Verstreken, 2017), but also in a more indirect way involving the remodelling of actin cytoskeleton. It is indeed known that an actin scaffold helps shaping the autophagosome, and that the severing protein cofilin takes part in actin redistribution (Mi et al., 2015). Thus, LRRK2 pathological mutations might lead to an aberrant activation of the PAK6/LIMK1/cofilin pathway, with defects in microfilament recruitment and/or mobilisation and, eventually, consequences on autophagosome formation. In addition to this, PAK1 has been implicated in autophagy and, in particular, either downregulation or inhibition of its kinase activity have been identified as the trigger of the AKT/mTOR/ULK1 cascade (Dou et al., 2016; Wang et al., 2016; Wang et al., 2017b). Even though PAK6 has yet to be associated to this event, we cannot exclude the involvement of the LRRK2-PAK6 axis in multiple, parallel pathways ultimately converging to the same cellular process.

10. Results

The robust results generated in our laboratory in support of a key role for the LRRK2-PAK6 complex in shaping the neuronal network (Civiero et al., 2015; Civiero et al., 2017b), with possible implications for PD, led us to pursue the investigation of possible additional pathways in which the complex is involved, as well as the mechanisms that might underlie the deregulated processes during pathology. As an initial confirmation of the close interplay between these two proteins, we obtained some preliminary data suggesting that the expression of both Lrrk2 and Pak6 increases from DIV9 to DIV14 in primary murine cortical neurons (Figure 22A). Moreover, when we compared Lrrk2 and Pak6 expression levels during postnatal mouse development in WT versus BAC-G2019S brains, we similarly observed a coupled pattern of expression, with a maximum for both proteins at P28 in the range of time analysed. Strikingly, Pak6 levels were dramatically reduced in BAC-G2019S brains (Figure 22B and C), pointing towards a possible negative regulation on Pak6 expression operated by Lrrk2. Considered the role of PAK6 in promoting neurite outgrowth, this observation might, at least partially, justify the reduced length and complexity of the neurites observed in neurons cultured from these mice (Figure 21). In such a scenario, during these years I had the possibility to begin the exploration of the involvement of the LRRK2-PAK6 complex in multiple cellular processes and analyse different biochemical aspects of the interaction. In particular, we first aimed at further characterising the physiological role(s) of PAK6, by investigating its possible involvement in a novel pathway, i.e. autophagy. Second, we performed a biochemical, cellular and functional characterisation of the LRRK2-PAK6 complex in presence of a putative *de novo* mutation in PAK6. Finally, we evaluated how the presence of a PD mutation in LRRK2 affects the binding with PAK6. The following paragraphs will provide an overview of our work in different contexts and through the use of several models and techniques.

Figure 22. Lrrk2 and Pak6 show overlapping expression profiles in mouse brain. Preliminary data from time courses of Lrrk2 and Pak6 expression in (A) primary cortical neurons and (B) whole brain lysates from postnatal day 0 to postnatal day 28 reveal compatible patterns of expression for the two proteins (n=1). (C) The trend of Pak6 expression -normalised to Gapdh - over time is maintained but the BAC-G2019S brains show reduced levels of Pak6 at all time points.

10.1 Exploring the role of the LRRK2-PAK6 complex in the autophagic pathway

10.1.1 Pharmacological inhibition of PAKs alters autophagic markers

The fact that a functional cytoskeleton is essential for a proper autophagic flux (Kast and Dominguez, 2017), the influence exerted by the LRRK2-PAK6 complex in regulating actin dynamics (Civiero et al., 2015; Civiero et al., 2017b), the established role of LRRK2 and the possible impact of PAK6 on the autophagic pathway (Dou et al., 2016; Wang et al., 2016; Manzoni, 2017), led us to wonder whether PAK6 plays a role in the autophagic process and whether this is LRRK2-

dependent.

Using a pharmacological approach with the small ATP analogue PF-3758309 (hereafter referred to as PAKs PF) active against type II PAKs, we have initially evaluated the autophagic response of H4 cells (human brain neuroglioma) to different doses of inhibitor. We selected this cell line given that it was previously shown to constitute a good model to follow autophagy (Manzoni et al., 2013a; Manzoni et al., 2016), and it endogenously expresses PAK6 (Figure 23).
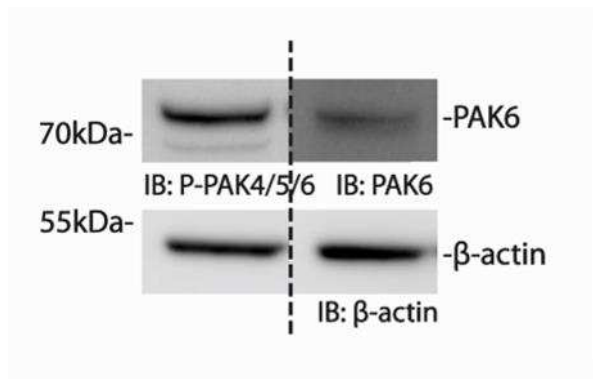
Figure 23. Endogenous expression of PAK6 in H4 cells. Antibodies against total PAK6 and the autophosphorylation Ser560 residue in PAK6 (Ser474 in PAK4, Ser602 in PAK5) were employed for the detection. The lower band in the top left gel is likely to be phospho-PAK4.

We initially subjected H4 cells to either 2.5 or 10µM PAKs PF for 90 minutes, and included 200nm Torin-1 as a positive control. Figure 24 shows how inhibition of type II PAKs with the highest dose of PAKs PF, i.e. 10µM, induces an alteration in the monitored autophagic markers, particularly in LC3 lipidation. Of note, 10µM corresponds to the dose that was previously shown to effectively inhibit PAK6 in a number of cell systems (Civiero et al., 2017b). Since the results obtained from this initial treatment looked promising, we followed this up and performed an additional dose-response experiment with additional inhibitor doses to evaluate whether 10µM was the optimal concentration to adopt in our experimental conditions. We therefore tested 1, 2.5, 5 and 10µM PAKs PF and observed a dose-dependent response to the treatment by H4 cells (Figure 25A). The interpretation of this experiment is partially impeded by some technical issues. First, the negative control is unexpectedly activated in terms of autophagy, as can be appreciated by the high levels of LC3-II. Second, the treatment with Torin-1, predicted to act as a positive control, did not give the expected response, especially for ULK1 dephosphorylation, which is expected to be completely

abolished. However, when we plotted LC3-II levels normalised to β-actin against the employed dose of PAKs PF inhibitor, we could clearly appreciate the concentration-dependent behaviour, suggesting that we were observing an autophagic response proportional to the degree of PAKs inhibition (Figure 25B).
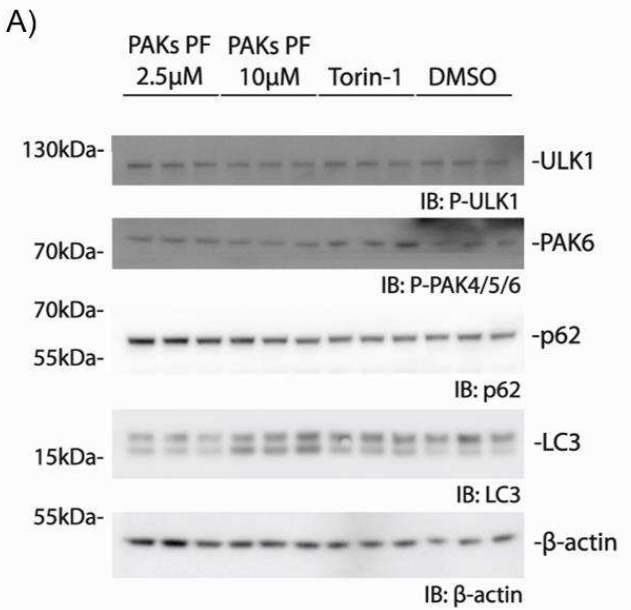
Figure 24. Inhibition of PAKs induces LC3 lipidation. (A) WB showing the impact of type II PAKs inhibition on the autophagic markers analysed. In particular, 10µM PAKs PF promotes the production of LC3-II. Quantification of LC3 and p62 is shown in (B) (n=3 technical replicates; mean ± SEM; one-way ANOVA with Turkey's multiple comparison test; *P≤0.05; **P≤0.01; ***P≤0.001).
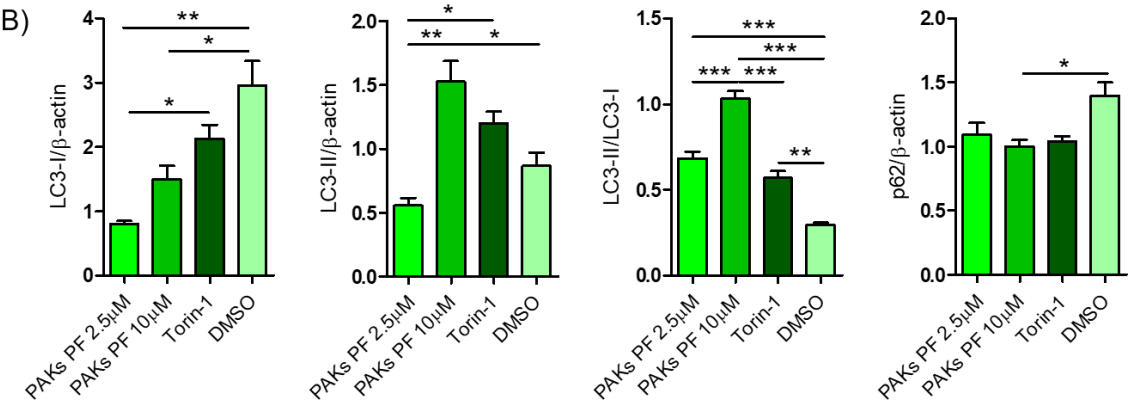
Once established 10µM PAKs PF as a working condition, we wondered whether the duration of the treatment could also influence the autophagic response. We therefore performed a time-course experiment subjecting H4 cells to different times of treatment (from 1 to 4 hours). We indeed inferred that the alteration in the autophagic markers induced by 10µM PAKs PF increases over time, since after 4 hours of treatment we could appreciate a clear

dephosphorylation of ULK1, a neat degradation of p62 and a sharp LC3-II band as compared to controls (Figure 26).
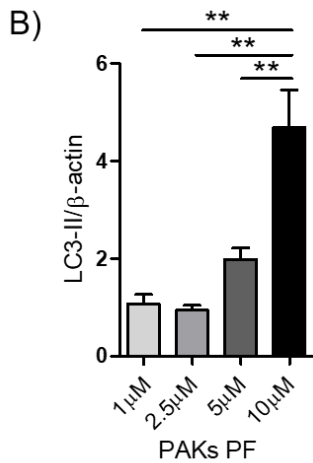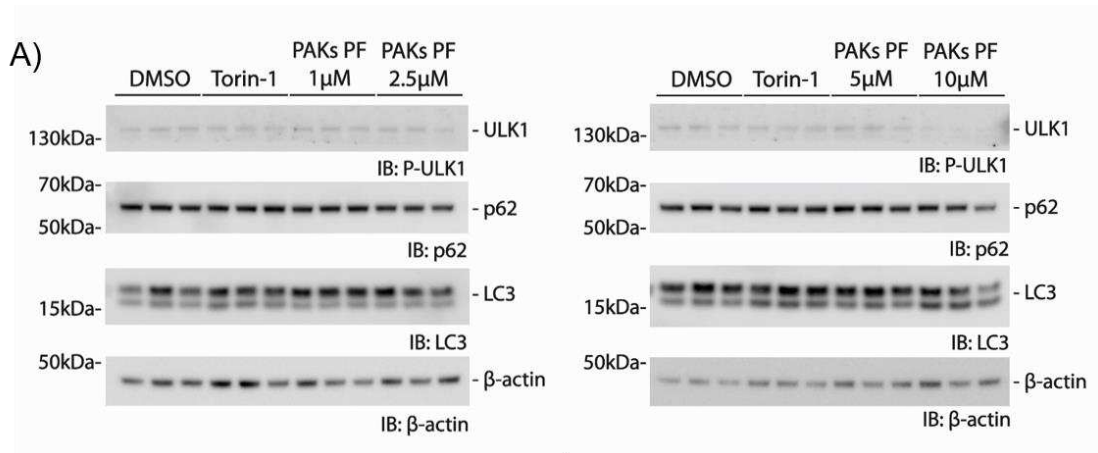
Figure 25. 10µM PAKs PF induces alterations in autophagic markers. Representative (A) WB and (B) histogram related to LC3-II/β-actin increase in dependence of the dose of PAKs PF inhibitor administered to H4 cells. Cells were treated with increasing concentrations of PAKs PF to establish i) the working dose and ii) the possible presence of an impact on the autophagic pathway. Torin-1 was employed as a positive control for autophagy induction (n=2 independent experiments; n=3 technical replicates per experiment; mean ± SEM; normalisation over the mean of DMSO control samples was employed to compare values between different gels; one-way ANOVA with Turkey's multiple comparison test; **P≤0.01).
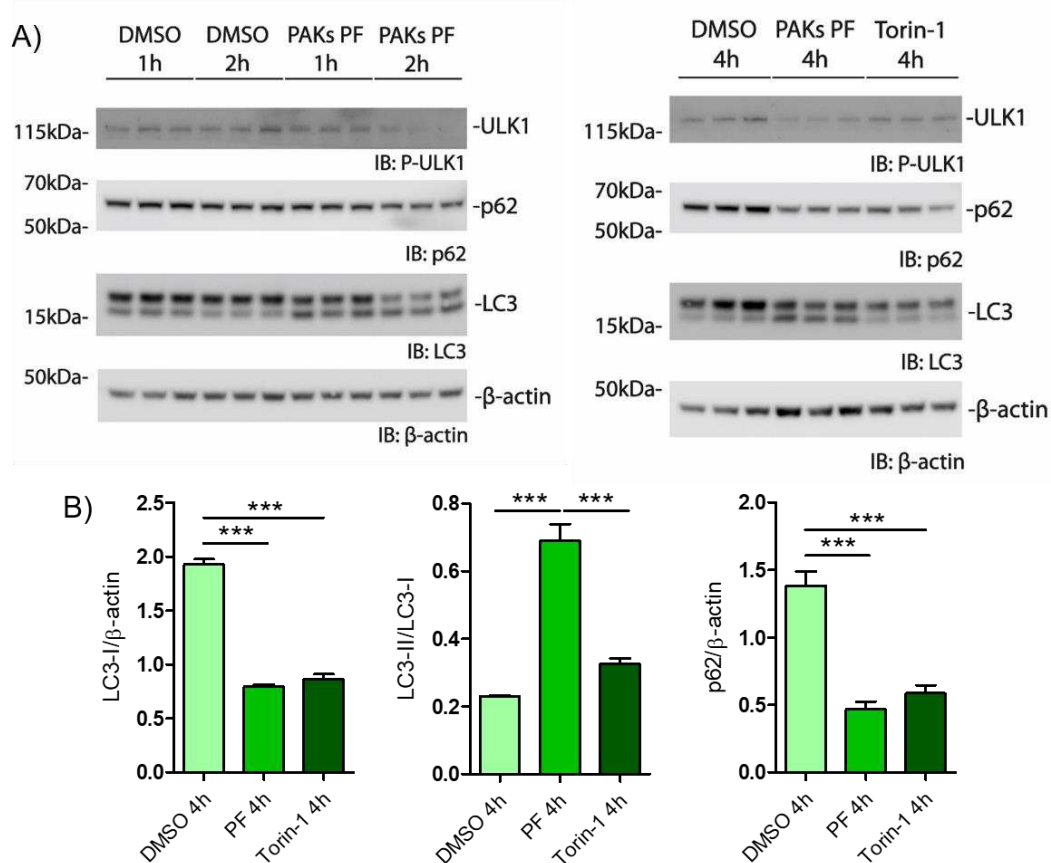
Figure 26. PAKs PF treatment has a time-dependent effect on autophagic markers. H4 cells show a clear alteration in ULK1 phosphorylation, LC3 lipidation and p62 levels after a 4-hour treatment with PAKs PF. (A) Representative WB with the relative quantification shown in (B). Torin-1 was employed as a positive control for autophagy induction (n=2 independent experiments; n=3 technical replicates per experiment; mean ± SEM; one-way ANOVA with Turkey's multiple comparison test; ***P≤0.001).

10.1.2   LRRK2 and PAK6 likely exert independent effects on autophagy

Finally, we wanted to address whether the effect of PAKs inhibition on the autophagic process was dependent on LRRK2. We therefore looked at the consequences of single and combined inhibition of LRRK2 and PAK6 kinase activities, employing LRRK2 IN-1 together with PAKs PF. Interestingly, we observed that the two proteins appear to influence autophagy through two different pathways: while LRRK2 inhibition operates *via* Beclin-1, as previously

reported (Manzoni et al., 2016), our data suggest that PAK6 is involved in the mTOR/ULK1 cascade, as PAK6 inhibition causes dephosphorylation of ULK1, which is absent when LRRK2 kinase activity is pharmacologically blocked (Figure 27). Interestingly, in terms of LC3 lipidation, a combination of the two compounds resulted in an intermediate phenotype with respect to the single treatment.
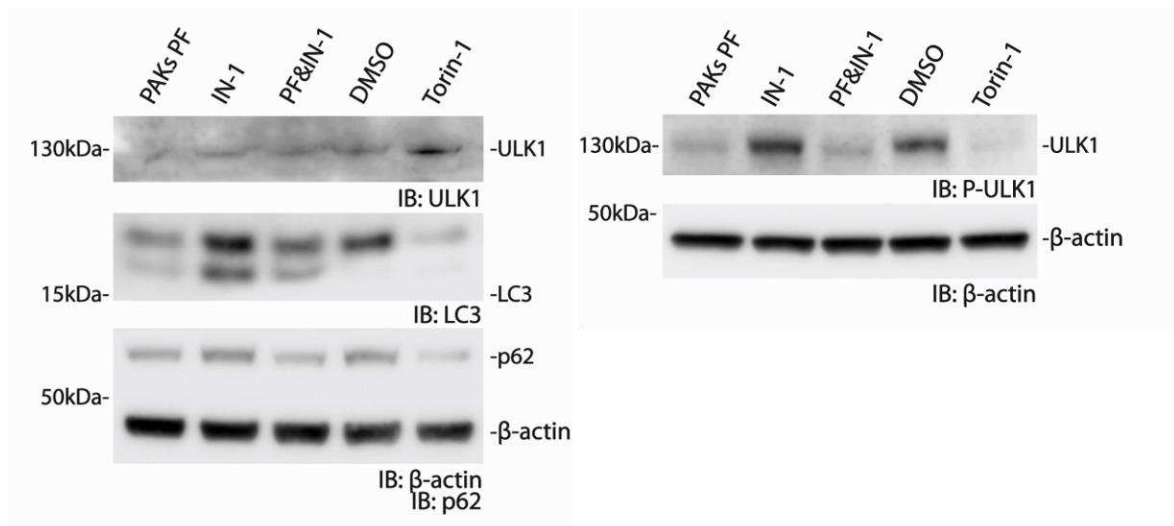
Figure 27. PAK6 and LRRK2 kinase inhibition induces autophagy through parallel pathways. Representative image of single and combined inhibition of PAK6 and LRRK2 kinase activity with PAKs PF and IN-1, respectively, showing that the two proteins have a different impact on the autophagic markers analysed (n=4 independent experiments; n=3 technical replicates per experiment).

10.2 Biochemical, cellular and functional characterisation of the *de novo* S236L substitution in PAK6

In the context of the LRRK2-PAK6 interaction, we had the possibility to collaborate in a very exciting project aimed at the identification of a *de novo*, causative mutation leading to a form of infantile parkinsonism, in collaboration with Simone Martinelli's group at the Istituto Superiore di Sanità in Rome. The young subject displayed clear motor symptoms at 6 months of age and severe neurological deterioration at 10 months of age. After exclusion of the known variants in known juvenile parkinsonism/dystonia-associated genes, whole exome

sequencing (WES) revealed three *de novo* substitutions within candidate genes having an established role in the nervous system, namely *CHRNA6* and *PAK6*, or highly expressed in cultured neurons, i.e. *HIBADH*. *CHRNA6* codes for the α6 subunit of neuronal nicotinic acetylcholine receptors (Albuquerque et al., 2009) while *HIBADH* encodes a mitochondrial 3-hydroxyisobutyrate dehydrogenase enzyme, which is highly expressed in the liver, kidney, muscle, and cultured neurons (Murín et al., 2008). The missense change in PAK6 leads to the S236L mutation. Despite the poor conservation of the residue, the predicted weak impact of the aminoacid variation and its position in the N-terminal region far away from the kinase domain, given the interaction between PAK6 and LRRK2 and the established association of *LRRK2* with PD (Civiero et al., 2015), we characterised the effects of the S236L substitution in terms of kinase activity, binding to LRRK2, subcellular localisation and impact on neurite outgrowth.

10.2.1 Biochemical and cellular characterisation of S236L-PAK6

Given that PAK6 ability of mediating neurite outgrowth depends on its kinase activity (Civiero et al., 2015), we initially tested whether the S236L mutation interferes with PAK6 kinase activity. To do so, we performed *in vitro* kinase assays using purified proteins to measure autophosphorylation activity with radiolabelled γ^{33}P-ATP *in vitro* or assessed autophosphorylation of PAK6 Ser560 – which is a reliable indicator of PAK6 activation *status* (Civiero et al., 2015) – in HEK293T cells. As shown in Figure 28A-B, both assays demonstrated that WT and mutant PAK6 display similar catalytic activity, which is in line with the location of Ser236 outside of the kinase domain. The next step was to evaluate whether S236L-PAK6 interferes with the binding to LRRK2 as compared with WT-PAK6, using pull-down assays. We therefore immunopurified 3xFlag-tagged WT or S236L-PAK6, as well as 3xFlag-GFP as a negative control, and incubated them with a cell lysate overexpressing GFP-LRRK2. As shown in Figure 28C-D, we did not observe any differential binding between LRRK2 and WT or S236L-PAK6. Since LRRK2 is required to promote PAK6 activation in cells (Civiero et al., 2015), we then measured the activation state of S236L-PAK6 compared to WT in the presence of LRRK2 overexpression in HEK293T cells. WB analysis with anti-

phospho-Ser560 did not reveal any aberrant activation in S236L-PAK6 (Figure 28E-F).
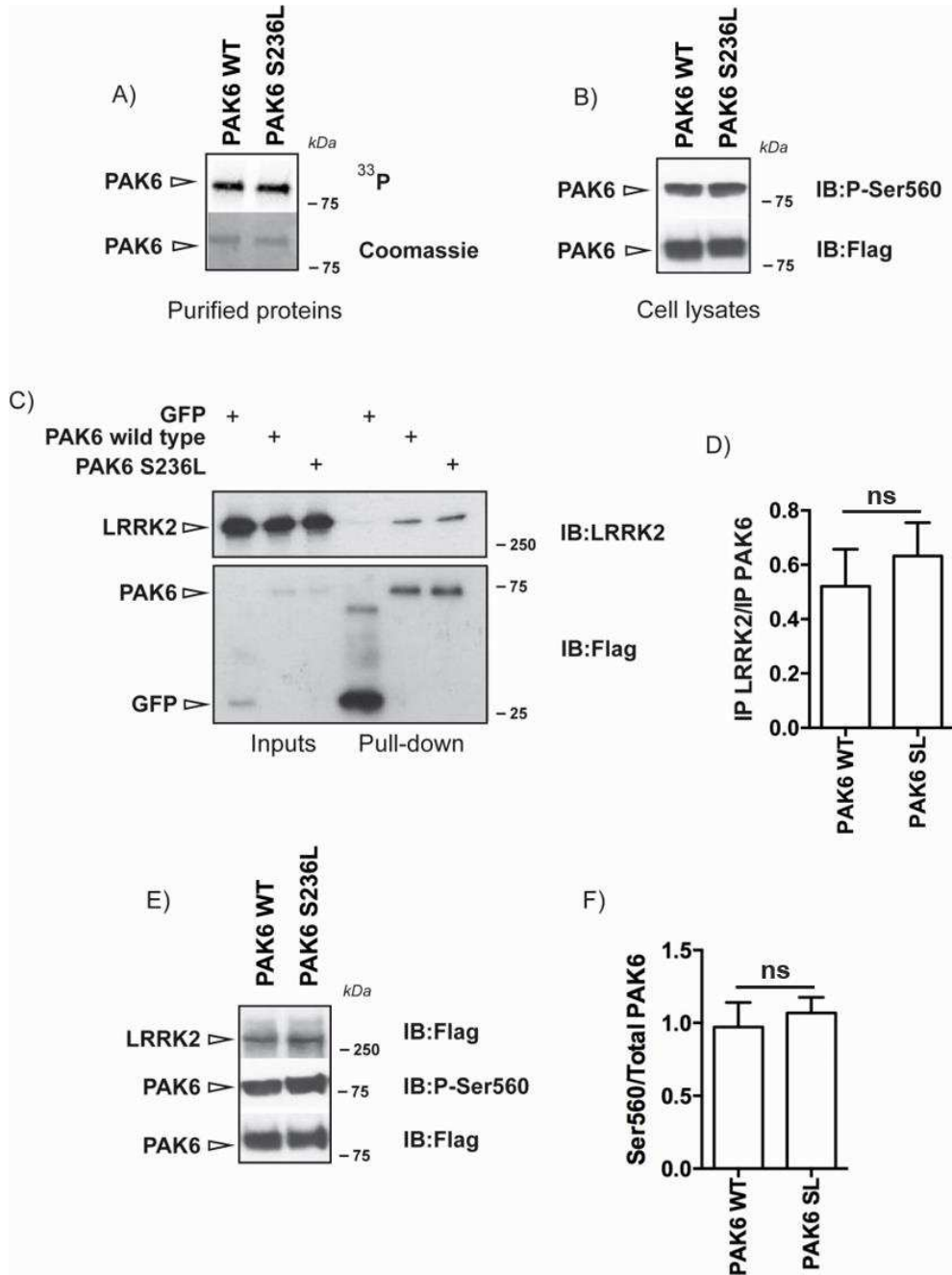
Figure 28. Biochemical characterization of S236L-PAK6. (A) S236L-PAK6 does not display differential kinase activity compared to WT *in vitro*. Recombinant 3xFlag-PAK6 WT and S236L were purified and subjected to kinase assays *in vitro* upon the addition of γ^{33}P-ATP-Mg^{2+}. PAK6 kinase activity was measured by monitoring the incorporation of ^{33}P. (B) Mutant PAK6 does not show aberrant activation compared to WT. 3xFlag-PAK6 WT and S236L were transfected in HEK293T

cells and PAK6 activation was monitored by WB analysis of cell lysates with an α-phospho-Ser560 antibody. (C-D) WT and mutant PAK6 display similar affinity for LRRK2. 3xFlag-PAK6 WT, S236L or control 3xFlag-GFP bound to M2-Flag agarose beads were incubated with cell lysates expressing GFP-LRRK2. After washing, interaction was revealed by WB with α-LRRK2 antibody. Quantification of bound LRRK2 normalised by pulled-down PAK6 is shown in (D) (n=3 independent experiments; n=3 technical replicates per experiment; mean ± SEM; one-way ANOVA with Turkey's multiple comparison test). (E-F) Phosphorylation tone of mutant PAK6 in cells does not show any difference compared to WT in the presence of LRRK2. 3xFlag-PAK6 WT and S236L were transfected in HEK293T cells together with GFP-LRRK2 and PAK6 activation was monitored by probing cell lysates with α-phospho-Ser560 antibody. Quantifications of phospho-PAK6 normalised by total protein are shown in F (n=3 independent experiments; n=3 technical replicates per experiment; mean ± SEM; unpaired t-test) (adapted from Martinelli et al., in preparation).

Finally, the subcellular distribution of WT and S236L-PAK6 were similar, as well as the degree of co-localisation with F-actin both in absence and presence of LRRK2 overexpression (Figure 29).
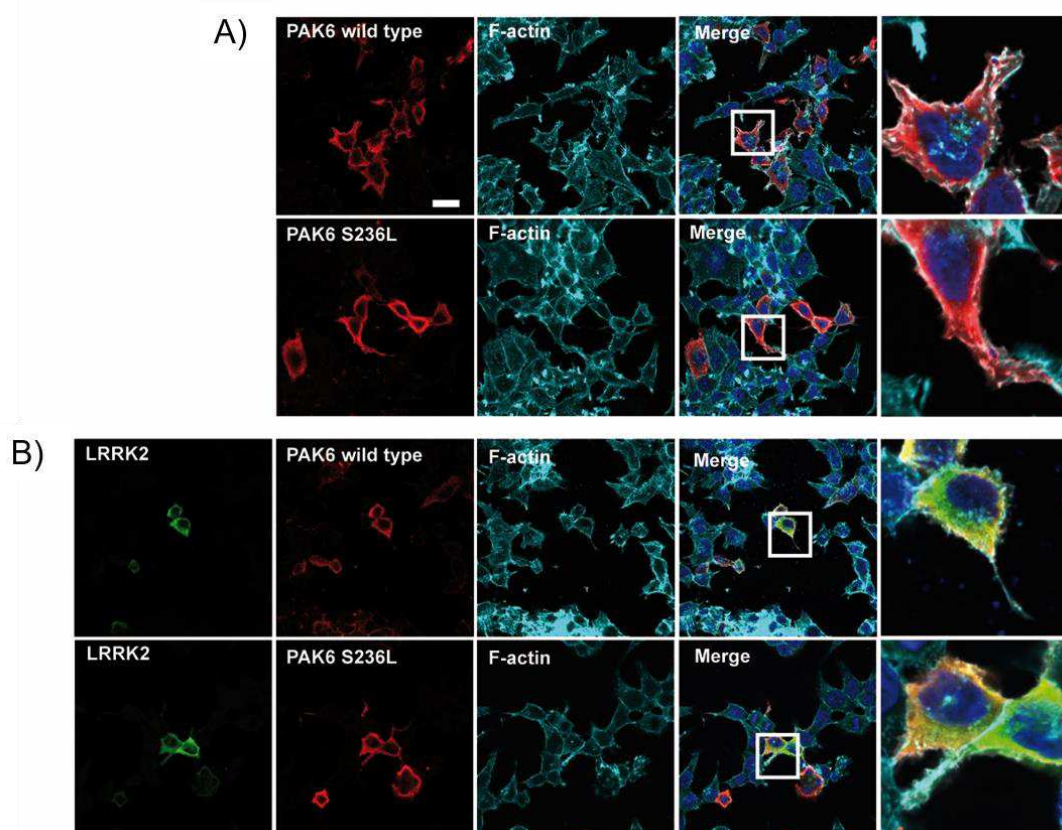
Figure 29. Cellular localization of S236L-PAK6. (A) Mutant PAK6 does not show differential cellular localisation compared to WT. 3xFlag-PAK6 WT and S236L were transfected in HEK293T

cells and their localisation analysed using an antibody against PAK6 (red). Cells were co-stained with phalloidin to mark F-actin (cyan). DAPI stains nuclei in blue. Scale bar is 20 μm. (B) Expression of LRRK2 does not induce re-localisation of WT neither of mutant PAK6. 3xFlag-PAK6 WT or S236L were co-transfected with GFP-LRRK2 (green) in HEK293T cells and their localisation was assessed using antibodies against PAK6 (red). GFP is in green, phalloidin in cyan. DAPI stains nuclei in blue. Scale bar is 20 μm (adapted from Martinelli et al., in preparation).

10.2.2 The S236L substitution in PAK6 does not affect neurite outgrowth

Since PAK6 promotes neurite outgrowth and branching in its active conformation (Civiero et al., 2015), we next investigated whether S236L-PAK6 affects this process. Primary cortical neurons were transfected with 3xFlag-PAK6 WT or S236L together with GFP, or with GFP only as a control, and the fluorescent signal from GFP was exploited to trace the processes. Coherently with the previous observations that S236L-PAK6 does not alter kinase activity, we did not observe any significant differences in the number of neurites and in the total neurite length in primary neurons overexpressing S236L-PAK6 compared with cells expressing the WT protein or the GFP vector (Figure 30).
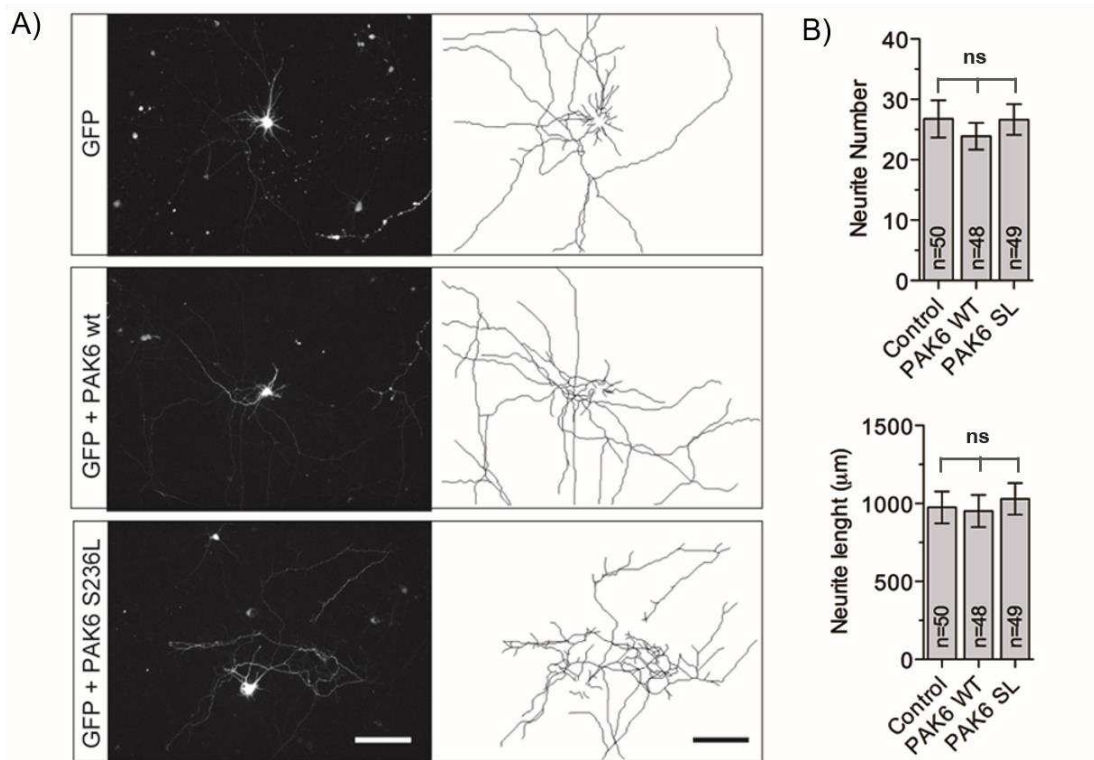
Figure 30. The S236L substitution in PAK6 does not influence its ability to promote neurite outgrowth. (A) Representative images of primary neurons transfected with GFP together with 3xFlag-PAK6 WT or 3xFlag-PAK6 S236L and GFP alone as a control. Scale bar is 30μm. (B) Quantification of neurite length and number by two-way ANOVA with Bonferroni *post-hoc* test for all variants. Data were collected from two independent cultures. Around 50 transfected neurons were traced in total (bars represent the mean ± SEM) (adapted from Martinelli et al., in preparation).

10.3 How do Roc-COR pathological mutations impact on the interaction with PAK6?

Given the robustly confirmed interaction between LRRK2 and PAK6 (Beilina et al., 2014; Civiero et al., 2015; Civiero et al., 2017b) and their established role in shaping the neuritic network, both in physiological (WT versus KO models) and pathological (WT versus BAC-G2019S models) conditions, we subsequently focused on a more "pathologically-relevant" scenario. Indeed, we are currently assessing whether and how Roc-COR mutations influence the interaction.

10.3.1 The variability of pull-down assays makes them inadequate to detect differences in the interaction between mutant LRRK2 and PAK6

Firstly, to compare the binding affinity of WT and mutant – R1441C and Y1699C – LRRK2 towards PAK6, we set up a pull-down assay between immuno-purified 3xFlag-PAK6 from HEK293T cells and HEK293T cell lysates over-expressing either 2xmyc-GFP, GFP-LRRK2 WT, GFP-LRRK2 R1441C or GFP-LRRK2 Y1699C. With this assay, we confirmed that GFP-LRRK2 WT, R1441C and Y1699C, are able to interact with PAK6. However, we did not appreciate a significant difference in the interaction between GFP-LRRK2 WT and mutants (Figure 31), which could be partially due to the high variability we observed during this experiment. Indeed, in contrast to the interaction between WT-LRRK2 and WT or S236L-PAK6 where we have obtained very reproducible data among the replicates, this was not the case when comparing the binding between WT-PAK6 and mutant LRRK2, indicating that the strategic location of the mutations could

potentially have a subtle effect on the binding, but the experimental setup was not sensitive enough to reveal statistically significant differences.
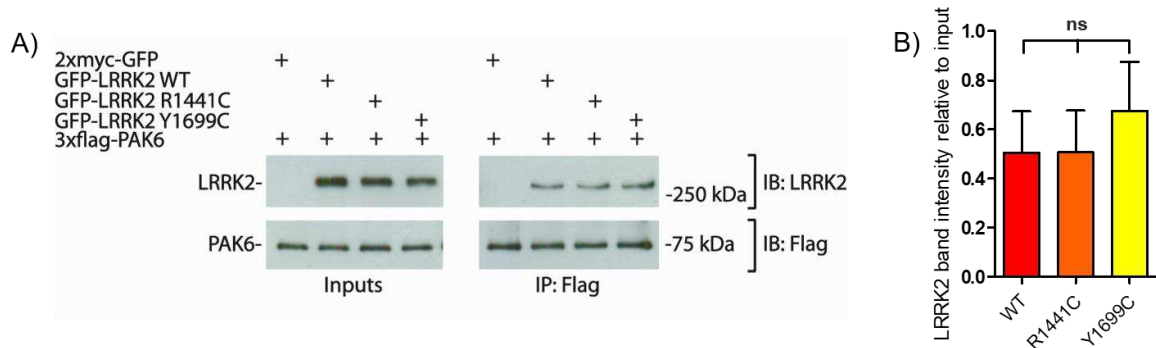
Figure 31. Pull-down assays are not sensitive enough to detect variations in the binding between LRRK2 and PAK6. (A) 3xFlag-PAK6 WT bound to M2-Flag agarose beads was incubated with cell lysates expressing 2xmyc-GFP, GFP-LRRK2 WT, R1441C or Y1699C. After washing, interaction was revealed by WB with an α-LRRK2 antibody. Quantification of bound LRRK2 normalised by the input is shown in (B) (n=3 technical replicates; mean ± SEM; one-way ANOVA with Turkey's multiple comparison test).

10.3.2   SPR reveals a reduced affinity of R1441C-Roc for PAK6

To acquire sensitivity in measuring the interaction between LRRK2 and PAK6, we decided to move to SPR. With this technique, we were able to further confirm the formation of the complex, in presence of the full-length proteins. More interestingly, we could also compare the binding affinities of WT and mutant Roc-COR fragments, purified from *E. coli*, for PAK6, chemically immobilised on a chip.

The data obtained from these experiments are summarised in Table 3. Briefly, since it was possible to calculate the K_D for all the tested conditions, we could appreciate an affinity in the nM range (0.080±0.004µM) between full-length LRRK2 and PAK6. With respect to the Roc-COR fragments, the affinity was approximately 10-fold lower for what concerns WT and Y1699C-Roc-COR as compared to full-length LRRK2, but as much as 100-fold lower for R1441C-Roc-COR. These data suggest that mutations in the Roc, but not in the COR domain,

display a weakening effect on the interaction with PAK6. Additional replicates are required to gain the statistical power to test this robustly.

Ligand	Analyte	K_D (µM)	Chip configuration
Roc-COR WT	PAK6	0.46±0.03	
PAK6	Roc-COR WT	0.37±0.12	
PAK6	Roc-COR R1441C	3.81±0.92	
PAK6	Roc-COR Y1699C	0.87±0.04	
PAK6	LRRK2	0.080±0.004	

*In the presence of GppCp, DTT and MgCl$_2$

Table 3. SPR results suggest that the R1441C pathological mutation in the Roc domain, but not the Y1699C in the COR, affects the binding to PAK6. GppCp is a non-hydrolysable analogue of GTP.

11.   Discussion

We previously showed that PAK6 interacts with LRRK2 Roc domain in its GTP bound state (Civiero et al., 2015), thus representing a putative effector of Roc/GTPase domain. PAK6 and LRRK2 interact to promote neurite complexity in the *striatum* by modulating actin dynamics via the LIMK/cofilin pathway. Given the robust link between LRRK2 and autophagy (reviewed in Manzoni, 2017) and between autophagy and the actin-cytoskeleton (Kast and Dominguez, 2017), combined with the evidence that a member of the PAK family has also been linked to this process (Dou et al., 2016; Wang et al., 2016), we asked whether PAK6 participates in the LRRK2-mediated autophagic pathway. We chose H4 cells as a model to test our hypothesis through a pharmacological approach based on the small ATP-analogue PF-3758309, which inhibits the kinase activity of type II PAKs. H4 cells derive from a human brain neuroglioma, and constitute an excellent model for our purposes for a handful of reasons. First, they on average display very low or null levels of basal autophagy, whose changes can therefore be easily detected and measured. However, some conditions such as the degree of confluency or the passage can promote basal autophagy in these cells – as in most cell lines –, therefore a careful experimental setup is required when analysing and/or manipulating this pathway. Second, PAK6 is highly and almost exclusively expressed in the brain (Mahfouz et al., 2016), meaning that i) we could work with the endogenous protein and ii) the data we obtained possibly refer to a conserved pathway in our tissue of interest. Overall, we can conclude from our preliminary evaluation that inhibition of type II PAKs has a clear and robust impact on autophagic markers. However, based on our current data, we are still unable to state whether we are observing an induction or a blockade of the flux, even though the decrease in p62 levels might point towards the direction of increased autophagic flux. Further experiments with a combination of PAKs PF and Bafilomycin A1 (which inhibits the fusion between the autophagosome and the lysosome) are required to answer this question. Moreover, the PAKs PF inhibitor selectively targets type II PAKs. Therefore, to definitely confirm that we are observing an effect dependent on PAK6 and not on another member of the kinase

family (i.e. PAK4 or PAK5), shRNA-mediated knockdown of all the members of the family is desirable. In addition, as most ATP competitors, PAKs PF potentially possesses cellular activity agains off-target proteins, such as AMPK (Murray et al., 2010). Even though we expect that an inhibition of AMPK should lead to a blockade of the autophagic flux, additional controls are required to confirm the specifity of the results. In general, the observation that type II PAKs inhibition alters autophagic markers is interesting and novel per se. Moreover, our data suggest that is happening independently of LRRK2. This finding appears in line with the fact that LRRK2 is known to induce autophagy *via* Beclin-1, whereas PAK1 operates through the AKT/mTOR axis (Dou et al., 2016; Manzoni et al., 2016). Further investigation is required to delineate the molecular details in the signalling cascade. In addition, it will be important to confirm the result employing more specific LRRK2 inhibitors in addition to IN-1, e.g. the MLi-2 compound from Merck (Fell et al., 2015).

In the second part of the chapter, we performed a biochemical characterisation of the LRRK2-PAK6 complex, in presence of both PAK6 variants and PD-pathological mutations in LRRK2.

Initially, WES was employed to identify the disease-causing mutation in a child who experienced progressive neurological deterioration leading to a complete derangement of dopaminergic striatal pathways. WES analysis highlighted the presence of three *de novo* variants within genes that are highly expressed in cultured neurons – *HIBADH* – or play an established role in the nervous system – *CHRNA6* and *PAK6* – (Murín et al., 2008; Albuquerque et al., 2009; Civiero and Greggio; 2018). The S236L mutation in PAK6 is located in a poorly conserved residue outside of the kinase domain (Kumar et al., 2017), therefore we did not expect it to have a major impact on the overall properties of the protein. However, given the interaction with LRRK2 in regulating a highly relevant pathway for neuronal cells and the link of *LRRK2* with PD, in combination with the parkinsonism-like phenotype of the subject, a functional evaluation of the *de novo* variant was required. As expected, we did not find significant differences between WT and S236L-PAK6 in terms of kinase activity, localisation and neurite development as well as interaction with LRRK2. Collectively, these data indicate that the *de novo PAK6* variant does not affect significantly protein function and

PAK6-mediated cellular processes, making this change unlikely to play a major role in the patient's phenotype. Functional analysis conducted on the other two candidate genes indicated as probably causative a missense mutation in the *CHRNA6* gene, encoding the α6 subunits of nicotinic receptors (Martinelli et al., in preparation).

On the contrary, the integrity of LRRK2-Roc domain is required to support the interaction with PAK6. LRRK2-Roc and PAK6-CRIB – a small peptide located in the N-terminal region of PAK6 – were mapped as the interface mediating the binding (Civiero et al., 2015). Indeed, data from SPR suggest that the R1441C mutation, but not the Y1699C, weakens the interaction. However, these results refer to the isolated Roc-COR fragments. The limited yields that can be reached when purifying full-length LRRK2 make SPR unsuitable to calculate the K_Ds for all the mutants, due to the high amount of material required. On the other hand, we managed to calculate a K_D value for full-length, WT-LRRK2, which has been extremely informative. The 10-fold increase in affinity with the entire protein as compared to the Roc-COR bidomain suggests that other portions of LRRK2 participate in stabilising the binding. This idea is corroborated by the compactness of LRRK2 structure, as highlighted by the fine model provided by Guaitoli and colleagues and confirmed by subsequent studies (Guaitoli et al., 2016; Sejwal et al., 2017).

Confirmation of the data from SPR in a more physiological system is mandatory. One possibility we are currently setting up to further verify that the R1441C mutation is impacting on the interaction is to apply the CETSA technique to a fully endogenous system. In particular, we aim to compare the denaturation curve of PAK6 in WT, KO and R1441C mouse embryonic fibroblasts (MEFs). In this case, we selected MEFs because i) we are able to directly derive them from the mice, without the need to knockdown or transfect mutant LRRK2 and ii) they express reasonable amounts of PAK6. We expect to observe an increase of T_{agg50} in the WT sample as compared to KO, since interactions tend to slow down the aggregation process, while the R1441C mutant should display an intermediate behaviour. This method is an indirect but elegant way to demonstrate that the binding between LRRK2 and PAK6 is impaired in presence of the R1441C mutation. Importantly, if future experiments confirm that variations in the R1441

residue are associated with a reduced interaction also in a cellular context, we predict that PAK6 should no longer be able to rescue the neurite shortening phenotype, which has been reported also for mutations in the Roc domain of LRRK2 (Lavalley et al., 2016).

Chapter 6

General discussion

12. General discussion

In this work, we focused on the Roc/GTPase domain of LRRK2, since a comprehensive overview of the intra- and extra-molecular mechanisms of regulation of the protein and the signalling pathways it mediates is mandatory in order to fully predict the consequences of therapeutically targeting LRRK2. Moreover, since Roc itself displays an enzymatic activity – that can influence the kinase (Taymans et al., 2011; Biosa et al., 2013) – and it also operates as a signalling platform, it constitutes per se an intriguing target for drug discovery. The characterisation of the RAW264.7 cell lines from the MJFF corroborated previous findings from the literature, suggestive of an instability of T1348N-Lrrk2, with consequences on kinase activity and on its ability to form dimers (reviewed in Nguyen and Moore, 2017). Here, for the first time with endogenous proteins, we confirmed reduced steady-state levels of Lrrk2 when GTP/GDP binding is genetically eliminated, and tried to understand the mechanistic basis of the process. One possibility is that the GTP-binding deficient T1348N mutation, located in a key residue in the active site of the GTPase core, affects Lrrk2 folding, either structurally or due to the lack of binding with key ligands (e.g. nucleotides) or protein partners. The CHX treatment did not reveal gross changes in the half-life of T1348N-Lrrk2 compared to WT in our experimental conditions, suggesting that the pool of T1348N-Lrrk2 that is maintained by the cell essentially behaves similarly to its WT counterpart. This might imply that the remainder, large population of T1348N-Lrrk2 molecules is either very rapidly degraded by the stress pathways dealing with unproperly folded proteins (e.g. the unfolded protein response in the ER – Almanza et al., 2018) or re-distributed in different cellular compartments, such as insoluble inclusion bodies. Further experiments are required to shed light on the cellular mediators of T1348N-Lrrk2 instability.

In support of the requirement of Roc integrity for the proper function of LRRK2, the pathological R1441C mutation impairs the binding with PAK6, an interactor of GTP-bound Roc (Civiero et al., 2015). In contrast, this is not happening in the presence of a putative parkinsonism-causing substitution in a neutral position of PAK6 sequence, namely S236L.

The data obtained by analysing postnatal brain expression in WT versus BAC-G2019S support the idea of a negative regulation operated by Lrrk2 on Pak6 levels. BAC-G2019S mice overexpress a hyper-active form of murine Lrrk2, therefore this phenotype might depend on the overexpression, on the increase in kinase activity, or both. In case this is a kinase-dependent phenotype, we expect to confirm it in G2019S-Lrrk2 KI mice, as well as in R1441C-Lrrk2 KI models, given that LRRK2-Roc mutants also display an increase in kinase activity (Steger et al., 2016). As previously mentioned, neurons cultured from these mice exhibit a peculiar neurite shortening phenotype (MacLeod et al., 2006; Sepulveda et al., 2013; Civiero et al., 2017b), which might be partially explained by the reduction in Pak6 levels. Of note, we were able to rescue the reduction in neurite length and complexity in BAC-G2019S primary neurons through overexpression of PAK6, *via* a 14-3-3γ-mediated pathway (Civiero et al., 2017b). It will be now important to understand whether and to which extent the ability of PAK6 to restore a functional network is affected as a consequence of the impaired interaction with Lrrk2 in R1441C models. In general, given the protective role of PAK6 toward mutant LRRK2, we hypothesise that increasing PAK6 kinase activity may represent an appealing therapeutic target worth exploring. Supporting our extensive observations made with PAK6/Pak6, a recent study showed that expression of a constitutively active form of the homologous kinase Pak4 protects from DA neuron loss in the 6-hydroxydopamine (6-OHDA) and α-syn rat models through the CRTC1-CREB pathway (Won et al., 2016). Future studies addressing whether PAK6 activity ameliorates PD-associated neurodegeneration will conclusively prove or disprove this hypothesis.

In conclusion, after fifteen years of research on LRRK2, the molecular mechanisms that underlie toxicity and potentially initiate neurodegeneration start to be uncovered in greater detail. Despite some dearth of knowledge regarding certain biochemical and cellular aspects of LRRK2-PD, research progresses at a rapid pace, preparing the ground for exciting advances in the therapeutic management of one of the most common neurodegenerative movement disorders.

Bibliography

Aasly, J.O., Vilariño-Güell, C., Dachsel, J.C., Webber, P.J., West, A.B., Haugarvoll, K., Johansen, K.K., Toft, M., Nutt, J.G., Payami, H., et al. (2010). Novel pathogenic LRRK2 p.Asn1437His substitution in familial Parkinson's disease. Mov. Disord. *25*, 2156–2163.

Agalliu, I., San Luciano, M., Mirelman, A., Giladi, N., Waro, B., Aasly, J., Inzelberg, R., Hassin-Baer, S., Friedman, E., Ruiz-Martinez, J., et al. (2015). Higher frequency of certain cancers in LRRK2 G2019S mutation carriers with Parkinson disease: a pooled analysis. JAMA Neurol *72*, 58–65.

Aguilera, M.O., Berón, W., and Colombo, M.I. (2012). The actin cytoskeleton participates in the early events of autophagosome formation upon starvation induced autophagy. Autophagy *8*, 1590–1603.

Albuquerque, E.X., Pereira, E.F.R., Alkondon, M., and Rogers, S.W. (2009). Mammalian Nicotinic Acetylcholine Receptors: From Structure to Function. Physiological Reviews *89*, 73–120.

Alegre-Abarrategui, J., Christian, H., Lufino, M.M.P., Mutihac, R., Venda, L.L., Ansorge, O., and Wade-Martins, R. (2009). LRRK2 regulates autophagic activity and localizes to specific membrane microdomains in a novel human genomic reporter cellular model. Hum. Mol. Genet. *18*, 4022–4034.

Almanza, A., Carlesso, A., Chintha, C., Creedican, S., Doultsinos, D., Leuzzi, B., Luís, A., McCarthy, N., Montibeller, L., More, S., et al. (2018). Endoplasmic reticulum stress signalling - from basic mechanisms to clinical applications. FEBS J.

Andén, N.E., Carlsson, A., Kerstell, J., Magnusson, T., Olsson, R., Roos, B.E., Steen, B., Steg, G., Svanborg, A., Thieme, G., et al. (1970). Oral L-dopa treatment of parkinsonism. Acta Med Scand *187*, 247–255.

Antecol, M.H., Darveau, A., Sonenberg, N., and Mukherjee, B.B. (1986). Altered biochemical properties of actin in normal skin fibroblasts from individuals predisposed to dominantly inherited cancers. Cancer Res. *46*, 1867–1873.

Athanasopoulos, P.S., Jacob, W., Neumann, S., Kutsch, M., Wolters, D., Tan, E.K., Bichler, Z., Herrmann, C., and Heumann, R. (2016). Identification of protein phosphatase 2A as an interacting protein of leucine-rich repeat kinase 2. Biol. Chem. *397*, 541–554.

Axelsson, H., Almqvist, H., Seashore-Ludlow, B., and Lundbäck, T. (2004). Screening for Target Engagement using the Cellular Thermal Shift Assay - CETSA. In Assay Guidance Manual, G.S. Sittampalam, N.P. Coussens, K. Brimacombe, A. Grossman, M. Arkin, D. Auld, C. Austin, J. Baell, B. Bejcek, J.M.M. Caaveiro, et al., eds. (Bethesda (MD): Eli Lilly & Company and the National Center for Advancing Translational Sciences), p.

Bah, A., and Vergne, I. (2017). Macrophage Autophagy and Bacterial Infections. Front Immunol *8*, 1483.

Ballatore, C., Lee, V.M.-Y., and Trojanowski, J.Q. (2007). Tau-mediated neurodegeneration in Alzheimer's disease and related disorders. Nat. Rev. Neurosci. *8*, 663–672.

Bang, Y., Kim, K.-S., Seol, W., and Choi, H.J. (2016). LRRK2 interferes with aggresome formation for autophagic clearance. Mol. Cell. Neurosci. *75*, 71–80

Batzoglou, S. (2000). Human and Mouse Gene Structure: Comparative Analysis and Application to Exon Prediction. Genome Research *10*, 950–958.

Beach, T.G., Adler, C.H., Lue, L., Sue, L.I., Bachalakuri, J., Henry-Watson, J., Sasse, J., Boyer, S., Shirohi, S., et al. (2009). Unified staging system for Lewy body disorders: correlation with nigrostriatal degeneration, cognitive impairment and motor dysfunction. Acta Neuropathologica *117*, 613–634.

Beilina, A., Rudenko, I.N., Kaganovich, A., Civiero, L., Chau, H., Kalia, S.K., Kalia, L.V., Lobbestael, E., Chia, R., Ndukwe, K., et al. (2014). Unbiased screen for interactors of leucine-rich repeat kinase 2 supports a common pathway for sporadic and familial Parkinson disease. Proc. Natl. Acad. Sci. U.S.A. *111*, 2626–2631.

Belluzzi, E., Gonnelli, A., Cirnaru, M.-D., Marte, A., Plotegher, N., Russo, I., Civiero, L., Cogo, S., Carrion, M.P., Franchin, C., et al. (2016). LRRK2 phosphorylates pre-synaptic N-ethylmaleimide sensitive fusion (NSF) protein enhancing its ATPase activity and SNARE complex disassembling rate. Mol Neurodegener *11*, 1.

Berger, Z., Smith, K.A., and Lavoie, M.J. (2010). Membrane localization of LRRK2 is associated with increased formation of the highly active LRRK2 dimer and changes in its phosphorylation. Biochemistry *49*, 5511–5523.

Biosa, A., Trancikova, A., Civiero, L., Glauser, L., Bubacco, L., Greggio, E., and Moore, D.J. (2013). GTPase activity regulates kinase activity and cellular phenotypes of Parkinson's disease-associated LRRK2. Hum. Mol. Genet. *22*, 1140–1156.

Birkmayer, W., and Hornykiewicz, O. (1961). [The L-3,4-dioxyphenylalanine (DOPA)-effect in Parkinson-akinesia]. Wien. Klin. Wochenschr. *73*, 787–788.

Bjørkøy, G., Lamark, T., Pankiv, S., Øvervatn, A., Brech, A., and Johansen, T. (2009). Chapter 12 Monitoring Autophagic Degradation of p62/SQSTM1. In Methods in Enzymology, (Elsevier), pp. 181–197.

Blauwendraat, C., Reed, X., Kia, D.A., Gan-Or, Z., Lesage, S., Pihlstrøm, L., Guerreiro, R., Gibbs, J.R., Sabir, M., Ahmed, S., et al. (2018). Frequency of Loss

of Function Variants in LRRK2 in Parkinson Disease. JAMA Neurol *75*, 1416–1422.

Bonifati, V. (2003). Mutations in the DJ-1 Gene Associated with Autosomal Recessive Early-Onset Parkinsonism. Science *299*, 256–259.

Bové, J., Prou, D., Perier, C., and Przedborski, S. (2005). Toxin-induced models of Parkinson's disease. NeuroRx *2*, 484–494.

Braak, H., Vos, R.A.I. de, Jansen, E.N.H., Bratzke, H., and Braak, E. (1998). Chapter 20 Neuropathological hallmarks of Alzheimer's and Parkinson's diseases. In Progress in Brain Research, (Elsevier), pp. 267–285.

Braak, H., Del Tredici, K., Rüb, U., de Vos, R.A.I., Jansen Steur, E.N.H., and Braak, E. (2003). Staging of brain pathology related to sporadic Parkinson's disease. Neurobiol. Aging *24*, 197–211.

Bravo-San Pedro, J.M., Niso-Santano, M., Gómez-Sánchez, R., Pizarro-Estrella, E., Aiastui-Pujana, A., Gorostidi, A., Climent, V., López de Maturana, R., Sanchez-Pernaute, R., López de Munain, A., et al. (2013). The LRRK2 G2019S mutant exacerbates basal autophagy through activation of the MEK/ERK pathway. Cell. Mol. Life Sci. *70*, 121–136.

Cao, M., Wu, Y., Ashrafi, G., McCartney, A.J., Wheeler, H., Bushong, E.A., Boassa, D., Ellisman, M.H., Ryan, T.A., and De Camilli, P. (2017). Parkinson Sac Domain Mutation in Synaptojanin 1 Impairs Clathrin Uncoating at Synapses and Triggers Dystrophic Changes in Dopaminergic Axons. Neuron *93*, 882–896.e5.

Carlsson, A., Lindqvist, M., and Magnusson, T. (1957). 3,4-Dihydroxyphenylalanine and 5-hydroxytryptophan as reserpine antagonists. Nature *180*, 1200.

Carlsson, A., Lindqvist, M., Magnusson, T., and Waldeck, B. (1958). On the presence of 3-hydroxytyramine in brain. Science *127*, 471.

Chang, D., Nalls, M.A., Hallgrímsdóttir, I.B., Hunkapiller, J., van der Brug, M., Cai, F., International Parkinson's Disease Genomics Consortium, 23andMe Research Team, Kerchner, G.A., Ayalon, G., et al. (2017). A meta-analysis of genome-wide association studies identifies 17 new Parkinson's disease risk loci. Nat. Genet. *49*, 1511–1516.

Chartier-Harlin, M.-C., Kachergus, J., Roumier, C., Mouroux, V., Douay, X., Lincoln, S., Levecque, C., Larvor, L., Andrieux, J., Hulihan, M., et al. (2004). Alpha-synuclein locus duplication as a cause of familial Parkinson's disease. Lancet *364*, 1167–1169.

Chen, R., Zou, Y., Mao, D., Sun, D., Gao, G., Shi, J., Liu, X., Zhu, C., Yang, M., Ye, W., et al. (2014). The general amino acid control pathway regulates mTOR and autophagy during serum/glutamine starvation. J. Cell Biol. *206*, 173–182.

Chia, R., Haddock, S., Beilina, A., Rudenko, I.N., Mamais, A., Kaganovich, A., Li, Y., Kumaran, R., Nalls, M.A., and Cookson, M.R. (2014). Phosphorylation of LRRK2 by casein kinase 1α regulates trans-Golgi clustering via differential interaction with ARHGEF7. Nature Communications *5*.

Cho, H.J., Yu, J., Xie, C., Rudrabhatla, P., Chen, X., Wu, J., Parisiadou, L., Liu, G., Sun, L., Ma, B., et al. (2014). Leucine-rich repeat kinase 2 regulates Sec16A at ER exit sites to allow ER-Golgi export. EMBO J. *33*, 2314–2331.

Choi, I., Kim, B., Byun, J.-W., Baik, S.H., Huh, Y.H., Kim, J.-H., Mook-Jung, I., Song, W.K., Shin, J.-H., Seo, H., et al. (2015). LRRK2 G2019S mutation attenuates microglial motility by inhibiting focal adhesion kinase. Nature Communications *6*, 8255.

Ciechanover, A., and Kwon, Y.T. (2015). Degradation of misfolded proteins in neurodegenerative diseases: therapeutic targets and strategies. Exp. Mol. Med. *47*, e147.

Cingolani, L.A., and Goda, Y. (2008). Actin in action: the interplay between the actin cytoskeleton and synaptic efficacy. Nat. Rev. Neurosci. *9*, 344–356.

Civiero, L., Vancraenenbroeck, R., Belluzzi, E., Beilina, A., Lobbestael, E., Reyniers, L., Gao, F., Micetic, I., De Maeyer, M., Bubacco, L., et al. (2012). Biochemical characterization of highly purified leucine-rich repeat kinases 1 and 2 demonstrates formation of homodimers. PLoS ONE *7*, e43472.

Civiero, L., Cirnaru, M.D., Beilina, A., Rodella, U., Russo, I., Belluzzi, E., Lobbestael, E., Reyniers, L., Hondhamuni, G., Lewis, P.A., et al. (2015). Leucine-rich repeat kinase 2 interacts with p21-activated kinase 6 to control neurite complexity in mammalian brain. J. Neurochem. *135*, 1242–1256.

Civiero, L., Russo, I., Bubacco, L., and Greggio, E. (2017a). Molecular Insights and Functional Implication of LRRK2 Dimerization. In Leucine-Rich Repeat Kinase 2 (LRRK2), H.J. Rideout, ed. (Cham: Springer International Publishing), pp. 107–121.

Civiero, L., Cogo, S., Kiekens, A., Morganti, C., Tessari, I., Lobbestael, E., Baekelandt, V., Taymans, J.-M., Chartier-Harlin, M.-C., Franchin, C., et al. (2017b). PAK6 Phosphorylates 14-3-3γ to Regulate Steady State Phosphorylation of LRRK2. Front Mol Neurosci *10*, 417.

Civiero, L., and Greggio, E. (2018). PAKs in the brain: Function and dysfunction. Biochim Biophys Acta Mol Basis Dis *1864*, 444–453.

Cirnaru, M.D., Marte, A., Belluzzi, E., Russo, I., Gabrielli, M., Longo, F., Arcuri, L., Murru, L., Bubacco, L., Matteoli, M., et al. (2014). LRRK2 kinase activity regulates synaptic vesicle trafficking and neurotransmitter release through modulation of LRRK2 macro-molecular complex. Front Mol Neurosci *7*, 49.

Cogo, S., Greggio, E., and Lewis, P.A. (2017). Leucine Rich Repeat Kinase 2: beyond Parkinson's and beyond kinase inhibitors. Expert Opin. Ther. Targets *21*, 751–753.

Cook, D.A., Kannarkat, G.T., Cintron, A.F., Butkovich, L.M., Fraser, K.B., Chang, J., Grigoryan, N., Factor, S.A., West, A.B., Boss, J.M., et al. (2017). LRRK2 levels in immune cells are increased in Parkinson's disease. NPJ Parkinsons Dis *3*, 11.

Cromm, P.M., Spiegel, J., Grossmann, T.N., and Waldmann, H. (2015). Direct Modulation of Small GTPase Activity and Function. Angew. Chem. Int. Ed. Engl. *54*, 13516–13537.

Daniëls, V., Vancraenenbroeck, R., Law, B.M.H., Greggio, E., Lobbestael, E., Gao, F., De Maeyer, M., Cookson, M.R., Harvey, K., Baekelandt, V., et al. (2011). Insight into the mode of action of the LRRK2 Y1699C pathogenic mutant. J. Neurochem. *116*, 304–315.

Dauer, W., and Przedborski, S. (2003). Parkinson's disease: mechanisms and models. Neuron *39*, 889–909.

Davies, P., Hinkle, K.M., Sukar, N.N., Sepulveda, B., Mesias, R., Serrano, G., Alessi, D.R., Beach, T.G., Benson, D.L., White, C.L., et al. (2013). Comprehensive characterization and optimization of anti-LRRK2 (leucine-rich repeat kinase 2) monoclonal antibodies. Biochem. J. *453*, 101–113.

De Duve, C. (1963). The lysosome. Sci. Am. *208*, 64–72.

Deng, X., Dzamko, N., Prescott, A., Davies, P., Liu, Q., Yang, Q., Lee, J.-D., Patricelli, M.P., Nomanbhoy, T.K., Alessi, D.R., et al. (2011). Characterization of a selective inhibitor of the Parkinson's disease kinase LRRK2. Nat. Chem. Biol. *7*, 203–205.

Deng, H., Gao, K., and Jankovic, J. (2013). The VPS35 gene and Parkinson's disease. Mov. Disord. *28*, 569–575.

Deng, H., and Yuan, L. (2014). Genetic variants and animal models in SNCA and Parkinson disease. Ageing Research Reviews *15*, 161–176.

Deng, H., Wang, P., and Jankovic, J. (2018). The genetics of Parkinson disease. Ageing Res. Rev. *42*, 72–85.

Desplats, P., Lee, H.-J., Bae, E.-J., Patrick, C., Rockenstein, E., Crews, L., Spencer, B., Masliah, E., and Lee, S.-J. (2009). Inclusion formation and neuronal cell death through neuron-to-neuron transmission of -synuclein. Proceedings of the National Academy of Sciences *106*, 13010–13015.

Deyaert, E., Wauters, L., Guaitoli, G., Konijnenberg, A., Leemans, M., Terheyden, S., Petrovic, A., Gallardo, R., Nederveen-Schippers, L.M., Athanasopoulos, P.S., et al. (2017a). A homologue of the Parkinson's disease-associated protein LRRK2

undergoes a monomer-dimer transition during GTP turnover. Nat Commun *8*, 1008.

Deyaert, E., Kortholt, A., and Versées, W. (2017b). The LRR-Roc-COR module of the Chlorobium tepidum Roco protein: crystallization and X-ray crystallographic analysis. Acta Crystallogr F Struct Biol Commun *73*, 520–524.

Deverman, B.E., Ravina, B.M., Bankiewicz, K.S., Paul, S.M., and Sah, D.W.Y. (2018). Gene therapy for neurological disorders: progress and prospects. Nat Rev Drug Discov *17*, 641–659.

Devine, M.J., Kaganovich, A., Ryten, M., Mamais, A., Trabzuni, D., Manzoni, C., McGoldrick, P., Chan, D., Dillman, A., Zerle, J., et al. (2011). Pathogenic LRRK2 mutations do not alter gene expression in cell model systems or human brain tissue. PLoS ONE *6*, e22489.

Dodson, M.W., Leung, L.K., Lone, M., Lizzio, M.A., and Guo, M. (2014). Novel ethyl methanesulfonate (EMS)-induced null alleles of the Drosophila homolog of LRRK2 reveal a crucial role in endolysosomal functions and autophagy in vivo. Dis Model Mech *7*, 1351–1363.

Dou, Q., Chen, H.-N., Wang, K., Yuan, K., Lei, Y., Li, K., Lan, J., Chen, Y., Huang, Z., Xie, N., et al. (2016). Ivermectin Induces Cytostatic Autophagy by Blocking the PAK1/Akt Axis in Breast Cancer. Cancer Research *76*, 4457–4469.

Edvardson, S., Cinnamon, Y., Ta-Shma, A., Shaag, A., Yim, Y.-I., Zenvirt, S., Jalas, C., Lesage, S., Brice, A., Taraboulos, A., et al. (2012). A Deleterious Mutation in DNAJC6 Encoding the Neuronal-Specific Clathrin-Uncoating Co-Chaperone Auxilin, Is Associated with Juvenile Parkinsonism. PLoS ONE *7*, e36458.

Ehringer, H., and Hornykiewicz, O. (1960). [Distribution of noradrenaline and dopamine (3-hydroxytyramine) in the human brain and their behavior in diseases of the extrapyramidal system]. Klin. Wochenschr. *38*, 1236–1239.

Eriksen, J.L., Wszolek, Z., and Petrucelli, L. (2005). Molecular pathogenesis of Parkinson disease. Arch. Neurol. *62*, 353–357.

Farrer, M.J., Stone, J.T., Lin, C.-H., Dächsel, J.C., Hulihan, M.M., Haugarvoll, K., Ross, O.A., and Wu, R.-M. (2007). Lrrk2 G2385R is an ancestral risk factor for Parkinson's disease in Asia. Parkinsonism & Related Disorders *13*, 89–92.

Fell, M.J., Mirescu, C., Basu, K., Cheewatrakoolpong, B., DeMong, D.E., Ellis, J.M., Hyde, L.A., Lin, Y., Markgraf, C.G., Mei, H., et al. (2015). MLi-2, a Potent, Selective, and Centrally Active Compound for Exploring the Therapeutic Potential and Safety of LRRK2 Kinase Inhibition. J. Pharmacol. Exp. Ther. *355*, 397–409.

Ferree, A., Guillily, M., Li, H., Smith, K., Takashima, A., Squillace, R., Weigele, M., Collins, J.J., and Wolozin, B. (2012). Regulation of physiologic actions of LRRK2: focus on autophagy. Neurodegener Dis *10*, 238–241.

Ferreira, M., and Massano, J. (2017). An updated review of Parkinson's disease genetics and clinicopathological correlations. Acta Neurol. Scand. *135*, 273–284.

Foo, J.-N., Liany, H., Bei, J.-X., Yu, X.-Q., Liu, J., Au, W.-L., Prakash, K.M., Tan, L.C., and Tan, E.-K. (2013). Rare lysosomal enzyme gene SMPD1 variant (p.R591C) associates with Parkinson's disease. Neurobiol. Aging *34*, 2890.e13-15.

Franke, A., McGovern, D.P.B., Barrett, J.C., Wang, K., Radford-Smith, G.L., Ahmad, T., Lees, C.W., Balschun, T., Lee, J., Roberts, R., et al. (2010). Genome-wide meta-analysis increases to 71 the number of confirmed Crohn's disease susceptibility loci. Nat. Genet. *42*, 1118–1125.

Fuji, R.N., Flagella, M., Baca, M., Baptista, M.A.S., Brodbeck, J., Chan, B.K., Fiske, B.K., Honigberg, L., Jubb, A.M., Katavolos, P., et al. (2015). Effect of selective LRRK2 kinase inhibition on nonhuman primate lung. Sci Transl Med *7*, 273ra15.

Funayama, M., Hasegawa, K., Kowa, H., Saito, M., Tsuji, S., and Obata, F. (2002). A new locus for Parkinson's disease (PARK8) maps to chromosome 12p11.2-q13.1. Ann. Neurol. *51*, 296–301.

Funayama, M., Ohe, K., Amo, T., Furuya, N., Yamaguchi, J., Saiki, S., Li, Y., Ogaki, K., Ando, M., Yoshino, H., et al. (2015). CHCHD2 mutations in autosomal dominant late-onset Parkinson's disease: a genome-wide linkage and sequencing study. Lancet Neurol *14*, 274–282.

Gandhi, P.N., Wang, X., Zhu, X., Chen, S.G., and Wilson-Delfosse, A.L. (2008). The Roc domain of leucine-rich repeat kinase 2 is sufficient for interaction with microtubules. J. Neurosci. Res. *86*, 1711–1720.

Gan-Or, Z., Ozelius, L.J., Bar-Shira, A., Saunders-Pullman, R., Mirelman, A., Kornreich, R., Gana-Weisz, M., Raymond, D., Rozenkrantz, L., Deik, A., et al. (2013). The p.L302P mutation in the lysosomal enzyme gene SMPD1 is a risk factor for Parkinson disease. Neurology *80*, 1606–1610.

Gardet, A., Benita, Y., Li, C., Sands, B.E., Ballester, I., Stevens, C., Korzenik, J.R., Rioux, J.D., Daly, M.J., Xavier, R.J., et al. (2010). LRRK2 is involved in the IFN-gamma response and host response to pathogens. J. Immunol. *185*, 5577–5585.

Gasser, T. (2015). Usefulness of Genetic Testing in PD and PD Trials: A Balanced Review. Journal of Parkinson's Disease *5*, 209–215.

Geel, T.M., Ruiters, M.H.J., Cool, R.H., Halby, L., Voshart, D.C., Andrade Ruiz, L., Niezen-Koning, K.E., Arimondo, P.B., and Rots, M.G. (2018). The past and presence of gene targeting: from chemicals and DNA via proteins to RNA. Philos. Trans. R. Soc. Lond., B, Biol. Sci. *373*.

Gehrke, S., Imai, Y., Sokol, N., and Lu, B. (2010). Pathogenic LRRK2 negatively regulates microRNA-mediated translational repression. Nature *466*, 637–641.

Gelb, D.J., Oliver, E., and Gilman, S. (1999). Diagnostic criteria for Parkinson disease. Arch. Neurol. *56*, 33–39.

Giaime, E., Tong, Y., Wagner, L.K., Yuan, Y., Huang, G., and Shen, J. (2017). Age-Dependent Dopaminergic Neurodegeneration and Impairment of the Autophagy-Lysosomal Pathway in LRRK -Deficient Mice. Neuron *96*, 796–807.e6.

Gillardon, F. (2009). Leucine-rich repeat kinase 2 phosphorylates brain tubulin-beta isoforms and modulates microtubule stability--a point of convergence in parkinsonian neurodegeneration? J. Neurochem. *110*, 1514–1522.

Gilsbach, B.K., Ho, F.Y., Vetter, I.R., van Haastert, P.J.M., Wittinghofer, A., and Kortholt, A. (2012). Roco kinase structures give insights into the mechanism of Parkinson disease-related leucine-rich-repeat kinase 2 mutations. Proc. Natl. Acad. Sci. U.S.A. *109*, 10322–10327.

Giordana, M.T., D'Agostino, C., Albani, G., Mauro, A., Di Fonzo, A., Antonini, A., and Bonifati, V. (2007). Neuropathology of Parkinson's disease associated with the LRRK2 Ile1371Val mutation. Mov. Disord. *22*, 275–278.

Gloeckner, C.J., Boldt, K., and Ueffing, M. (2009). Strep/FLAG tandem affinity purification (SF-TAP) to study protein interactions. Curr Protoc Protein Sci *Chapter 19*, Unit19.20.

Gloeckner, C.J., Boldt, K., von Zweydorf, F., Helm, S., Wiesent, L., Sarioglu, H., and Ueffing, M. (2010). Phosphopeptide analysis reveals two discrete clusters of phosphorylation in the N-terminus and the Roc domain of the Parkinson-disease associated protein kinase LRRK2. J. Proteome Res. *9*, 1738–1745.

Godena, V.K., Brookes-Hocking, N., Moller, A., Shaw, G., Oswald, M., Sancho, R.M., Miller, C.C.J., Whitworth, A.J., and De Vos, K.J. (2014). Increasing microtubule acetylation rescues axonal transport and locomotor deficits caused by LRRK2 Roc-COR domain mutations. Nat Commun *5*, 5245.

Goldman, S.M. (2014). Environmental toxins and Parkinson's disease. Annu. Rev. Pharmacol. Toxicol. *54*, 141–164.

Goldwurm, S., Di Fonzo, A., Simons, E.J., Rohé, C.F., Zini, M., Canesi, M., Tesei, S., Zecchinelli, A., Antonini, A., Mariani, C., et al. (2005). The G6055A (G2019S) mutation in LRRK2 is frequent in both early and late onset Parkinson's disease and originates from a common ancestor. J. Med. Genet. *42*, e65.

Gómez-Suaga, P., Luzón-Toro, B., Churamani, D., Zhang, L., Bloor-Young, D., Patel, S., Woodman, P.G., Churchill, G.C., and Hilfiker, S. (2012). Leucine-rich repeat kinase 2 regulates autophagy through a calcium-dependent pathway involving NAADP. Hum. Mol. Genet. *21*, 511–525.

Gotthardt, K., Weyand, M., Kortholt, A., Van Haastert, P.J.M., and Wittinghofer, A. (2008). Structure of the Roc-COR domain tandem of C. tepidum, a prokaryotic homologue of the human LRRK2 Parkinson kinase. EMBO J. *27*, 2239–2249.

Greggio, E., Jain, S., Kingsbury, A., Bandopadhyay, R., Lewis, P., Kaganovich, A., van der Brug, M.P., Beilina, A., Blackinton, J., Thomas, K.J., et al. (2006). Kinase activity is required for the toxic effects of mutant LRRK2/dardarin. Neurobiol. Dis. *23*, 329–341.

Greggio, E., Lewis, P.A., van der Brug, M.P., Ahmad, R., Kaganovich, A., Ding, J., Beilina, A., Baker, A.K., and Cookson, M.R. (2007). Mutations in LRRK2/dardarin associated with Parkinson disease are more toxic than equivalent mutations in the homologous kinase LRRK1. J. Neurochem. *102*, 93–102.

Greggio, E., Zambrano, I., Kaganovich, A., Beilina, A., Taymans, J.-M., Daniëls, V., Lewis, P., Jain, S., Ding, J., Syed, A., et al. (2008). The Parkinson disease-associated leucine-rich repeat kinase 2 (LRRK2) is a dimer that undergoes intramolecular autophosphorylation. J. Biol. Chem. *283*, 16906–16914.

Greggio, E., and Cookson, M.R. (2009). Leucine-rich repeat kinase 2 mutations and Parkinson's disease: three questions. ASN Neuro *1*.

Greggio, E., Taymans, J.-M., Zhen, E.Y., Ryder, J., Vancraenenbroeck, R., Beilina, A., Sun, P., Deng, J., Jaffe, H., Baekelandt, V., et al. (2009). The Parkinson's disease kinase LRRK2 autophosphorylates its GTPase domain at multiple sites. Biochem. Biophys. Res. Commun. *389*, 449–454.

Greggio, E., Civiero, L., Bisaglia, M., and Bubacco, L. (2012). Parkinson's disease and immune system: is the culprit LRRKing in the periphery? J Neuroinflammation *9*, 94.

Greggio, E., Bubacco, L., and Russo, I. (2017). Cross-talk between LRRK2 and PKA: implication for Parkinson's disease? Biochem. Soc. Trans. *45*, 261–267.

Guaitoli, G., Raimondi, F., Gilsbach, B.K., Gómez-Llorente, Y., Deyaert, E., Renzi, F., Li, X., Schaffner, A., Jagtap, P.K.A., Boldt, K., et al. (2016). Structural model of the dimeric Parkinson's protein LRRK2 reveals a compact architecture involving distant interdomain contacts. Proc. Natl. Acad. Sci. U.S.A. *113*, E4357-4366.

Haebig, K., Gloeckner, C.J., Miralles, M.G., Gillardon, F., Schulte, C., Riess, O., Ueffing, M., Biskup, S., and Bonin, M. (2010). ARHGEF7 (Beta-PIX) acts as guanine nucleotide exchange factor for leucine-rich repeat kinase 2. PLoS ONE *5*, e13762.

Hansen, C., Angot, E., Bergström, A.-L., Steiner, J.A., Pieri, L., Paul, G., Outeiro, T.F., Melki, R., Kallunki, P., Fog, K., et al. (2011). α-Synuclein propagates from mouse brain to grafted dopaminergic neurons and seeds aggregation in cultured human cells. J. Clin. Invest. *121*, 715–725.

Hakimi, M., Selvanantham, T., Swinton, E., Padmore, R.F., Tong, Y., Kabbach, G., Venderova, K., Girardin, S.E., Bulman, D.E., Scherzer, C.R., et al. (2011). Parkinson's disease-linked LRRK2 is expressed in circulating and tissue immune cells and upregulated following recognition of microbial structures. J Neural Transm (Vienna) *118*, 795–808.

Hardie, D.G., and Lin, S.-C. (2017). AMP-activated protein kinase - not just an energy sensor. F1000Res *6*, 1724.

Hardy, J., and Lees, A.J. (2005). Parkinson's disease: A broken nosology. Movement Disorders *20*, S2–S4.

Härtlova, A., Herbst, S., Peltier, J., Rodgers, A., Bilkei-Gorzo, O., Fearns, A., Dill, B.D., Lee, H., Flynn, R., Cowley, S.A., et al. (2018). LRRK2 is a negative regulator of Mycobacterium tuberculosis phagosome maturation in macrophages. EMBO J. *37*.

Hatano, T., Kubo, S., Imai, S., Maeda, M., Ishikawa, K., Mizuno, Y., and Hattori, N. (2007). Leucine-rich repeat kinase 2 associates with lipid rafts. Human Molecular Genetics *16*, 678–690.

Henry, A.G., Aghamohammadzadeh, S., Samaroo, H., Chen, Y., Mou, K., Needle, E., and Hirst, W.D. (2015). Pathogenic LRRK2 mutations, through increased kinase activity, produce enlarged lysosomes with reduced degradative capacity and increase ATP13A2 expression. Hum. Mol. Genet. *24*, 6013–6028.

Hernandez, D.G., Reed, X., and Singleton, A.B. (2016). Genetics in Parkinson disease: Mendelian versus non-Mendelian inheritance. Journal of Neurochemistry *139*, 59–74.

Herzig, M.C., Kolly, C., Persohn, E., Theil, D., Schweizer, T., Hafner, T., Stemmelen, C., Troxler, T.J., Schmid, P., Danner, S., et al. (2011). LRRK2 protein levels are determined by kinase function and are crucial for kidney and lung homeostasis in mice. Human Molecular Genetics *20*, 4209–4223.

Hockey, L.N., Kilpatrick, B.S., Eden, E.R., Lin-Moshier, Y., Brailoiu, G.C., Brailoiu, E., Futter, C.E., Schapira, A.H., Marchant, J.S., and Patel, S. (2015). Dysregulation of lysosomal morphology by pathogenic LRRK2 is corrected by TPC2 inhibition. J. Cell. Sci. *128*, 232–238.

Hornykiewicz, O. (2002). Dopamine miracle: from brain homogenate to dopamine replacement. Mov. Disord. *17*, 501–508.

Hurley, J.H., and Young, L.N. (2017). Mechanisms of Autophagy Initiation. Annu. Rev. Biochem. *86*, 225–244.

Ibáñez, P., Bonnet, A.-M., Débarges, B., Lohmann, E., Tison, F., Pollak, P., Agid, Y., Dürr, A., and Brice, A. (2004). Causal relation between alpha-synuclein gene duplication and familial Parkinson's disease. Lancet *364*, 1169–1171.

Imai, Y., Gehrke, S., Wang, H.-Q., Takahashi, R., Hasegawa, K., Oota, E., and Lu, B. (2008). Phosphorylation of 4E-BP by LRRK2 affects the maintenance of dopaminergic neurons in Drosophila. EMBO J. *27*, 2432–2443.

Inoshita, T., Arano, T., Hosaka, Y., Meng, H., Umezaki, Y., Kosugi, S., Morimoto, T., Koike, M., Chang, H.-Y., Imai, Y., et al. (2017). Vps35 in cooperation with LRRK2 regulates synaptic vesicle endocytosis through the endosomal pathway in Drosophila. Hum. Mol. Genet. *26*, 2933–2948.

Islam, M.S., Nolte, H., Jacob, W., Ziegler, A.B., Pütz, S., Grosjean, Y., Szczepanowska, K., Trifunovic, A., Braun, T., Heumann, H., et al. (2016). Human R1441C LRRK2 regulates the synaptic vesicle proteome and phosphoproteome in a Drosophila model of Parkinson's disease. Hum. Mol. Genet. *25*, 5365–5382.

Jafari, R., Almqvist, H., Axelsson, H., Ignatushchenko, M., Lundbäck, T., Nordlund, P., and Martinez Molina, D. (2014). The cellular thermal shift assay for evaluating drug target interactions in cells. Nat Protoc *9*, 2100–2122.

Jaleel, M., Nichols, R.J., Deak, M., Campbell, D.G., Gillardon, F., Knebel, A., and Alessi, D.R. (2007). LRRK2 phosphorylates moesin at threonine-558: characterization of how Parkinson's disease mutants affect kinase activity. Biochem. J. *405*, 307–317.

Jankovic, J. (2008). Parkinson's disease: clinical features and diagnosis. J. Neurol. Neurosurg. Psychiatry *79*, 368–376.

Jankovic, J., Goodman, I., Safirstein, B., Marmon, T.K., Schenk, D.B., Koller, M., Zago, W., Ness, D.K., Griffith, S.G., Grundman, M., et al. (2018). Safety and Tolerability of Multiple Ascending Doses of PRX002/RG7935, an Anti-α-Synuclein Monoclonal Antibody, in Patients With Parkinson Disease: A Randomized Clinical Trial. JAMA Neurol.

Jankovic, J. (2018). An update on new and unique uses of botulinum toxin in movement disorders. Toxicon *147*, 84–88.

Jellinger, K.A. (1991). Pathology of Parkinson's disease. Changes other than the nigrostriatal pathway. Mol. Chem. Neuropathol. *14*, 153–197.

Jellinger, K.A. (2003). Neuropathological spectrum of synucleinopathies. Movement Disorders *18*, 2–12.

Jellinger, K.A. (2008). A critical reappraisal of current staging of Lewy-related pathology in human brain. Acta Neuropathologica *116*, 1–16.

Kalinderi, K., Bostantjopoulou, S., and Fidani, L. (2016). The genetic background of Parkinson's disease: current progress and future prospects. Acta Neurol. Scand. *134*, 314–326.

Kalogeropulou, A.F., Zhao, J., Bolliger, M.F., Memou, A., Narasimha, S., Molitor, T.P., Wilson, W.H., Rideout, H.J., and Nichols, R.J. (2018). P62/SQSTM1 is a novel leucine-rich repeat kinase 2 (LRRK2) substrate that enhances neuronal toxicity. Biochemical Journal *475*, 1271–1293.

Kamikawaji, S., Ito, G., and Iwatsubo, T. (2009). Identification of the autophosphorylation sites of LRRK2. Biochemistry *48*, 10963–10975.

Kapitein, L.C., and Hoogenraad, C.C. (2015). Building the Neuronal Microtubule Cytoskeleton. Neuron *87*, 492–506.

Kast, D.J., and Dominguez, R. (2017). The Cytoskeleton-Autophagy Connection. Curr. Biol. *27*, R318–R326.

Keller, M.F., Saad, M., Bras, J., Bettella, F., Nicolaou, N., Simon-Sanchez, J., Mittag, F., Buchel, F., Sharma, M., Gibbs, J.R., et al. (2012). Using genome-wide complex trait analysis to quantify "missing heritability" in Parkinson's disease. Human Molecular Genetics *21*, 4996–5009.

Kett, L.R., Boassa, D., Ho, C.C.-Y., Rideout, H.J., Hu, J., Terada, M., Ellisman, M., and Dauer, W.T. (2012). LRRK2 Parkinson disease mutations enhance its microtubule association. Human Molecular Genetics *21*, 890–899.

Khan, S.H., and Kumar, R. (2012). Role of an intrinsically disordered conformation in AMPK-mediated phosphorylation of ULK1 and regulation of autophagy. Mol. BioSyst. *8*, 91–96.

Kim, B., Yang, M.-S., Choi, D., Kim, J.-H., Kim, H.-S., Seol, W., Choi, S., Jou, I., Kim, E.-Y., and Joe, E.-H. (2012). Impaired inflammatory responses in murine Lrrk2-knockdown brain microglia. PLoS ONE *7*, e34693.

Kim, K.S., Marcogliese, P.C., Yang, J., Callaghan, S.M., Resende, V., Abdel-Messih, E., Marras, C., Visanji, N.P., Huang, J., Schlossmacher, M.G., et al. (2018). Regulation of myeloid cell phagocytosis by LRRK2 via WAVE2 complex stabilization is altered in Parkinson's disease. Proc. Natl. Acad. Sci. U.S.A. *115*, E5164–E5173.

Kitada, T., Asakawa, S., Hattori, N., Matsumine, H., Yamamura, Y., Minoshima, S., Yokochi, M., Mizuno, Y., and Shimizu, N. (1998). Mutations in the parkin gene cause autosomal recessive juvenile parkinsonism. Nature *392*, 605–608.

Klionsky, D.J., Abdelmohsen, K., Abe, A., Abedin, M.J., Abeliovich, H., Acevedo Arozena, A., Adachi, H., Adams, C.M., Adams, P.D., Adeli, K., et al. (2016). Guidelines for the use and interpretation of assays for monitoring autophagy (3rd edition). Autophagy *12*, 1–222.

Kozina, E., Sadasivan, S., Jiao, Y., Dou, Y., Ma, Z., Tan, H., Kodali, K., Shaw, T., Peng, J., and Smeyne, R.J. (2018). Mutant LRRK2 mediates peripheral and central immune responses leading to neurodegeneration in vivo. Brain *141*, 1753–1769.

Kordower, J.H., Chu, Y., Hauser, R.A., Freeman, T.B., and Olanow, C.W. (2008). Lewy body–like pathology in long-term embryonic nigral transplants in Parkinson's disease. Nature Medicine *14*, 504–506.

Kortholt, A., van Egmond, W.N., Plak, K., Bosgraaf, L., Keizer-Gunnink, I., and van Haastert, P.J.M. (2012). Multiple regulatory mechanisms for the Dictyostelium Roco protein GbpC. J. Biol. Chem. *287*, 2749–2758.

Krebs, C.E., Karkheiran, S., Powell, J.C., Cao, M., Makarov, V., Darvish, H., Di Paolo, G., Walker, R.H., Shahidi, G.A., Buxbaum, J.D., et al. (2013). The Sac1 Domain of *SYNJ1* Identified Mutated in a Family with Early-Onset Progressive Parkinsonism with Generalized Seizures. Human Mutation *34*, 1200–1207.

Kruppa, A.J., Kendrick-Jones, J., and Buss, F. (2016). Myosins, Actin and Autophagy. Traffic *17*, 878–890.

Kumar, R., Sanawar, R., Li, X., and Li, F. (2017). Structure, biochemistry, and biology of PAK kinases. Gene *605*, 20–31.

Lang, A.E. (2011). A critical appraisal of the premotor symptoms of Parkinson's disease: potential usefulness in early diagnosis and design of neuroprotective trials. Mov. Disord. *26*, 775–783.

Langston, R.G., Rudenko, I.N., Kumaran, R., Hauser, D.N., Kaganovich, A., Ponce, L.B., Mamais, A., Ndukwe, K., Dillman, A.A., Al-Saif, A.M., et al. (2018). Differences in Stability, Activity and Mutation Effects Between Human and Mouse Leucine-Rich Repeat Kinase 2. Neurochemical Research.

Lavalley, N.J., Slone, S.R., Ding, H., West, A.B., and Yacoubian, T.A. (2016). 14-3-3 Proteins regulate mutant LRRK2 kinase activity and neurite shortening. Hum. Mol. Genet. *25*, 109–122.

Law, B.M.H., Spain, V.A., Leinster, V.H.L., Chia, R., Beilina, A., Cho, H.J., Taymans, J.-M., Urban, M.K., Sancho, R.M., Blanca Ramírez, M., et al. (2014). A direct interaction between leucine-rich repeat kinase 2 and specific β-tubulin isoforms regulates tubulin acetylation. J. Biol. Chem. *289*, 895–908.

Lee, S., Liu, H.-P., Lin, W.-Y., Guo, H., and Lu, B. (2010). LRRK2 kinase regulates synaptic morphology through distinct substrates at the presynaptic and

postsynaptic compartments of the Drosophila neuromuscular junction. J. Neurosci. *30*, 16959–16969.

Lee, J.S., and Lee, S.-J. (2016). Mechanism of Anti-α-Synuclein Immunotherapy. J Mov Disord *9*, 14–19.

Lee, D.J., Dallapiazza, R.F., De Vloo, P., and Lozano, A.M. (2018). Current surgical treatments for Parkinson's disease and potential therapeutic targets. Neural Regen Res *13*, 1342–1345.

Lesage, S., Drouet, V., Majounie, E., Deramecourt, V., Jacoupy, M., Nicolas, A., Cormier-Dequaire, F., Hassoun, S.M., Pujol, C., Ciura, S., et al. (2016). Loss of VPS13C Function in Autosomal-Recessive Parkinsonism Causes Mitochondrial Dysfunction and Increases PINK1/Parkin-Dependent Mitophagy. Am. J. Hum. Genet. *98*, 500–513.

Lewis, P.A. (2018). Mutations in LRRK2 amplify cell-to-cell protein aggregate propagation: a hypothesis. Acta Neuropathol. *135*, 973–976.

Lewy, F. (1912). *Paralysis agitans. I. Pathologische anatomie.* In: Lewandowsky, M., editor. *Handbuch der neurologie.* (Berlin). Springer, 920–933.

Li, J.-Y., Englund, E., Holton, J.L., Soulet, D., Hagell, P., Lees, A.J., Lashley, T., Quinn, N.P., Rehncrona, S., Björklund, A., et al. (2008). Lewy bodies in grafted neurons in subjects with Parkinson's disease suggest host-to-graft disease propagation. Nat. Med. *14*, 501–503.

Li, T., He, X., Thomas, J.M., Yang, D., Zhong, S., Xue, F., and Smith, W.W. (2015). A Novel GTP-Binding Inhibitor, FX2149, Attenuates LRRK2 Toxicity in Parkinson's Disease Models. PLOS ONE *10*, e0122461.

Liao, J., Wu, C.-X., Burlak, C., Zhang, S., Sahm, H., Wang, M., Zhang, Z.-Y., Vogel, K.W., Federici, M., Riddle, S.M., et al. (2014). Parkinson disease-associated mutation R1441H in LRRK2 prolongs the "active state" of its GTPase domain. Proc. Natl. Acad. Sci. U.S.A. *111*, 4055–4060.

Lin, X., Parisiadou, L., Gu, X.-L., Wang, L., Shim, H., Sun, L., Xie, C., Long, C.-X., Yang, W.-J., Ding, J., et al. (2009). Leucine-rich repeat kinase 2 regulates the progression of neuropathology induced by Parkinson's-disease-related mutant alpha-synuclein. Neuron *64*, 807–827.

Lis, P., Burel, S., Steger, M., Mann, M., Brown, F., Diez, F., Tonelli, F., Holton, J.L., Ho, P.W., Ho, S.-L., et al. (2018). Development of phospho-specific Rab protein antibodies to monitor in vivo activity of the LRRK2 Parkinson's disease kinase. Biochem. J. *475*, 1–22.

Liu, Z., Lee, J., Krummey, S., Lu, W., Cai, H., and Lenardo, M.J. (2011). The kinase LRRK2 is a regulator of the transcription factor NFAT that modulates the severity of inflammatory bowel disease. Nat. Immunol. *12*, 1063–1070.

Liu, Z., Mobley, J.A., DeLucas, L.J., Kahn, R.A., and West, A.B. (2016). LRRK2 autophosphorylation enhances its GTPase activity. FASEB J. *30*, 336–347.

Liu, Z., Bryant, N., Kumaran, R., Beilina, A., Abeliovich, A., Cookson, M.R., and West, A.B. (2018). LRRK2 phosphorylates membrane-bound Rabs and is activated by GTP-bound Rab7L1 to promote recruitment to the trans-Golgi network. Hum. Mol. Genet. *27*, 385–395.

Lystad, A.H., and Simonsen, A. (2016). Phosphoinositide-binding proteins in autophagy. FEBS Lett. *590*, 2454–2468.

Lobbestael, E., Zhao, J., Rudenko, I.N., Beylina, A., Gao, F., Wetter, J., Beullens, M., Bollen, M., Cookson, M.R., Baekelandt, V., et al. (2013). Identification of protein phosphatase 1 as a regulator of the LRRK2 phosphorylation cycle. Biochemical Journal *456*, 119–128.

Longo, F., Russo, I., Shimshek, D.R., Greggio, E., and Morari, M. (2014). Genetic and pharmacological evidence that G2019S LRRK2 confers a hyperkinetic phenotype, resistant to motor decline associated with aging. Neurobiol. Dis. *71*, 62–73.

Lotia, M., and Jankovic, J. (2016). New and emerging medical therapies in Parkinson's disease. Expert Opin Pharmacother *17*, 895–909.

Ma, B., Xu, L., Pan, X., Sun, L., Ding, J., Xie, C., Koliatsos, V.E., and Cai, H. (2016). LRRK2 modulates microglial activity through regulation of chemokine (C-X3-C) receptor 1 -mediated signalling pathways. Hum. Mol. Genet. *25*, 3515–3523.

MacLeod, D., Dowman, J., Hammond, R., Leete, T., Inoue, K., and Abeliovich, A. (2006). The familial Parkinsonism gene LRRK2 regulates neurite process morphology. Neuron *52*, 587–593.

Madero-Pérez, J., Fdez, E., Fernández, B., Lara Ordóñez, A.J., Blanca Ramírez, M., Gómez-Suaga, P., Waschbüsch, D., Lobbestael, E., Baekelandt, V., Nairn, A.C., et al. (2018). Parkinson disease-associated mutations in LRRK2 cause centrosomal defects via Rab8a phosphorylation. Mol Neurodegener *13*, 3.

Maekawa, T., Sasaoka, T., Azuma, S., Ichikawa, T., Melrose, H.L., Farrer, M.J., and Obata, F. (2016). Leucine-rich repeat kinase 2 (LRRK2) regulates α-synuclein clearance in microglia. BMC Neurosci *17*, 77.

Mahfouz, A., Lelieveldt, B.P.F., Grefhorst, A., van Weert, L.T.C.M., Mol, I.M., Sips, H.C.M., van den Heuvel, J.K., Datson, N.A., Visser, J.A., Reinders, M.J.T., et al. (2016). Genome-wide coexpression of steroid receptors in the mouse brain: Identifying signaling pathways and functionally coordinated regions. Proceedings of the National Academy of Sciences *113*, 2738–2743.

Mangeat, P., Roy, C., and Martin, M. (1999). ERM proteins in cell adhesion and membrane dynamics. Trends Cell Biol. *9*, 187–192.

Manzoni, C., Mamais, A., Dihanich, S., Abeti, R., Soutar, M.P.M., Plun-Favreau, H., Giunti, P., Tooze, S.A., Bandopadhyay, R., and Lewis, P.A. (2013a). Inhibition of LRRK2 kinase activity stimulates macroautophagy. Biochim. Biophys. Acta *1833*, 2900–2910.

Manzoni, C., Mamais, A., Dihanich, S., McGoldrick, P., Devine, M.J., Zerle, J., Kara, E., Taanman, J.-W., Healy, D.G., Marti-Masso, J.-F., et al. (2013b). Pathogenic Parkinson's disease mutations across the functional domains of LRRK2 alter the autophagic/lysosomal response to starvation. Biochem. Biophys. Res. Commun. *441*, 862–866.

Manzoni, C., Denny, P., Lovering, R.C., and Lewis, P.A. (2015). Computational analysis of the LRRK2 interactome. PeerJ *3*, e778.

Manzoni, C., Mamais, A., Roosen, D.A., Dihanich, S., Soutar, M.P.M., Plun-Favreau, H., Bandopadhyay, R., Hardy, J., Tooze, S.A., Cookson, M.R., et al. (2016). mTOR independent regulation of macroautophagy by Leucine Rich Repeat Kinase 2 via Beclin-1. Sci Rep *6*, 35106.

Manzoni, C. (2017). The LRRK2–macroautophagy axis and its relevance to Parkinson's disease. Biochemical Society Transactions *45*, 155–162.

Martin, I., Kim, J.W., Lee, B.D., Kang, H.C., Xu, J.-C., Jia, H., Stankowski, J., Kim, M.-S., Zhong, J., Kumar, M., et al. (2014a). Ribosomal protein s15 phosphorylation mediates LRRK2 neurodegeneration in Parkinson's disease. Cell *157*, 472–485.

Martin, I., Abalde-Atristain, L., Kim, J.W., Dawson, T.M., and Dawson, V.L. (2014b). Abberant protein synthesis in G2019S LRRK2 Drosophila Parkinson disease-related phenotypes. Fly (Austin) *8*, 165–169.

Mata, I.F., Davis, M.Y., Lopez, A.N., Dorschner, M.O., Martinez, E., Yearout, D., Cholerton, B.A., Hu, S.-C., Edwards, K.L., Bird, T.D., et al. (2016). The discovery of LRRK2 p.R1441S, a novel mutation for Parkinson's disease, adds to the complexity of a mutational hotspot. Am. J. Med. Genet. B Neuropsychiatr. Genet. *171*, 925–930.

Matikainen-Ankney, B.A., Kezunovic, N., Mesias, R.E., Tian, Y., Williams, F.M., Huntley, G.W., and Benson, D.L. (2016). Altered Development of Synapse Structure and Function in Striatum Caused by Parkinson's Disease-Linked LRRK2-G2019S Mutation. J. Neurosci. *36*, 7128–7141.

Matta, S., Van Kolen, K., da Cunha, R., van den Bogaart, G., Mandemakers, W., Miskiewicz, K., De Bock, P.-J., Morais, V.A., Vilain, S., Haddad, D., et al. (2012). LRRK2 controls an EndoA phosphorylation cycle in synaptic endocytosis. Neuron *75*, 1008–1021.

Meixner, A., Boldt, K., Van Troys, M., Askenazi, M., Gloeckner, C.J., Bauer, M., Marto, J.A., Ampe, C., Kinkl, N., and Ueffing, M. (2011). A QUICK screen for Lrrk2 interaction partners--leucine-rich repeat kinase 2 is involved in actin cytoskeleton dynamics. Mol. Cell Proteomics *10*, M110.001172.

Meijering, E., Jacob, M., Sarria, J.-C.F., Steiner, P., Hirling, H., and Unser, M. (2004). Design and validation of a tool for neurite tracing and analysis in fluorescence microscopy images. Cytometry A *58*, 167–176.

Mi, N., Chen, Y., Wang, S., Chen, M., Zhao, M., Yang, G., Ma, M., Su, Q., Luo, S., Shi, J., et al. (2015). CapZ regulates autophagosomal membrane shaping by promoting actin assembly inside the isolation membrane. Nat. Cell Biol. *17*, 1112–1123.

Minden, A. (2012). PAK4–6 in cancer and neuronal development. Cellular Logistics *2*, 95–104.

Mir, R., Tonelli, F., Lis, P., Macartney, T., Polinski, N.K., Martinez, T.N., Chou, M.-Y., Howden, A.J.M., König, T., Hotzy, C., et al. (2018). The Parkinson's disease VPS35[D620N] mutation enhances LRRK2-mediated Rab protein phosphorylation in mouse and human. Biochem. J. *475*, 1861–1883.

Mizushima, N., and Yoshimori, T. (2007). How to Interpret LC3 Immunoblotting. Autophagy *3*, 542–545.

Moehle, M.S., Webber, P.J., Tse, T., Sukar, N., Standaert, D.G., DeSilva, T.M., Cowell, R.M., and West, A.B. (2012). LRRK2 inhibition attenuates microglial inflammatory responses. J. Neurosci. *32*, 1602–1611.

Monastyrska, I., Rieter, E., Klionsky, D.J., and Reggiori, F. (2009). Multiple roles of the cytoskeleton in autophagy. Biol Rev Camb Philos Soc *84*, 431–448.

Muda, K., Bertinetti, D., Gesellchen, F., Hermann, J.S., von Zweydorf, F., Geerlof, A., Jacob, A., Ueffing, M., Gloeckner, C.J., and Herberg, F.W. (2014). Parkinson-related LRRK2 mutation R1441C/G/H impairs PKA phosphorylation of LRRK2 and disrupts its interaction with 14-3-3. Proc. Natl. Acad. Sci. U.S.A. *111*, E34-43.

Murín, R., Schaer, A., Kowtharapu, B.S., Verleysdonk, S., and Hamprecht, B. (2008). Expression of 3-hydroxyisobutyrate dehydrogenase in cultured neural cells. J. Neurochem. *105*, 1176–1186.

Murray, B.W., Guo, C., Piraino, J., Westwick, J.K., Zhang, C., Lamerdin, J., Dagostino, E., Knighton, D., Loi, C.-M., Zager, M., et al. (2010). Small-molecule p21-activated kinase inhibitor PF-3758309 is a potent inhibitor of oncogenic signaling and tumor growth. Proceedings of the National Academy of Sciences *107*, 9446–9451.

Nalls, M.A., Pankratz, N., Lill, C.M., Do, C.B., Hernandez, D.G., Saad, M., DeStefano, A.L., Kara, E., Bras, J., Sharma, M., et al. (2014). Large-scale meta-

analysis of genome-wide association data identifies six new risk loci for Parkinson's disease. Nat. Genet. *46*, 989–993.

Nekrasova, T., Jobes, M.L., Ting, J.H., Wagner, G.C., and Minden, A. (2008). Targeted disruption of the Pak5 and Pak6 genes in mice leads to deficits in learning and locomotion. Developmental Biology *322*, 95–108.

Nguyen, A.P.T., and Moore, D.J. (2017). Understanding the GTPase Activity of LRRK2: Regulation, Function, and Neurotoxicity. Adv Neurobiol *14*, 71–88.

Nguyen, M., and Krainc, D. (2018). LRRK2 phosphorylation of auxilin mediates synaptic defects in dopaminergic neurons from patients with Parkinson's disease. Proc. Natl. Acad. Sci. U.S.A. *115*, 5576–5581.

Nguyen, A.P.T., Daniel, G., Valdés, P., Islam, M.S., Schneider, B.L., and Moore, D.J. (2018). G2019S LRRK2 enhances the neuronal transmission of tau in the mouse brain. Hum. Mol. Genet. *27*, 120–134.

Nichols, R.J., Dzamko, N., Morrice, N.A., Campbell, D.G., Deak, M., Ordureau, A., Macartney, T., Tong, Y., Shen, J., Prescott, A.R., et al. (2010). 14-3-3 binding to LRRK2 is disrupted by multiple Parkinson's disease-associated mutations and regulates cytoplasmic localization. Biochemical Journal *430*, 393–404.

Niesen, F.H., Berglund, H., and Vedadi, M. (2007). The use of differential scanning fluorimetry to detect ligand interactions that promote protein stability. Nat Protoc *2*, 2212–2221.

Nikonova, E.V., Xiong, Y., Tanis, K.Q., Dawson, V.L., Vogel, R.L., Finney, E.M., Stone, D.J., Reynolds, I.J., Kern, J.T., and Dawson, T.M. (2012). Transcriptional responses to loss or gain of function of the leucine-rich repeat kinase 2 (LRRK2) gene uncover biological processes modulated by LRRK2 activity. Hum. Mol. Genet. *21*, 163–174.

Nixon-Abell, J., Berwick, D.C., Grannó, S., Spain, V.A., Blackstone, C., and Harvey, K. (2016). Protective LRRK2 R1398H Variant Enhances GTPase and Wnt Signaling Activity. Front Mol Neurosci *9*, 18.

Novello, S., Arcuri, L., Dovero, S., Dutheil, N., Shimshek, D.R., Bezard, E., and Morari, M. (2018). G2019S LRRK2 mutation facilitates α-synuclein neuropathology in aged mice. Neurobiol. Dis. *120*, 21–33.

Obeso, J.A., Stamelou, M., Goetz, C.G., Poewe, W., Lang, A.E., Weintraub, D., Burn, D., Halliday, G.M., Bezard, E., Przedborski, S., et al. (2017). Past, present, and future of Parkinson's disease: A special essay on the 200th Anniversary of the Shaking Palsy. Mov. Disord. *32*, 1264–1310.

Orenstein, S.J., Kuo, S.-H., Tasset, I., Arias, E., Koga, H., Fernandez-Carasa, I., Cortes, E., Honig, L.S., Dauer, W., Consiglio, A., et al. (2013). Interplay of LRRK2 with chaperone-mediated autophagy. Nat. Neurosci. *16*, 394–406.

Ostrowska, Z., and Moraczewska, J. (2017). Cofilin - a protein controlling dynamics of actin filaments. Postepy Hig Med Dosw (Online) *71*, 339–351.

Paisán-Ruíz, C., Jain, S., Evans, E.W., Gilks, W.P., Simón, J., van der Brug, M., de Munain, A.L., Aparicio, S., Gil, A.M., Khan, N., et al. (2004). Cloning of the Gene Containing Mutations that Cause PARK8-Linked Parkinson's Disease. Neuron *44*, 595–600.

Paisan-Ruiz, C., Bhatia, K.P., Li, A., Hernandez, D., Davis, M., Wood, N.W., Hardy, J., Houlden, H., Singleton, A., and Schneider, S.A. (2009). Characterization of PLA2G6 as a locus for dystonia-parkinsonism. Ann. Neurol. *65*, 19–23.

Paisán-Ruiz, C., Lewis, P.A., and Singleton, A.B. (2013). LRRK2: cause, risk, and mechanism. J Parkinsons Dis *3*, 85–103.

Papinski, D., and Kraft, C. (2016). Regulation of Autophagy By Signaling Through the Atg1/ULK1 Complex. J. Mol. Biol. *428*, 1725–1741.

Parisiadou, L., Xie, C., Cho, H.J., Lin, X., Gu, X.-L., Long, C.-X., Lobbestael, E., Baekelandt, V., Taymans, J.-M., Sun, L., et al. (2009). Phosphorylation of ezrin/radixin/moesin proteins by LRRK2 promotes the rearrangement of actin cytoskeleton in neuronal morphogenesis. J. Neurosci. *29*, 13971–13980.

Parisiadou, L., and Cai, H. (2010). LRRK2 function on actin and microtubule dynamics in Parkinson disease. Commun Integr Biol *3*, 396–400.

Parisiadou, L., Yu, J., Sgobio, C., Xie, C., Liu, G., Sun, L., Gu, X.-L., Lin, X., Crowley, N.A., Lovinger, D.M., et al. (2014). LRRK2 regulates synaptogenesis and dopamine receptor activation through modulation of PKA activity. Nat. Neurosci. *17*, 367–376.

Park, S., Han, S., Choi, I., Kim, B., Park, S.P., Joe, E.-H., and Suh, Y.H. (2016). Interplay between Leucine-Rich Repeat Kinase 2 (LRRK2) and p62/SQSTM-1 in Selective Autophagy. PLoS ONE *11*, e0163029.

Parkinson, J. (1817). An essay on the shaking palsy. Sherwood, Neely and Jones (London).

Parkinson, J. (2002). An essay on the shaking palsy. 1817. J Neuropsychiatry Clin Neurosci *14*, 223–236; discussion 222.

Parkkinen, L., Pirttilä, T., and Alafuzoff, I. (2008). Applicability of current staging/categorization of α-synuclein pathology and their clinical relevance. Acta Neuropathologica *115*, 399–407.

Pezzoli, G., and Cereda, E. (2013). Exposure to pesticides or solvents and risk of Parkinson disease. Neurology *80*, 2035–2041.

Piccoli, G., Onofri, F., Cirnaru, M.D., Kaiser, C.J.O., Jagtap, P., Kastenmüller, A., Pischedda, F., Marte, A., von Zweydorf, F., Vogt, A., et al. (2014). Leucine-rich repeat kinase 2 binds to neuronal vesicles through protein interactions mediated by its C-terminal WD40 domain. Mol. Cell. Biol. *34*, 2147–2161.

Plowey, E.D., Cherra, S.J., Liu, Y.-J., and Chu, C.T. (2008). Role of autophagy in G2019S-LRRK2-associated neurite shortening in differentiated SH-SY5Y cells. J. Neurochem. *105*, 1048–1056.

Poewe, W., Seppi, K., Tanner, C.M., Halliday, G.M., Brundin, P., Volkmann, J., Schrag, A.-E., and Lang, A.E. (2017). Parkinson disease. Nat Rev Dis Primers *3*, 17013.

Polymeropoulos, M.H., Lavedan, C., Leroy, E., Ide, S.E., Dehejia, A., Dutra, A., Pike, B., Root, H., Rubenstein, J., Boyer, R., et al. (1997). Mutation in the alpha-synuclein gene identified in families with Parkinson's disease. Science *276*, 2045–2047.

Pugsley, H.R. (2017). Quantifying autophagy: Measuring LC3 puncta and autolysosome formation in cells using multispectral imaging flow cytometry. Methods *112*, 147–156.

Purlyte, E., Dhekne, H.S., Sarhan, A.R., Gomez, R., Lis, P., Wightman, M., Martinez, T.N., Tonelli, F., Pfeffer, S.R., and Alessi, D.R. (2018). Rab29 activation of the Parkinson's disease-associated LRRK2 kinase. EMBO J. *37*, 1–18.

Quadri, M., Fang, M., Picillo, M., Olgiati, S., Breedveld, G.J., Graafland, J., Wu, B., Xu, F., Erro, R., Amboni, M., et al. (2013). Mutation in the *SYNJ1* Gene Associated with Autosomal Recessive, Early-Onset Parkinsonism. Human Mutation *34*, 1208–1215.

Rajput, A., Dickson, D.W., Robinson, C.A., Ross, O.A., Dächsel, J.C., Lincoln, S.J., Cobb, S.A., Rajput, M.L., and Farrer, M.J. (2006). Parkinsonism, Lrrk2 G2019S, and tau neuropathology. Neurology *67*, 1506–1508.

Ramirez, A., Heimbach, A., Gründemann, J., Stiller, B., Hampshire, D., Cid, L.P., Goebel, I., Mubaidin, A.F., Wriekat, A.-L., Roeper, J., et al. (2006). Hereditary parkinsonism with dementia is caused by mutations in ATP13A2, encoding a lysosomal type 5 P-type ATPase. Nat. Genet. *38*, 1184–1191.

Ramonet, D., Daher, J.P.L., Lin, B.M., Stafa, K., Kim, J., Banerjee, R., Westerlund, M., Pletnikova, O., Glauser, L., Yang, L., et al. (2011). Dopaminergic neuronal loss, reduced neurite complexity and autophagic abnormalities in transgenic mice expressing G2019S mutant LRRK2. PLoS ONE *6*, e18568.

Rassu, M., Del Giudice, M.G., Sanna, S., Taymans, J.M., Morari, M., Brugnoli, A., Frassineti, M., Masala, A., Esposito, S., Galioto, M., et al. (2017). Role of LRRK2 in the regulation of dopamine receptor trafficking. PLoS ONE *12*, e0179082.

Reggiori, F., Monastyrska, I., Shintani, T., and Klionsky, D.J. (2005). The actin cytoskeleton is required for selective types of autophagy, but not nonspecific autophagy, in the yeast Saccharomyces cerevisiae. Mol. Biol. Cell *16*, 5843–5856.

Roosen, D.A., and Cookson, M.R. (2016). LRRK2 at the interface of autophagosomes, endosomes and lysosomes. Mol Neurodegener *11*, 73.

Ross, O.A., Spanaki, C., Griffith, A., Lin, C.-H., Kachergus, J., Haugarvoll, K., Latsoudis, H., Plaitakis, A., Ferreira, J.J., Sampaio, C., et al. (2009). Haplotype analysis of Lrrk2 R1441H carriers with parkinsonism. Parkinsonism Relat. Disord. *15*, 466–467.

Rudi, K., Ho, F.Y., Gilsbach, B.K., Pots, H., Wittinghofer, A., Kortholt, A., and Klare, J.P. (2015). Conformational heterogeneity of the Roc domains in C. tepidum Roc-COR and implications for human LRRK2 Parkinson mutations. Biosci. Rep. *35*.

Russo, I., Berti, G., Plotegher, N., Bernardo, G., Filograna, R., Bubacco, L., and Greggio, E. (2015). Leucine-rich repeat kinase 2 positively regulates inflammation and down-regulates NF-κB p50 signaling in cultured microglia cells. J Neuroinflammation *12*, 230.

Saez-Atienzar, S., Bonet-Ponce, L., Blesa, J.R., Romero, F.J., Murphy, M.P., Jordan, J., and Galindo, M.F. (2014). The LRRK2 inhibitor GSK2578215A induces protective autophagy in SH-SY5Y cells: involvement of Drp-1-mediated mitochondrial fission and mitochondrial-derived ROS signaling. Cell Death Dis *5*, e1368.

Saha, S., Ash, P.E.A., Gowda, V., Liu, L., Shirihai, O., and Wolozin, B. (2015). Mutations in LRRK2 potentiate age-related impairment of autophagic flux. Mol Neurodegener *10*, 26.

Sánchez-Danés, A., Richaud-Patin, Y., Carballo-Carbajal, I., Jiménez-Delgado, S., Caig, C., Mora, S., Di Guglielmo, C., Ezquerra, M., Patel, B., Giralt, A., et al. (2012). Disease-specific phenotypes in dopamine neurons from human iPS-based models of genetic and sporadic Parkinson's disease. EMBO Mol Med *4*, 380–395.

Schapansky, J., Nardozzi, J.D., Felizia, F., and LaVoie, M.J. (2014). Membrane recruitment of endogenous LRRK2 precedes its potent regulation of autophagy. Hum. Mol. Genet. *23*, 4201–4214.

Schapansky, J., Nardozzi, J.D., and LaVoie, M.J. (2015). The complex relationships between microglia, alpha-synuclein, and LRRK2 in Parkinson's disease. Neuroscience *302*, 74–88.

Schapansky, J., Khasnavis, S., DeAndrade, M.P., Nardozzi, J.D., Falkson, S.R., Boyd, J.D., Sanderson, J.B., Bartels, T., Melrose, H.L., and LaVoie, M.J. (2018). Familial knockin mutation of LRRK2 causes lysosomal dysfunction and

accumulation of endogenous insoluble α-synuclein in neurons. Neurobiology of Disease *111*, 26–35.

Schreij, A.M.A., Chaineau, M., Ruan, W., Lin, S., Barker, P.A., Fon, E.A., and McPherson, P.S. (2015). LRRK2 localizes to endosomes and interacts with clathrin-light chains to limit Rac1 activation. EMBO Rep. *16*, 79–86.

Schuchman, E.H., and Desnick, R.J. (2017). Types A and B Niemann-Pick disease. Mol. Genet. Metab. *120*, 27–33.

Seirafi, M., Kozlov, G., and Gehring, K. (2015). Parkin structure and function. FEBS Journal *282*, 2076–2088.

Sejwal, K., Chami, M., Rémigy, H., Vancraenenbroeck, R., Sibran, W., Sütterlin, R., Baumgartner, P., McLeod, R., Chartier-Harlin, M.-C., Baekelandt, V., et al. (2017). Cryo-EM analysis of homodimeric full-length LRRK2 and LRRK1 protein complexes. Sci Rep *7*, 8667.

Sepulveda, B., Mesias, R., Li, X., Yue, Z., and Benson, D.L. (2013). Short- and long-term effects of LRRK2 on axon and dendrite growth. PLoS ONE *8*, e61986.

Shanley, M.R., Hawley, D., Leung, S., Zaidi, N.F., Dave, R., Schlosser, K.A., Bandopadhyay, R., Gerber, S.A., and Liu, M. (2015). LRRK2 Facilitates tau Phosphorylation through Strong Interaction with tau and cdk5. Biochemistry *54*, 5198–5208.

Sheng, Z., Zhang, S., Bustos, D., Kleinheinz, T., Le Pichon, C.E., Dominguez, S.L., Solanoy, H.O., Drummond, J., Zhang, X., Ding, X., et al. (2012). Ser1292 Autophosphorylation Is an Indicator of LRRK2 Kinase Activity and Contributes to the Cellular Effects of PD Mutations. Science Translational Medicine *4*, 164ra161-164ra161.

Shojaee, S., Sina, F., Banihosseini, S.S., Kazemi, M.H., Kalhor, R., Shahidi, G.-A., Fakhrai-Rad, H., Ronaghi, M., and Elahi, E. (2008). Genome-wide linkage analysis of a Parkinsonian-pyramidal syndrome pedigree by 500 K SNP arrays. Am. J. Hum. Genet. *82*, 1375–1384.

Sidransky, E., Nalls, M.A., Aasly, J.O., Aharon-Peretz, J., Annesi, G., Barbosa, E.R., Bar-Shira, A., Berg, D., Bras, J., Brice, A., et al. (2009). Multicenter analysis of glucocerebrosidase mutations in Parkinson's disease. N. Engl. J. Med. *361*, 1651–1661.

Simón-Sánchez, J., Schulte, C., Bras, J.M., Sharma, M., Gibbs, J.R., Berg, D., Paisan-Ruiz, C., Lichtner, P., Scholz, S.W., Hernandez, D.G., et al. (2009). Genome-wide association study reveals genetic risk underlying Parkinson's disease. Nature Genetics *41*, 1308–1312.

Singleton, A.B., Farrer, M., Johnson, J., Singleton, A., Hague, S., Kachergus, J., Hulihan, M., Peuralinna, T., Dutra, A., Nussbaum, R., et al. (2003). alpha-Synuclein locus triplication causes Parkinson's disease. Science *302*, 841.

Singleton, A., and Gwinn-Hardy, K. (2004). Parkinson's disease and dementia with Lewy bodies: a difference in dose? The Lancet *364*, 1105–1107.

Singleton, A., and Hardy, J. (2011). A generalizable hypothesis for the genetic architecture of disease: pleomorphic risk loci. Hum. Mol. Genet. *20*, R158-162.

Singleton, A., and Hardy, J. (2016). The Evolution of Genetics: Alzheimer's and Parkinson's Diseases. Neuron *90*, 1154–1163.

Smith, W.W., Pei, Z., Jiang, H., Dawson, V.L., Dawson, T.M., and Ross, C.A. (2006). Kinase activity of mutant LRRK2 mediates neuronal toxicity. Nat. Neurosci. *9*, 1231–1233.

Sossi, V., de la Fuente-Fernández, R., Nandhagopal, R., Schulzer, M., McKenzie, J., Ruth, T.J., Aasly, J.O., Farrer, M.J., Wszolek, Z.K., and Stoessl, J.A. (2010). Dopamine turnover increases in asymptomatic LRRK2 mutations carriers. Mov. Disord. *25*, 2717–2723.

Soukup, S.-F., Kuenen, S., Vanhauwaert, R., Manetsberger, J., Hernández-Díaz, S., Swerts, J., Schoovaerts, N., Vilain, S., Gounko, N.V., Vints, K., et al. (2016). A LRRK2-Dependent EndophilinA Phosphoswitch Is Critical for Macroautophagy at Presynaptic Terminals. Neuron *92*, 829–844.

Soukup, S.-F., and Verstreken, P. (2017). EndoA/Endophilin-A creates docking stations for autophagic proteins at synapses. Autophagy *13*, 971–972.

Spillantini, M.G., Schmidt, M.L., Lee, V.M., Trojanowski, J.Q., Jakes, R., and Goedert, M. (1997). Alpha-synuclein in Lewy bodies. Nature *388*, 839–840.

Steger, M., Tonelli, F., Ito, G., Davies, P., Trost, M., Vetter, M., Wachter, S., Lorentzen, E., Duddy, G., Wilson, S., et al. (2016). Phosphoproteomics reveals that Parkinson's disease kinase LRRK2 regulates a subset of Rab GTPases. Elife *5*.

Tain, L.S., Mortiboys, H., Tao, R.N., Ziviani, E., Bandmann, O., and Whitworth, A.J. (2009). Rapamycin activation of 4E-BP prevents parkinsonian dopaminergic neuron loss. Nat. Neurosci. *12*, 1129–1135.

Takeshige, K., Baba, M., Tsuboi, S., Noda, T., and Ohsumi, Y. (1992). Autophagy in yeast demonstrated with proteinase-deficient mutants and conditions for its induction. J. Cell Biol. *119*, 301–311.

Tanida, I., Ueno, T., and Kominami, E. (2008). LC3 and Autophagy. Methods Mol. Biol. *445*, 77–88.

Tarakad, A., and Jankovic, J. (2017). Diagnosis and Management of Parkinson's Disease. Semin Neurol *37*, 118–126.

Taymans, J.-M., Vancraenenbroeck, R., Ollikainen, P., Beilina, A., Lobbestael, E., De Maeyer, M., Baekelandt, V., and Cookson, M.R. (2011). LRRK2 kinase activity is dependent on LRRK2 GTP binding capacity but independent of LRRK2 GTP binding. PLoS ONE *6*, e23207.

Taymans, J.-M. (2012). The GTPase function of LRRK2. Biochemical Society Transactions *40*, 1063–1069.

Taymans, J.-M., and Greggio, E. (2016). LRRK2 Kinase Inhibition as a Therapeutic Strategy for Parkinson's Disease, Where Do We Stand? Curr Neuropharmacol *14*, 214–225.

Tomkins, J.E., Dihanich, S., Beilina, A., Ferrari, R., Ilacqua, N., Cookson, M.R., Lewis, P.A., and Manzoni, C. (2018). Comparative Protein Interaction Network Analysis Identifies Shared and Distinct Functions for the Human ROCO Proteins. Proteomics *18*, e1700444.

Tong, Y., Yamaguchi, H., Giaime, E., Boyle, S., Kopan, R., Kelleher, R.J., and Shen, J. (2010). Loss of leucine-rich repeat kinase 2 causes impairment of protein degradation pathways, accumulation of alpha-synuclein, and apoptotic cell death in aged mice. Proc. Natl. Acad. Sci. U.S.A. *107*, 9879–9884.

Tong, Y., Giaime, E., Yamaguchi, H., Ichimura, T., Liu, Y., Si, H., Cai, H., Bonventre, J.V., and Shen, J. (2012). Loss of leucine-rich repeat kinase 2 causes age-dependent bi-phasic alterations of the autophagy pathway. Mol Neurodegener *7*, 2.

Trenkwalder, C., and Arnulf, I. (2011). Parkinsonism. In Principles and Practice of Sleep Medicine, (Elsevier), pp. 980–992.

Tretiakoff, C. (1919). *Contribution a l'etude de l'anatomie pathologique du locus niger de Soemmering avec quelques deductions relatives a la pathogenie des troubles du tonus musculaire et de la maladie de Parkinson.* (Paris).

Vancraenenbroeck, R., De Raeymaecker, J., Lobbestael, E., Gao, F., De Maeyer, M., Voet, A., Baekelandt, V., and Taymans, J.-M. (2014). In silico, in vitro and cellular analysis with a kinome-wide inhibitor panel correlates cellular LRRK2 dephosphorylation to inhibitor activity on LRRK2. Front Mol Neurosci *7*, 51.

van Egmond, W.N., Kortholt, A., Plak, K., Bosgraaf, L., Bosgraaf, S., Keizer-Gunnink, I., and van Haastert, P.J.M. (2008). Intramolecular activation mechanism of the Dictyostelium LRRK2 homolog Roco protein GbpC. J. Biol. Chem. *283*, 30412–30420.

Vilariño-Güell, C., Wider, C., Ross, O.A., Dachsel, J.C., Kachergus, J.M., Lincoln, S.J., Soto-Ortolaza, A.I., Cobb, S.A., Wilhoite, G.J., Bacon, J.A., et al. (2011).

VPS35 Mutations in Parkinson Disease. The American Journal of Human Genetics *89*, 162–167.

Visanji, N.P., Brooks, P.L., Hazrati, L.-N., and Lang, A.E. (2013). The prion hypothesis in Parkinson's disease: Braak to the future. Acta Neuropathol Commun *1*, 2.

Volpicelli-Daley, L.A., Abdelmotilib, H., Liu, Z., Stoyka, L., Daher, J.P.L., Milnerwood, A.J., Unni, V.K., Hirst, W.D., Yue, Z., Zhao, H.T., et al. (2016). G2019S-LRRK2 Expression Augments -Synuclein Sequestration into Inclusions in Neurons. Journal of Neuroscience *36*, 7415–7427.

Volta, M., and Melrose, H. (2017). LRRK2 mouse models: dissecting the behavior, striatal neurochemistry and neurophysiology of PD pathogenesis. Biochem. Soc. Trans. *45*, 113–122.

Volta, M., Beccano-Kelly, D.A., Paschall, S.A., Cataldi, S., MacIsaac, S.E., Kuhlmann, N., Kadgien, C.A., Tatarnikov, I., Fox, J., Khinda, J., et al. (2017). Initial elevations in glutamate and dopamine neurotransmission decline with age, as does exploratory behavior, in LRRK2 G2019S knock-in mice. Elife *6*.

Vural, A., and Kehrl, J.H. (2014). Autophagy in Macrophages: Impacting Inflammation and Bacterial Infection. Scientifica *2014*, 1–13.

Wandu, W.S., Tan, C., Ogbeifun, O., Vistica, B.P., Shi, G., Hinshaw, S.J.H., Xie, C., Chen, X., Klinman, D.M., Cai, H., et al. (2015). Leucine-Rich Repeat Kinase 2 (Lrrk2) Deficiency Diminishes the Development of Experimental Autoimmune Uveitis (EAU) and the Adaptive Immune Response. PLoS ONE *10*, e0128906.

Wang, L., Xie, C., Greggio, E., Parisiadou, L., Shim, H., Sun, L., Chandran, J., Lin, X., Lai, C., Yang, W.-J., et al. (2008). The chaperone activity of heat shock protein 90 is critical for maintaining the stability of leucine-rich repeat kinase 2. J. Neurosci. *28*, 3384–3391.

Wang, K., Gao, W., Dou, Q., Chen, H., Li, Q., Nice, E.C., and Huang, C. (2016). Ivermectin induces PAK1-mediated cytostatic autophagy in breast cancer. Autophagy *12*, 2498–2499.

Wang, S., Liu, Z., Ye, T., Mabrouk, O.S., Maltbie, T., Aasly, J., and West, A.B. (2017a). Elevated LRRK2 autophosphorylation in brain-derived and peripheral exosomes in LRRK2 mutation carriers. Acta Neuropathol Commun *5*, 86.

Wang, Z., Jia, G., Li, Y., Liu, J., Luo, J., Zhang, J., Xu, G., and Chen, G. (2017b). Clinicopathological signature of p21-activated kinase 1 in prostate cancer and its regulation of proliferation and autophagy via the mTOR signaling pathway. Oncotarget *8*, 22563–22580.

West, A.B., Moore, D.J., Choi, C., Andrabi, S.A., Li, X., Dikeman, D., Biskup, S., Zhang, Z., Lim, K.-L., Dawson, V.L., et al. (2007). Parkinson's disease-associated

mutations in LRRK2 link enhanced GTP-binding and kinase activities to neuronal toxicity. Hum. Mol. Genet. *16*, 223–232.

West, A.B., Cowell, R.M., Daher, J.P.L., Moehle, M.S., Hinkle, K.M., Melrose, H.L., Standaert, D.G., and Volpicelli-Daley, L.A. (2014). Differential LRRK2 expression in the cortex, striatum, and substantia nigra in transgenic and nontransgenic rodents: LRRK2 distribution in the nigrostriatal pathway. Journal of Comparative Neurology *522*, 2465–2480.

Won, S.-Y., Park, M.-H., You, S.-T., Choi, S.-W., Kim, H.-K., McLean, C., Bae, S.-C., Kim, S.R., Jin, B.K., Lee, K.H., et al. (2016). Nigral dopaminergic PAK4 prevents neurodegeneration in rat models of Parkinson's disease. Sci Transl Med *8*, 367ra170.

Wu, X., and Brewer, G. (2012). The regulation of mRNA stability in mammalian cells: 2.0. Gene *500*, 10–21.

Xiong, Y., Yuan, C., Chen, R., Dawson, T.M., and Dawson, V.L. (2012). ArfGAP1 is a GTPase activating protein for LRRK2: reciprocal regulation of ArfGAP1 by LRRK2. J. Neurosci. *32*, 3877–3886.

Xiong, J. (2015). Atg7 in development and disease: panacea or Pandora's Box? Protein Cell *6*, 722–734.

Xiong, Y., Dawson, T.M., and Dawson, V.L. (2017). Models of LRRK2-Associated Parkinson's Disease. Adv Neurobiol *14*, 163–191.

Yu, L., Chen, Y., and Tooze, S.A. (2017). Autophagy pathway: Cellular and molecular mechanisms. Autophagy 1–9.

Yun, H.J., Kim, H., Ga, I., Oh, H., Ho, D.H., Kim, J., Seo, H., Son, I., and Seol, W. (2015). An early endosome regulator, Rab5b, is an LRRK2 kinase substrate. J. Biochem. *157*, 485–495.

Zabetian, C.P., Samii, A., Mosley, A.D., Roberts, J.W., Leis, B.C., Yearout, D., Raskind, W.H., and Griffith, A. (2005). A clinic-based study of the LRRK2 gene in Parkinson disease yields new mutations. Neurology *65*, 741–744.

Zhang, F.-R., Huang, W., Chen, S.-M., Sun, L.-D., Liu, H., Li, Y., Cui, Y., Yan, X.-X., Yang, H.-T., Yang, R.-D., et al. (2009). Genomewide association study of leprosy. N. Engl. J. Med. *361*, 2609–2618.

Zhao, J., Hermanson, S.B., Carlson, C.B., Riddle, S.M., Vogel, K.W., Bi, K., and Nichols, R.J. (2012). Pharmacological inhibition of LRRK2 cellular phosphorylation sites provides insight into LRRK2 biology. Biochem. Soc. Trans. *40*, 1158–1162.

Zharikov, A.D., Cannon, J.R., Tapias, V., Bai, Q., Horowitz, M.P., Shah, V., El Ayadi, A., Hastings, T.G., Greenamyre, J.T., and Burton, E.A. (2015). shRNA

targeting α-synuclein prevents neurodegeneration in a Parkinson's disease model. J. Clin. Invest. *125*, 2721–2735.

Zhuo, C., Ji, Y., Chen, Z., Kitazato, K., Xiang, Y., Zhong, M., Wang, Q., Pei, Y., Ju, H., and Wang, Y. (2013). Proteomics analysis of autophagy-deficient Atg7−/− MEFs reveals a close relationship between F-actin and autophagy. Biochemical and Biophysical Research Communications *437*, 482–488.

Zimprich, A., Biskup, S., Leitner, P., Lichtner, P., Farrer, M., Lincoln, S., Kachergus, J., Hulihan, M., Uitti, R.J., Calne, D.B., et al. (2004). Mutations in LRRK2 cause autosomal-dominant parkinsonism with pleomorphic pathology. Neuron *44*, 601–607.

Zimprich, A., Benet-Pagès, A., Struhal, W., Graf, E., Eck, S.H., Offman, M.N., Haubenberger, D., Spielberger, S., Schulte, E.C., Lichtner, P., et al. (2011). A mutation in VPS35, encoding a subunit of the retromer complex, causes late-onset Parkinson disease. Am. J. Hum. Genet. *89*, 168–175.